

DEVELOPMENT OF NANOFIBER BASED ACTIVE PACKAGING MATERIAL
BY ELECTROSPINNING TECHNIQUE AND FOOD VALIDATION

A THESIS SUBMITTED TO
THE GRADUATE SCHOOL OF NATURAL AND APPLIED SCIENCES
OF
MIDDLE EAST TECHNICAL UNIVERSITY

BY

AYÇA AYDOĞDU

IN PARTIAL FULFILLMENT OF THE REQUIREMENTS
FOR
THE DEGREE OF DOCTOR OF PHILOSOPHY
IN
FOOD ENGINEERING

SEPTEMBER 2019

Approval of the thesis:

**DEVELOPMENT OF NANOFIBER BASED ACTIVE PACKAGING
MATERIAL BY ELECTROSPINNING TECHNIQUE AND FOOD
VALIDATION**

submitted by **AYÇA AYDOĞDU** in partial fulfillment of the requirements for the degree of **Doctor of Philosophy in Food Engineering Department, Middle East Technical University** by,

Prof. Dr. Halil Kalıpçılar
Dean, Graduate School of **Natural and Applied Sciences**

Prof. Dr. Serpil Şahin
Head of Department, **Food Engineering**

Prof. Dr. Gülüm Şumnu
Supervisor, **Food Engineering, METU**

Prof. Dr. Serpil Şahin
Co-Supervisor, **Food Engineering, METU**

Examining Committee Members:

Prof. Dr. Zehra Ayhan
Food Engineering, Sakarya University

Prof. Dr. Gülüm Şumnu
Food Engineering, METU

Assoc. Prof. Dr. Halil Mecit Öztop
Food Engineering, METU

Assoc. Prof. Dr. Özge Şakıyan Demirkol
Food Engineering, Ankara University

Dr. Leyla Nesrin Kahyaoğlu
Food Engineering, METU

Date: 06.09.2019

I hereby declare that all information in this document has been obtained and presented in accordance with academic rules and ethical conduct. I also declare that, as required by these rules and conduct, I have fully cited and referenced all material and results that are not original to this work.

Name, Surname: Ayça Aydođdu

Signature:

ABSTRACT

DEVELOPMENT OF NANOFIBER BASED ACTIVE PACKAGING MATERIAL BY ELECTROSPINNING TECHNIQUE AND FOOD VALIDATION

Aydođdu, Ayça
Doctor of Philosophy, Food Engineering
Supervisor: Prof. Dr. Glm Őumnu
Co-Supervisor: Prof. Dr. Serpil Őahin

September 2019, 173 pages

The main objective of this study was to encapsulate gallic acid in Hydroxypropyl methylcellulose (HPMC) and legume flours (lentil and pea) based nanofiber by electrospinning and to examine the usage of nanofibers as active packaging materials. Firstly, HPMC based homogenous nanofibers were fabricated and it was observed that the morphology of the fibers changed from the beaded structure to the uniform fiber structure by increasing the concentrations of the solutions. By choosing optimum HPMC concentration, gallic acid was encapsulated successfully in HPMC based nanofibers by electrospinning and the antioxidant activity of gallic acid were preserved in the nanofibers. When gallic acid loaded HPMC nanofiber was used as active package material to pack walnut, it reduced the oxidation of walnut during storage. Then, gallic acid was encapsulated into lentil flour/polyethylene oxide (PEO) nanofibers. To promote the solubility of lentil proteins, pH of solutions was adjusted to pH 1 and pH 10. It should be noted that alkaline nanofibers showed homogenous structure and antioxidant activity after electrospinning. Therefore, alkaline nanofibers were used to pack walnuts and active packages provided stability to walnuts against oxidation. Moreover, gallic acid was also incorporated into pea flour nanofiber successfully. To prove incorporation of gallic acid into nanofibers, physical and

thermal properties of gallic acid encapsulated nanofibers were examined by Fourier transform infrared spectroscopy (FTIR), thermal gravimetric analysis (TGA) and differential scanning calorimeter (DSC) analyses. Finally, bilayer nanofiber sheets composed of Poly (lactic acid) (PLA) and soy protein/HPMC were produced to be suggested to pack of light sensitive foods.

Keywords: electrospinning, HPMC, lentil flour, pea flour, packaging

ÖZ

ELEKTROEĞİRME YÖNTEMİ İLE NANOLİF BAZLI AKTİF AMBALAJ MALZEMESİ GELİŞTİRİLMESİ VE GIDA VALİDASYONU

Aydoğdu, Ayça
Doktora, Gıda Mühendisliği
Tez Danışmanı: Prof. Dr. Gülüm Şumnu
Ortak Tez Danışmanı: Prof. Dr. Serpil Şahin

Eylül 2019, 173 sayfa

Bu çalışmanın temel amacı, elektroegirme ile galik asitin hidrokispropil metilselüloz (HPMC) ve baklagil unu (mercimek ve bezelye) bazlı nanoliflerin içine enkapsüle etmek ve nanoliflerin aktif paketleme malzemesi olarak kullanılabilirliğini incelemektir. İlk olarak, HPMC bazlı homojen nanolifler üretilmiştir ve çözeltilerin konsantrasyonlarını arttırdıkça, nanoliflerin morfolojisinin boncuklu yapıdan homojen yapıya deęiştigi gözlenmiştir. Optimum HPMC konsantrasyonunun seçilerek, galik asit HPMC bazlı nanoliflere elektroegirme ile başarılı bir şekilde kapsüllenmiş ve gallik asidin antioksidan aktivitesi nanoliflerde korunmuştur. Galik asit yüklü HPMC nanolifler ceviz ambalajlamak için aktif ambalaj malzemesi olarak kullanıldığında, depolama sırasında cevizin oksidasyonunu azaltmıştır. Daha sonra, gallik asit mercimek unu / polietilen oksit (PEO) nanoliflere enkapsüle edilmiştir. Mercimek proteinlerinin çözünürlüğünü arttırmak için, çözeltilerin pH'ı 1 ve 10'a ayarlanmıştır. Alkali nanoliflerin, elektroegirmeden sonra homojen yapı ve antioksidan aktivite gösterdiği belirtilmiştir. Bu nedenle, ceviz ambalajlamak için alkali nanolifler kullanılmış ve aktif ambalajlar cevizlerin oksidasyona karşı stabilite sağlamıştır. Gallik asidin nanoliflere enkapsüle olduğunu kanıtlamak için, gallik asit kapsüllenmiş nanoliflerin fiziksel ve termal özellikleri Fourier dönüşümü kızılötesi spektroskopisi

(FTIR), termal gravimetrik analiz (TGA) ve diferansiyel taramalı kalorimetre (DSC) analizleriyle incelenmiştir. Son olarak, ışığa duyarlı yiyeceklerin ambalajlanması için Poly (laktik asit) (PLA) ve soya proteini / HPMC'den oluşan iki tabakalı nanofiber tabakalar önerilmiştir.

Anahtar Kelimeler: Elektroğirme, HPMC, mercimek unu, bezelye unu, ambalajlama

To my family...

ACKNOWLEDGMENTS

This research was funded by The Scientific and Technological Research Council of Turkey (TUBITAK) (Project no: 215O569). I would like to thank TUBITAK for giving the opportunity to complete the study.

I would like to express my deepest gratitude and respect to my supervisor Prof. Dr. Gülüm Şumnu for her encouragement, guidance, valuable suggestions and kindly attitude throughout this study. I would also thank to my co-supervisor, Prof. Dr. Serpil Şahin for her assistive suggestions throughout my thesis. I am also grateful to Prof. Dr. Zehra Ayhan for her experimental support.

I would like to thank Seren Oguz and Nilay Tam who are valuable part of this project. We are not just collaborators; we are such a great team. They are definitely the most responsible and planned students that I have seen and I am really happy to choose them to work together. Although we spent lots of time to solve unsolvable electrospinning problems, at the end we achieved the impossible and finished the project.

My invaluable gratitude goes to Eda Berk Yıldız and certainly I could not complete this thesis without her help. She not only helped me with the experiments but also listened my whole complaints even if when I was in USA. I feel myself really lucky to have such a great friend.

The most difficulty of this study is waiting until midnight to turn of the set up and in that part I am really grateful to Selen Güner, Kübra Ertan and Emrah Kırtıl to do that.

I am also so thankful to Serkan Yılmaz for SEM experiments that last for many hours. I would like to express my thanks to Cansu Kabakcı, Şahin Namlı, Serap Namlı, Derya Uçbaş, Esmâ İlhan and Özge Güven for all the good times spent. I also would like to thank Armağan Cabadağ for technical help during my study.

I would like to express my special thanks to Emrah Kırtıl, Sevil Çıkrıkcı and Bade Tonyalı for their endless friendship through all those years. The word of “friend” is not enough to define our relationship, I feel that they are members of my family. Whenever I need a help or I feel unhappy and stressful, they are always there for me. I value of their contributions to this study and their effort to make me feel always motivated and happy.

Last and certainly not least, my deepest appreciation goes to my family; my mother Ayşe Aydoğdu, my father Yıldırım Aydoğdu, and my sister Asena Aydoğdu for their unconditional love and tireless devotion throughout my life. They have always faith in me and without their support and encouragement, it would be impossible to finish this work. Words are incapable to express my gratitude and love to them. I would like to express special thanks to my father Yıldırım Aydoğdu. He was like my another supervisor during PhD and helped for experiments.

TABLE OF CONTENTS

ABSTRACT	v
ÖZ	vii
ACKNOWLEDGMENTS	x
TABLE OF CONTENTS	xii
LIST OF TABLES.....	xvii
LIST OF FIGURES	xxii
CHAPTERS	
1. INTRODUCTION.....	1
1.1. Electrospinning	1
1.1.1. Electrospinning Principles and Setup.....	1
1.1.2. Parameters Affecting Electrospinning.....	2
1.1.2.1. Solution parameters	3
1.1.2.2. Processing parameters	6
1.1.2.3. Ambient parameters.....	10
1.1.3. Applications of electrospinning.....	11
1.1.3.1. Enzyme immobilization.....	12
1.1.3.2. Encapsulation of bioactive compounds	13
1.1.3.3. Food packaging.....	17
1.2. Objectives of the study.....	21
2. MATERIALS AND METHODS	23
2.1. Materials.....	23
2.2. Methods.....	23

2.2.1. Preparation of electrospinning solutions.....	23
2.2.1.1. HPMC solutions.....	23
2.2.1.2. HPMC/gallic acid solutions.....	24
2.2.1.3. Lentil flour/gallic acid solutions.....	24
2.2.1.4. Pea flour/gallic acid solutions.....	25
2.2.1.5. Soy protein solutions.....	25
2.2.1.6. Soy Protein/HPMC solutions.....	26
2.2.2. Characterization of solutions.....	26
2.2.2.1. Rheological properties.....	26
2.2.2.2. Electrical Conductivity.....	26
2.2.2.3. Total phenolic content of lentil and pea flour solutions.....	27
2.2.3. Electrospinning of solutions.....	27
2.2.4. Characterization of nanofibers.....	28
2.2.4.1. Morphological analysis.....	28
2.2.4.2. Loading efficiency of gallic acid in HPMC based electrospun fiber.....	28
2.2.4.3. Loading efficiency of gallic acid in lentil and pea flour based electrospun fiber.....	29
2.2.4.4. Antioxidant capacity of electrospun fiber.....	29
2.2.4.5. Water Vapor Permeability (WVP).....	30
2.2.4.6. Thermogravimetric Analysis (TGA).....	31
2.2.4.7. Differential Scanning Calorimetry (DSC).....	31
2.2.4.8. Fourier-transform infrared (FTIR) Analysis.....	31
2.2.4.9. Opacity.....	31
2.2.5. Packaging of walnuts and accelerated oxidation test.....	32

2.2.5.1. Oil extraction	32
2.2.5.2. Oxidation analyses	33
2.2.6. Statistical analysis	34
3. RESULTS AND DISCUSSION	35
3.1. Fabrication of HPMC/PEO nanofibers by electrospinning.....	35
3.1.1. Physical properties of solutions.....	35
3.1.1.1. Rheological properties	35
3.1.1.2. Electrical Conductivity	41
3.1.2. Characterization of nanofibers	42
3.1.2.1. Fiber morphology	42
3.1.2.2. Water Vapor Permeability (WVP).....	47
3.1.2.3. FTIR Analysis.....	48
3.1.2.4. Thermo-gravimetric Analysis (TGA)	50
3.1.2.5. DSC Analysis.....	52
3.2. Fabrication of gallic acid loaded HPMC/PEO nanofibers with electrospinning	54
3.2.1. Physical properties of solutions.....	54
3.2.1.1. Rheological properties	54
3.2.1.2. Electrical Conductivity	56
3.2.2. Characterization of electrospun nanofibers	56
3.2.2.1. Fiber Morphology.....	56
3.2.2.2. Loading efficiency and antioxidant activity of gallic acid in HPMC/PEO electrospun fiber	59
3.2.2.3. Thermo-gravimetric Analysis (TGA)	60

3.2.2.4. DSC Analysis	61
3.2.2.5. FTIR Analysis	62
3.2.3. Application of HPMC based nanofibers for packaging of walnuts	64
3.3. Fabrication of gallic acid loaded lentil flour/PEO nanofibers with electrospinning	66
3.3.1. Physical properties of solutions	66
3.3.1.1. Rheological properties	66
3.3.1.2. Electrical conductivity	67
3.3.2. Characterization of electrospun nanofibers	69
3.3.2.1. Fiber morphology	69
3.3.2.2. Total phenolic content (TPC) and antioxidant activity of solutions and nanofibers	72
3.3.2.3. Thermo-gravimetric analysis (TGA)	74
3.3.2.4. Differential scanning calorimetry (DSC) analysis	75
3.3.2.5. FTIR analysis	77
3.3.3. Application of lentil flour based nanofibers for packaging of walnuts	79
3.4. Fabrication of gallic acid loaded pea flour/PEO nanofibers with electrospinning	82
3.4.1. Physical properties of solutions	82
3.4.1.1. Rheological properties	82
3.4.1.2. Electrical conductivity	83
3.4.2. Characterization of electrospun nanofibers	83
3.4.2.1. Fiber morphology	83
3.4.2.2. Total phenolic content (TPC) and antioxidant activity of solutions and nanofibers	86

3.4.2.3. Thermo-gravimetric analysis (TGA)	87
3.4.2.4. Differential Scanning Calorimetry (DSC) Analysis	89
3.4.2.5. FTIR analysis	91
3.5. Fabrication of Poly(lactic acid)/Soy Protein/HPMC nanofibers with electrospinning	93
3.5.1. Physical properties of solutions	93
3.5.1.1. Rheological properties	93
3.5.1.2. Electrical Conductivity	95
3.5.2. Characterization of Nanofibers	97
3.5.2.1. Fiber Morphology	97
3.5.2.2. Opacity	101
3.5.2.3. Water Vapor Permeability (WVP)	102
3.5.2.4. FTIR Analysis	103
3.5.2.5. TGA Analysis	104
3.5.2.6. DSC Analysis	106
4. CONCLUSION	109
REFERENCES	111
APPENDICES	133
CURRICULUM VITAE	171

LIST OF TABLES

TABLES

Table 1.1 Examples of bioactive compounds encapsulated into different biopolymer-based matrices by electrospinning	16
Table 3.1 Rheological properties and electrical conductivities of solutions, the morphology and average diameters of the HPMC/PEO fibers	38
Table 3.2 WVP and thermal properties of fibers	47
Table 3.3 Rheological properties and electrical conductivities of solutions and average diameter of nanofibers.....	55
Table 3.4. Loading efficiency and total antioxidant activities of gallic acid loaded HPMC/PEO electrospun nanofibers	60
Table 3.5 Peroxide, p-anisidin, Totox and TBARS values of walnuts that packed in gallic acid loaded nanofibers containing packages	65
Table 3.6 Rheological properties, electrical conductivities, and TPC of solutions and average diameter of nanofibers	68
Table 3.7 Loading efficiency and total antioxidant activities of gallic acid loaded lentil flour based electrospun nanofibers prepared at different pH values.....	73
Table 3.8 Peroxide, p-anisidine, Totox and TBARS values of walnuts that packed in gallic acid loaded nanofibers containing packages	81
Table 3.9 Rheological properties, electrical conductivities, TPC of solutions and average diameter of nanofibers	83
Table 3.10 Loading efficiency and total antioxidant activities of gallic acid loaded pea flour/PEO electrospun nanofibers	87
Table 3.11 Rheological properties and electrical conductivities of solutions.....	95
Table 3.12 Average diameter, opacity and water vapor permeability of sheets	101

Table A. 1 One way Analysis of Variance (ANOVA) and Tukey’s comparison test for consistency index (k) values of solutions containing different amount of HPMC/PEO.	133
Table A. 2 One way Analysis of Variance (ANOVA) and Tukey’s comparison test for flow behavior index (n) values of solutions containing different amount of HPMC/PEO.	134
Table A. 3 One way Analysis of Variance (ANOVA) and Tukey’s comparison test for electrical conductivity values of solutions containing different amount of HPMC/PEO.	135
Table A. 4 One way Analysis of Variance (ANOVA) and Tukey’s comparison test for diameter values of nanofibers containing different amount of HPMC/PEO.	136
Table A. 5 One way Analysis of Variance (ANOVA) and Tukey’s comparison test for WVP values of nanofibers containing different amount of HPMC/PEO.	137
Table A. 6 One way Analysis of Variance (ANOVA) and Tukey’s comparison test for glass transition temperature (Tg) values of nanofibers containing different amount of HPMC/PEO.	138
Table A. 7 One way Analysis of Variance (ANOVA) and Tukey’s comparison test for melting temperature (Tm) values of nanofibers containing different amount of HPMC/PEO.	139
Table A. 8 One way Analysis of Variance (ANOVA) and Tukey’s comparison test for melting enthalpy (ΔH_m) values of nanofibers containing different amount of HPMC/PEO.	140
Table A. 9 One way Analysis of Variance (ANOVA) and Tukey’s comparison test for consistency index (k) values of HPMC/PEO solutions containing different amount of gallic acid.	141
Table A. 10 One way Analysis of Variance (ANOVA) and Tukey’s comparison test for flow behavior index (n) values of HPMC/PEO solutions containing different amount of gallic acid	142

Table A. 11 One way Analysis of Variance (ANOVA) and Tukey’s comparison test for electrical conductivity values of HPMC/PEO solutions containing different amount of gallic acid.....	143
Table A. 12 One way Analysis of Variance (ANOVA) and Tukey’s comparison test for diameter values of HPMC/PEO nanofibers containing different amount of gallic acid.....	144
Table A. 13 One way Analysis of Variance (ANOVA) and Tukey’s comparison test for gallic acid loading efficiency values of HPMC/PEO nanofibers containing different amount of gallic acid.....	145
Table A. 14 One way Analysis of Variance (ANOVA) and Tukey’s comparison test for antioxidant activity values of HPMC/PEO nanofibers containing different amount of gallic acid.....	146
Table A. 15 One way Analysis of Variance (ANOVA) and Tukey’s comparison test for p_anisidin values of walnuts packed in HPMC/PEO packages	147
Table A. 16 One way Analysis of Variance (ANOVA) and Tukey’s comparison test for peroxide value values of walnuts packed in HPMC/PEO packages	148
Table A. 17 One way Analysis of Variance (ANOVA) and Tukey’s comparison test for TBARS values of walnuts packed in HPMC/PEO packages	149
Table A. 18 Two way Analysis of Variance (ANOVA) and Tukey’s comparison test for the effect of pH and gallic acid on consistency index (k) values of solutions containing lentil flour/PEO.....	150
Table A. 19 Two way Analysis of Variance (ANOVA) and Tukey’s comparison test for the effect of pH and gallic acid on flow behavior index values (n) of solutions containing lentil flour/PEO.....	151
Table A. 20 Two way Analysis of Variance (ANOVA) and Tukey’s comparison test for the effect of pH and gallic acid on electrical conductivity values of solutions containing lentil flour/PEO.....	152
Table A. 21 Two way Analysis of Variance (ANOVA) and Tukey’s comparison test for the effect of pH and gallic acid on total phenolic content (TPC) values of solutions containing lentil flour/PEO.....	153

Table A. 22 One way Analysis of Variance (ANOVA) and Tukey’s comparison test for total phenolic content values of lentil flour/PEO nanofibers prepared at different pH values	154
Table A. 23 One way Analysis of Variance (ANOVA) and Tukey’s comparison test for antioxidant activity values of lentil flour/PEO nanofibers prepared at different pH values	155
Table A. 24 One way Analysis of Variance (ANOVA) and Tukey’s comparison test for per oxide values of walnuts packed in lentil flour/PEO packages	156
Table A. 25 One way Analysis of Variance (ANOVA) and Tukey’s comparison test for p-anisidin values of walnuts packed in lentil flour/PEO packages	157
Table A. 26 One way Analysis of Variance (ANOVA) and Tukey’s comparison test for TBARS values of walnuts packed in lentil flour/PEO packages	158
Table A. 27 One way Analysis of Variance (ANOVA) and Tukey’s comparison test for consistency index (k) values of Pea flour/PEO solutions containing different amount of gallic acid.	159
Table A. 28 One way Analysis of Variance (ANOVA) and Tukey’s comparison test for flow behavior index (n) values of pea flour/PEO solutions containing different amount of gallic acid.	160
Table A. 29 One way Analysis of Variance (ANOVA) and Tukey’s comparison test for electrical conductivity values of pea flour/PEO solutions containing different amount of gallic acid.	161
Table A. 30 One way Analysis of Variance (ANOVA) and Tukey’s comparison test for total phenolic content (TPC) values of pea flour/PEO solutions containing different amount of gallic acid.	162
Table A. 31 One way Analysis of Variance (ANOVA) and Tukey’s comparison test for diameter values of pea flour/PEO nanofibers containing different amount of gallic acid.....	163
Table A. 32 One way Analysis of Variance (ANOVA) and Tukey’s comparison test for total phenolic content (TPC) values of pea flour/PEO nanofibers containing different amount of gallic acid.....	164

Table A. 33 One way Analysis of Variance (ANOVA) and Tukey’s comparison test for antioxidant activity values of pea flour/PEO nanofibers containing different amount of gallic acid.....	165
Table A. 34 One way Analysis of Variance (ANOVA) and Tukey’s comparison test for consistency index (k) values of solutions containing PEO/soy protein/HPMC.	166
Table A. 35 One way Analysis of Variance (ANOVA) and Tukey’s comparison test for flow behavior index (n) values of solutions containing PEO/soy protein/HPMC.	167
Table A. 36 One way Analysis of Variance (ANOVA) and Tukey’s comparison test for diameter values of nanofibers containing PEO/soy protein/HPMC.....	168
Table A. 37 One way Analysis of Variance (ANOVA) and Tukey’s comparison test for opacity values of sheets containing PEO/soy protein/HPMC and PLA.....	169
Table A. 38 One way Analysis of Variance (ANOVA) and Tukey’s comparison test for WVP values of sheets containing PEO/soy protein/HPMC and PLA.....	170

LIST OF FIGURES

FIGURES

Figure 1.1 Schematic of electrospinning apparatus (Bharwaj & Kundu,2010).....	2
Figure 3.1 Flow curves of solutions containing different amount of HPMC/PEO ...	39
Figure 3.2 Variation of storage modulus (G') and loss modulus (G'') with frequency for solutions containing different amount of HPMC/PEO	40
Figure 3.3 SEM images of electrospun fibers containing 2% PEO with different HPMC contents: A: 2%, B: 3%, C: 4%......	45
Figure 3.4 SEM images of electrospun fibers containing 1% PEO with different HPMC contents: A: 2%, B: 3%, C: 4%......	46
Figure 3.5 FTIR spectra of nanofibers containing different amounts of HPMC and PEO.....	50
Figure 3.6 Thermo-gravimetric curves of nanofibers containing different amounts of HPMC and PEO.....	52
Figure 3.7 Flow curves of solutions containing different gallic acid concentration: \circ : control, Δ : 2%, \diamond : 5%, \square : 10%......	55
Figure 3.8 SEM images of electrospun nanofibers with different gallic acid concentration: a: control, b: 2%, c: 5%, d: 10%.	58
Figure 3.9 Thermo-gravimetric curves of gallic acid and electrospun nanofibers with different gallic acid concentration: a: gallic acid, b: control, c: 2%, d: 5%, e: 10%.	61
Figure 3.10 DSC curves of gallic acid and electrospun nanofibers with different gallic acid concentration: a: gallic acid, b: control, c: 2%, d: 5%, e: 10%.	62
Figure 3.11 FTIR spectra of gallic acid and electrospun nanofibers with different gallic acid concentration: a: gallic acid, b: control, c: 2%, d: 5%, e: 10%.	64
Figure 3.12 The packaged walnuts: A: packaged with 10% gallic acid loaded nanofibers, B&C: control.....	66

Figure 3.13 SEM images of electrospun nanofibers, A: pH10_nogallicacid, B: pH10_gallic acid. C: pH1_nogallicacid, D: pH1_gallic acid.....	71
Figure 3.14 Thermo-gravimetric curves of gallic acid and electrospun nanofibers: a: gallic acid, c: pH10_gallicacid, d: pH1_gallicacid. e: pH1_nogallicacid, f: pH10_nogallicacid.	75
Figure 3.15 DSC curves of gallic acid and electrospun nanofibers, a: gallic acid, b: pH10_nogallicacid, c: pH1_gallicacid. d: pH10_gallicacid, e: pH1_nogallicacid.	77
Figure 3.16 FTIR spectra of electrospun nanofibers, gallic acid and lentil flour, A: pH1_nogallicacid, B: pH1_gallicacid. C: pH10_nogallicacid, D: pH10_gallicacid, E: lentil flour, F: gallic acid.....	79
Figure 3.17 The packaged walnuts: A: control and B: packaged with gallic acid loaded nanofibers.....	82
Figure 3.18 SEM images of electrospun nanofibers with different gallic acid concentration: a: control, b: 5%, c: 10%.....	85
Figure 3.19 Thermo-gravimetric curves of gallic acid and electrospun nanofibers with different gallic acid concentration: a: gallic acid, b: 10%, c: 5%, d: control.	89
Figure 3.20 DSC curves of gallic acid and electrospun nanofibers with different gallic acid concentration: a: gallic acid, b: control, c: 10%, d: 5%.....	91
Figure 3.21 FTIR spectra of gallic acid, pea flour and electrospun nanofibers with different gallic acid concentration: a: control, b: 5%, c: 10%, d: pea flour, e: gallic acid.	92
Figure 3.22 Flow curves of solutions that used in electrospinning process: ○: PEO_Soy Protein, Δ: PEO_HPMC, ◇: PEO_HPMC_Soy Protein.	95
Figure 3.23 Surface (5000x magnification) and cross-section (2500x magnification) SEM images of nanofibers A-B PEO_HPMC, C-D: PEO_SoyProtein, E-F: PEO_HPMC_SoyProtein.....	99
Figure 3.24 Diameter distributions of nanofibers A: PEO_HPMC, B: PEO_SoyProtein, C: PEO_HPMC_SoyProtein.....	100
Figure 3.25 FTIR spectra of components and PLA-nanofiber sheets.....	104
Figure 3.26 TGA curves of components and PLA-nanofiber sheets.....	106

Figure 3.27 DSC curves of PLA and PLA-nanofiber sheets 107

CHAPTER 1

INTRODUCTION

1.1. Electrospinning

1.1.1. Electrospinning Principles and Setup

Electrospinning was first described by Rayleigh in 1897 and also studied by Zeleny in 1914 (Zeleny, 1914) and patented by Formhals in 1934 (Formhals, 1934) (US Patent Number: 2116942). With the study of Doshi & Reneker (1995), electrospinning was discovered again and started to use to produce nano-structured materials.

Electrospinning is a spinning technique which uses electrostatic forces to produce fibers having thinner diameter (from nanometer to micrometer) and larger surface area than conventional spinning process. The typical set up of electrospinning apparatus is shown in Figure 1.1. Electrospinning system consists of four main components: (1) a high voltage power supply that is operated generally in direct current (DC) mode; (2) a capillary tube with a needle or pipette; (3) a syringe pump; (4) a grounded collecting plate (flat plate or rotating drum) (Anu Bhushani & Anandharamakrishnan, 2014). Although there are two standard electrospinning setups, such as vertical and horizontal, alignment of syringe is usually horizontal. In vertical position, the syringe pump is not needed since polymer solution can exit capillary easily by the help of gravitational force. However, without syringe pump, the system is less controllable. Therefore, mostly the horizontal systems or vertical system with a syringe pump is preferred (Kriegel et al., 2008). In electrospinning, one electrode is connected to feedstock solution in syringe to raise the electrostatic potential of the fluid and the other one is attached to the collector. In the absence of electric field, the shape of volume of a fluid is maintained by the balance of gravitational force and surface tension of fluid. As the electrostatic potential increases, the surface charge of solution

increases, too. At the tip of the capillary, the application of the external electric field introduces additional forces namely the electrostatic repulsion of like charges and the Coulombic force of the external electric field which result in the fluid changing shape and forming a conical shape known as the Taylor cone. Once the electrical field attains a critical value in which repulsive electrostatic forces overcome the surface tension, a charged jet is ejected from the tip of the Taylor cone (Z.-M. Huang, Zhang, Kotaki, & Ramakrishna, 2003; Stanger, Tucker, & Staiger, 2005). The charged jet is exposed to several forces such as electrostatic force, drag force, gravity, Coulombic repulsion force, surface tension and viscoelastic forces. As the jet goes through the collector, it attenuates due to drag forces and evaporation of solvent occurs. Finally, continuous fibers are deposited on the collector (Ghorani & Tucker, 2015).

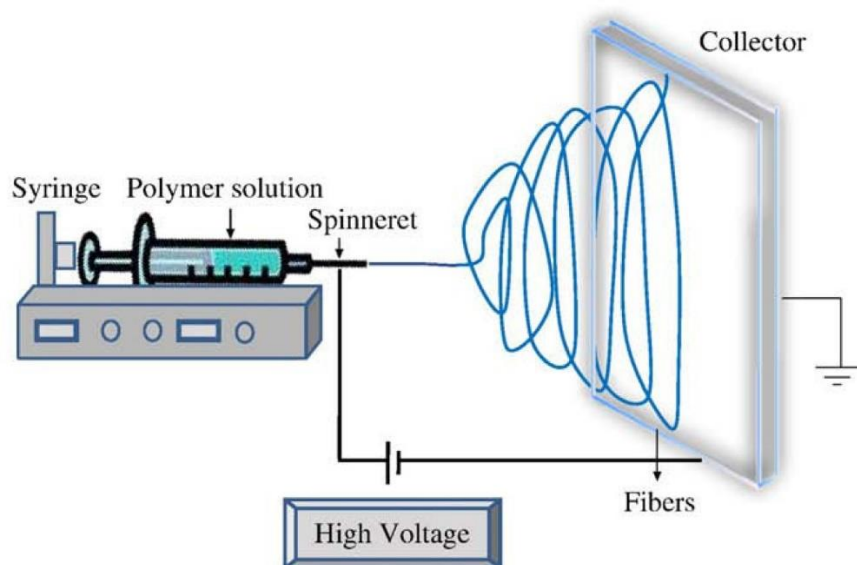


Figure 1.1 Schematic of electrospinning apparatus (Bharwaj & Kundu,2010)

1.1.2. Parameters Affecting Electrospinning

Electrospinning process strongly depends on several parameters which can be divided into three main groups: solution parameters (concentration, molecular weight, viscosity, surface tension, and conductivity), processing parameters (applied voltage, feed flow rate, types of collectors, tip to collector distance) and ambient parameters (humidity, temperature). These parameters may influence the fiber morphology

individually or synergistically. There are three significant criteria that show the successful electrospinning process: formation of Taylor cone and stable jet and homogeneous fibers containing no bead images. When optimum conditions are not provided, jet formation can not occur and small beads or fibers containing beads are obtained. Jet instabilities can be classified as axisymmetric Rayleigh instability, electric field induced axisymmetric instability and bending instability (Ramakrishna, Fujihara, Teo, Lim, & Ma, 2005a). Therefore, obtaining homogenous nanofibers by electrospinning require careful balancing of the parameters (Bhardwaj & Kundu, 2010).

1.1.2.1. Solution parameters

1.1.2.1.1. Viscosity of solutions

Solution viscosity plays an important role in fiber morphology and size during the electrospinning process. In general, the viscosity of the solution is associated to the extent of polymer molecule chain entanglement within the solution. The entanglement of polymers is crucial to the fiber formation (Ramakrishna et al., 2005a). The polymer solution should show high polymer entanglement without prevention of jet movement. In other words, below a critical viscosity value, applied voltage results in bead formation due to Rayleigh instability. The solution viscosity has been strongly related to the concentration of the solution and molecular weight of polymer. The effect of solution viscosity and/or concentration of polymers on fiber formation was proved in several studies. In the study of Gupta, Elkins, Long, & Wilkes (2005), the relationship between concentration and fiber formation was explored and polymer droplets and beaded structure was observed when dilute solutions were used due to insufficient overlap between molecular chains. With increasing concentration of poly (methyl methacrylate), uniform nanofibers were obtained by electrospinning. Similarly, Jia et al. (2007) observed that the structure of fibers changed gradually from the beads to the uniform structure with increasing concentration of polymers (PVA/chitosan). Zong et al. (2002) also demonstrated that up to a certain point increasing concentration

and viscosity of solution favored the formation of homogenous nanofibers. Viscosity of solutions affects not only the fiber formation but also the diameter of produced fibers. In general, as the higher viscosity discourages bending, and the jet path reduces. Reduced jet path resulted in less stretching of the solution so fiber diameter increases. (Ramakrishna et al., 2005). Demir, Yilgor, Yilgor, & Erman (2002) emphasized that concentration of polymer and the corresponding viscosity of polymer solution were one of the most effective parameters on fiber morphology. It was concluded that fiber diameter was proportional to the cube of the concentration of polymer. In the study of Ki et al. (2005), the increase in diameter of gelatin nanofibers was associated with the increased viscosity that was directly proportional with concentration of gelatin.

1.1.2.1.2. Electrical conductivity of solutions

Solution conductivity is mainly affected by the polymer and the solvent type. In general, the electrical conductivity of solvents is low due to having few free ions. The electrical conductivity of solutions can be increased by the addition of mineral salts, mineral and carboxylic acids. The general rule about electrospinning is that when the solution is not fully stretched, bead formation is observed. With solution having lower conductivity, the surface of droplet has no charge to form a Taylor cone, so electrospinning does not take place. If the electrical charges carried by the jet increase, under the electrical field the jet is exposed to higher elongation forces. Therefore, the possibility of obtaining uniform nanofibers increases (Ramakrishna et al., 2005a). In the study of Zong et al. (2002), it was found that the morphology of fibers changed from the beaded structure to uniform structure when the ionic salt added solutions were used, which was related with the increase in electrical conductivity of the solutions. Similarly, in the study of Choi et al. (2004), with the addition of small amount of benzyl triethylammonium chloride to poly(3-hydroxybutyrate-co-3-hydroxyvalerate) (PHBV) solution, the structure of nanofibers changed from bended shaped to straight shape. Increasing electrical conductivity of solutions affects not only production of homogenous nanofibers but also fiber diameter. Higher electrical conductivity leads to substantially smaller fiber diameter (Sun et al., 2014). In the study

of C. Zhang, Yuan, Wu, Han, & Sheng (2004), the diameters of nanofibers decreased from 214 nm to 159 nm with increasing NaCl content from 0.05% to 0.2% due to higher net charge density on jet. A number of research groups have studied the effect of electrical conductivity of solutions on the diameter of the nanofiber. Son, Youk, Lee, & Park (2004) reported that adding poly (allylamine hydrochloride) and poly (acrylic acid sodium salt) led to decrease in average diameters of electrospun PEO fibers. Similarly, in the study of Jia et al. (2007), it was observed that increasing chitosan content resulted in increase in electrical conductivity of solutions and decrease in average diameter of chitosan nanofibers. In general, higher electrical conductivity promotes to formation of uniform nanofibers but after a certain point, when solutions have very high charges, the electrostatic force generated by the applied electric field could be insufficient to form a Taylor cone and prevents initiation of electrospinning process (Haider, Haider, & Kang, 2018). That's why, similar to viscosity, an optimum electrical conductivity should be arranged to produce homogenous nanofibers.

1.1.2.1.3. Surface tension of solutions

Surface tension plays critical role in the electrospinning process and fiber morphology. To initiate electrospinning, the electrostatic forces must overcome the surface tension of solutions. Thus, the charged jet of polymer solution can be ejected from the tip of the Taylor cone. Therefore, high surface tension of solution could be the reason of instability of the jet. The effect of viscosity of solutions on fiber morphology is significantly correlated with surface tension. Especially, when the solutions have lower viscosity and high amount of free solvent molecules, under the influence of surface tension, solvent molecules congregate as spherical droplets. This favors bead formation during electrospinning. As the viscosity of solutions increases, polymer-solvent interaction dominates the interaction between solvent molecules and while stretching of solutions, it reduces the tendency of solvent molecules coming together by surface tension (Ramakrishna et al., 2005a). Moreover, decreasing surface tension of solutions minimizes the needed electric field to overcome surface tension during

electrospinning (Haghi & Akbari, 2007). Surface tension of solution strongly depends on the type of solvent that used for preparing polymer solutions. In the study of Yang et al. (2004), poly(vinyl pyrrolidone) (PVP) was dissolved in different solvents (dimethylformamide (DMF), dichloromethane (DCM) and ethanol) and solutions having different surface tension values were obtained. Thus, the effect of surface tension on fiber morphology was examined, and it was found that solutions prepared by using ethanol had lower surface tension and smooth nanofibers were obtained. On the contrary, bead formation was observed with polymer -DMF solutions having higher surface tension. In another study, mixing ethanol to water promoted formation of smooth nanofibers by reducing surface tension of polymer solutions (Fong, Chun, & Reneker, 1999). Another way to decrease surface tension is adding surfactant to solutions. Abutaleb, Lolla, Aljuhani, & Shin (2017) added the surfactants triton X-100 and hexadecyltrimethylammonium bromide (HTAB) to polyetherimide solutions and it was reported that bead formation gradually decreased with increasing surfactant amount. In the study of Zheng et al. (2014), the effect of surfactant on fiber morphology was studied and it was stated that surfactant addition enhanced homogenous nanofiber formation with lower fiber diameter.

1.1.2.2. Processing parameters

1.1.2.2.1. Applied voltage

In electrospinning process, applied voltage is the most significant processing parameter because it directly affects the electrostatic interaction forces in the solution. A critical value of applied voltage is needed to counteract the surface tension of solutions and so the polymer jet could be ejected from the Taylor cone (Anu Bhushani & Anandharamakrishnan, 2014). This critical voltage value changes from polymer to polymer. To initiate electrospinning, the specific external electric field must be provided. However, after a certain point, higher applied voltage results in bead formation. The effect of applied voltage magnitude was examined in detail in the study of Deitzel, Kleinmeyer, Harris, & Beck Tan (2001) by keeping the other parameters

(solution properties and processing conditions) constant. It was demonstrated that above critical voltage, the dependence of fiber morphology on voltage was correlated with droplet shape. When the voltage in the optimum range was applied, jet ejected from a cone at the bottom of the droplet is in agreement with an angle of Taylor cone theoretical prediction. On the other hand, under the effect of higher voltage, instead of droplet formation, jet appeared directly from the tip of syringe. It was observed that the fibers produced under these conditions had highly beaded structure. That's why, to obtain bead free nanofibers, adjustment of optimum voltage is necessary. In the study of Meechaisue, Dubin, Supaphol, Hoven, & Kohn (2006) strength below 20 kV was applied, fibers with beads were obtained from 15% (w/v) poly (DTE carbonate) solution. However, in the study of Sill & Von Recum (2008), it was stated that as the applied voltage was increased, the volume of the drop decreased until the Taylor cone formation and the jet was ejected from capillary instead of droplet that lead to an increase in bead defects. As can be understood from the studies, either weak or strong electric fields result in bead formation and the necessary optimal range of electric field for homogenous nanofiber formation depends on polymer solution characteristics. Applied voltage affects not only fiber formation but also fiber diameter significantly. As the electric field strength increases, greater volume of solution is ejected resulting in larger fiber diameter (Geoffrey Mitchell, 2015). There are several studies that confirms this theory. Torres-Giner, Ocio, & Lagaron, (2009) observed that fiber diameter of zein nanofibers increased gradually by increasing electric field due to drawing more material out of the syringe. In the study of Ramji & Shah (2014), when applied voltage was varied from 15 to 27kV, the average diameter increased 20 nm to 60 nm. Similar studies demonstrated the increase in fiber diameter with higher applied voltage (Neo, Ray, Easteal, Nikolaidis, & Quek, 2012; Coles et al., 2010). On the contrary, Lee et al. (2007) found that higher voltage lead to the reduction in the fiber diameter due to faster acceleration and more stretching of jet. The same result was verified by the study of Zhao, Wu, Wang, & Huang (2004) in which average fiber diameter decreased with increasing applied voltage. The effect of voltage is not only on the morphology of fibers but also on the crystallinity of the polymer fiber. The

crystallinity of nanofibers is affected by the degree of ordering and the time of crystallization during the elongation of jet. The electrostatic field induces in more ordered polymer molecules, so the crystallinity of the fibers is higher. In other words, the crystallinity of fibers is increased with increasing voltage. However, the acceleration of nanofiber formation increases with increased voltage which reduces the time of jet flight from anode to collector. Thus, the time of crystallization is shortened, and it is not sufficient to orientate polymer molecules, so the degree of crystallinity is decreased. When these two effects are combined, it is concluded that in sufficient elongation time, the crystallinity of the fiber is improved with higher voltage (Ramakrishna et al., 2005a). In the study of Zhao et al. (2004) while up to 50 kV, the crystallinity of electrospun ethyl–cyanoethyl cellulose nanofibers increased, above 50 kV, the crystallinity of the fibers decreased.

Although DC voltage supply has been commonly used in electrospinning, AC supply can be an alternative for electrospinning. With an AC supply, the charging of the solutions is faster and higher stretching of the jet causes smaller fiber diameter. The other advantage of AC voltage is that a thicker layer of electrospun fiber can be collected even in insulating collection plate due to fewer accumulation of like-charges on the fiber (Kessick & Tepper, 2004).

1.1.2.2.2. Flow Rate

During electrospinning, to hold a stable droplet at the tip of the needle, the polymer solution must be fed with enough pressure which can be done by syringe pump or gravity feed. To control the flow rate, syringe pump is mostly preferred (Geoffrey R Mitchell, 2015). The flow rate determines the amount of solution for electrospinning process and the jet velocity. To obtain nanofibers, the solvent must be evaporated so lower feed rate is desirable to get enough time for evaporation. The critical flow rate for fabrication of homogenous nanofibers depends on the polymer system. In the study of Yuan, Zhang, Dong, & Sheng (2004), decreasing flow rate from 0.66 ml/h to 0.40 ml/h resulted in changing fiber morphology from beaded to homogenous ones.

Megelski, Stephens, Chase, & Rabolt (2002) observed bead formation from polystyrene solution with flow rate of 0.1 mL/min due to non- evaporation of the solvent and low stretching of the solution. However, when the flow rate was decreased to 0.07 mL/min, homogenous nanofibers were produced. Flow rate also affects the fiber diameter. When greater volume of solution was drawn, the stretching of solution resulted in an increase in diameter of the nanofibers with increasing flow rate (Z. Li & Wang, 2013) . The same effect of higher flow rate was observed in the study of Megelski et al. (2002).

1.1.2.2.3. Tip to collector distance

The distance between tip and the collector is the other important process parameter that controls the fiber morphology and diameters. Tip to collector distance directly affects jet instability, deposition time and evaporation rate. Insufficient distance between needle tip and collector results in inadequate drying of fibers. In that condition, drying time is not enough to evaporate the solvent and partially dried fibers are deposited on the collector and instead of homogenous nanofibers, densely packed structure is obtained. Therefore, optimum distance between the tip and collector should be arranged to encourage evaporation of solvent from the nanofibers (Ghorani & Tucker, 2015). Bead formation is attributed to field strength between the needle tip and the collector which can be increased by decreasing distance. As mentioned before, with the higher field strength, jet instability promotes beads formation (Ramakrishna et al., 2005). The relationship between field strength and tip to collector distance is associated with fiber diameter, too. In the study of Y. Lin et al. (2008), the average fiber diameter reached minimum value as tip to collector distance increased but after that the increase in distance resulted in higher average diameter. In another study of Ying Yang, Zhidong Jia, Qiang Li, & Zhicheng Guan (2006), it was observed that when the ambient humidity was low, longer distance reduced the fiber diameter due to higher rate of evaporation. However, at higher humidity value, increased distance can not increase evaporation rate.

1.1.2.2.4. Types of collector

In order to initiate electrospinning process, there must be an electric field between collector and tip of needle. Therefore, the collector is made of conductive material and electrically grounded. In general, aluminum foil is covered to the collector to increase conductivity. The other collector used for electrospinning are conductive paper, wire mesh, pin, conductive cloth and parallel bar (Bhardwaj & Kundu, 2010). When the non-conductive collector is used, fewer fibers deposit and collected fibers have lower packing density due to repulsive forces of the accumulated charges on the collector. On the contrary, on the conducting collector, charges on the fibers are dissipated so more fibers are collected and fibers can pack closely together (Ramakrishna et al., 2005a). Different fiber morphology is observed by using different types of collectors. In the study of X. Wang et al. (2005), aluminum foil and wire screen were used for production of hyaluronic acid nanofibers by blowing-assisted electrospinning. It is difficult to separate nanofiber membrane from the aluminum collector. However, aluminum foil collector having larger conductive represented better performance than the wire screen collector. Bead formation was observed in fibers collected on wire screen due to having less conductive area. Different types of collectors are used to align electrospun nanofibers. Cylinder collector with high rotating speed, thin wheel with sharp edge, frame collector have been commonly used for fiber alignment (Z.-M. Huang et al., 2003).

1.1.2.3. Ambient parameters

In addition to solution properties and process parameters, ambient parameters including humidity and temperature also affect the electrospinning. Humidity of environment may affect solidification of charged jet. At high humidity, evaporation rate of solvent could be lower, and water could condense on the surface of fiber which may influence fiber morphology. In the study of Pelipenko, Kristl, Jankovi, Baumgartner, & Kocbek (2013), the effect of humidity on nanofiber diameter was investigated. Nanofibers having beaded structure was observed when electrospinning

was performed at higher relative humidity value (70%). However, the diameter of PVA nanofibers decreased from 667 nm to 161 nm when humidity was increased 4% to 60%. Moreover, it was reported the same humidity increase resulted in reduction of diameter of PEO nanofibers from 252 nm to 75 nm. Similar decrease in PEO fiber diameter was also observed in the study of Park & Lee (2010). It was also stated that humidity induced formation of porous nanofibers and at 60% relative humidity porous polystyrene fibers were obtained. Moreover, in the study of De Vrieze et al. (2009), at higher humidity values up to a certain point, poly(vinylpyrrolidone) fibers were thinner but after that nanofibers were stuck each other.

Temperature is another ambient parameter that affect the fiber morphology. Higher operation temperature could result higher rate of evaporation of solvent and decrease in viscosity of solutions. De Vrieze et al. (2009) found that higher temperature led to lower fiber diameter. Similarly, in the study of Mit-Uppatham, Nithitanakul, & Supaphol (2004), the effect of temperature on the morphology of electrospun polyamide-6 fibers and it was reported that temperature ranging from 25 to 60 °C attributed to decrease in fiber diameter due to inverse relationship between viscosity and temperature.

1.1.3. Applications of electrospinning

Since electrospun nanofibers have large surface to volume ratio, high porosity and superior mechanical properties, electrospinning has received increased attention to produce nanofibers. Although electrospinning is an old method to produce fibers, in recent years, it has been widely used in tissue engineering scaffolds (W.-J. Li, Laurencin, Catterson, Tuan, & Ko, 2002; F. Yang et al., 2004), wound healing (Katti, Robinson, Ko, & Laurencin, 2004; Rho et al., 2006), drug delivery (Jiang, Fang, Hsiao, Chu, & Chen, 2004; Zeng et al., 2003), filtration (Kattamuri et al., 2005; Lala et al., 2007), biosensors (Patel, Li, Yuan, & Wei, 2006; Wu & Yin, 2013), immobilization of enzymes (Ren et al., 2006; Xu, Sheardown, & Hoare, 2016) and in the textile industry (Deitzel et al., 2001; Lee, 2009). Recently, researchers have begun

to investigate the applicability of electrospinning for food industry such as enzyme immobilization, encapsulation of bioactive compounds and packaging.

1.1.3.1. Enzyme immobilization

Enzymes are natural catalysts, but their usage is limited due to their high cost, their sensitivity to temperature and pH and their difficulty in recovery from chemical reaction. To overcome these limitations, the immobilization of enzymes is the most common way. The aim of immobilization is to enhance enzyme stability to environmental changes (pH, temperature etc.). Between immobilization methods, electrospinning differentiates itself by being relatively simple and versatile method to fabricate enzyme immobilized nanofibers. Two different approaches have been followed to immobilize enzyme through electrospun nanofibers: adsorption of enzyme on the surface of nanofibers and encapsulation of enzyme into the nanofibers (Wen, Zong, Linhardt, Feng, & Wu, 2017). The porous structure of electrospun nanofibers can reduce the resistance to diffusion of substrates and can significantly increase the catalyzing ability of enzyme immobilized membranes due to having large surface area (Hong Wang, Shao, & Hu, 2006). Immobilized enzymes have been widely used in food industry for biosensor and bioactive food packaging. Glucose oxidase (GOD) have been commonly used to produce glucose biosensors and there are lots of studies that examined immobilization of GOD by electrospinning. In the study of Ren et al. (2006), GOD was successfully immobilized into PVA electrospun nanofibers and it was used to fabricate biosensor with lower detection limit for detection of the glucose in medical diagnosis. Sapountzi et al. (2017) immobilized GOD into poly(vinyl alcohol)/poly(ethyleneimine) nanofibers on the surface of gold electron and it was stated that production of novel glucose biosensor with good stability and low limit of detection achieved. Similarly, to design glucose biosensor, GOD was immobilized into chitosan and PVA biocomposite nanofibers with electrospinning. Horseradish peroxidase (HRP) is the other common enzyme that was immobilized to be used in food industry. Teepoo, Dawan, & Barnthip (2017) produced biosensor by immobilization of HRP through chitosan-gelatin electrospun nanofibers to detect

hydrogen peroxide. In other studies HRP was immobilized with glutaraldehyde vapor into electrospun polyvinyl alcohol/bovine serum albumin biocomposites (Fazel et al., 2016) and PVA nanofibers (Rodríguez-deLuna et al., 2017). Tyrosinase and laccase are employed widely for detection of phenolic compounds. For electrochemical detection of phenols, Oriero, Gyan, Bolshaw, Cheng, & Aston (2015) fabricated a fibrous electrode material of silica–PVA with immobilized tyrosinase enzyme onto an indium–tin oxide (ITO)-coated glass substrate. The produced biosensors were suggested due to having electrode response times, sensitivities and detection limits within feasible ranges to be replacements of more expensive techniques for phenolic sensing. Acta, Arecchi, Scampicchio, Drusch, & Mannino (2010) and Oriero, Jabal, Deobald, Weakley, & Aston (2011) studied the application of electrospinning as an immobilization technique to produce tyrosinase based biosensor for detection of phenolics. Similarly, Liu, Niu, Yin, & Jiang (2011) developed laccase based on biosensors for determination of phenolic compounds and electrospun PVA nanofibers was used as an matrix for enzyme immobilization. In numerous studies, the potential of electrospinning technique for immobilization of different enzymes were studied such as lipase (Xie & Hsieh, 2003), cellulase (Wu, Yuan, & Sheng, 2005), acetylcholinesterase (El-Moghazy et al., 2016), and β -Galactosidase (El-Aassar, 2013).

1.1.3.2. Encapsulation of bioactive compounds

Encapsulation is the entrapment of bioactive compounds such as antioxidants, vitamins, fatty acids etc. within a wall material. Encapsulation not only masks undesirable taste and odor but also improves the stability against environmental conditions (e.g., light, temperature, moisture, oxygen), bioavailability and controlled release properties of bioactive ingredients (de Vos, Faas, Spasojevic, & Sikkema, 2010). Moreover, the encapsulation matrices should be generally recognized as safe (GRAS) and natural biopolymers (proteins and polysaccharides) have been commonly used for encapsulation. There are lots of methods for encapsulation of compounds which are spray drying, freeze drying, emulsification, coacervation etc. (Anu

Bhushani & Anandharamakrishnan, 2014). Among them spray drying is one of the oldest and widely used method in food industry. Spray drying is an economical and flexible method and during spray drying, bioactive compounds are dispersed in carrier solution which is atomized into droplets with evaporation of solvent. Working temperatures that are used in spray drying process may cause heat degradation of active agents so the application of spray drying as encapsulation method is not suitable for thermally labile compounds (Drosou, Krokida, & Biliaderis, 2017). Therefore, in recent years, electrospinning has sparked a progressive interest in encapsulation of bioactive compounds. In general, studies demonstrated that electrospinning has been a promising method to encapsulate bioactive compounds due to the several reasons. It can produce nanofibers at room temperature, so deterioration of the active compound can be avoided. Moreover, it is possible to produce capsules at nano-sizes and the release of active compounds can be controlled by changing electrospinning conditions. In addition, limited surface area slows down the release of active substances. As the size of fibers goes from micron to nanosize, it offers very large surface area for controlled release (Anu Bhushani & Anandharamakrishnan, 2014). To encapsulate several antioxidants and antimicrobial agents, electrospinning technology has been successfully applied through the optimization of solution and processing conditions. Gallic acid is one of the antioxidant agent that is encapsulated by electrospinning. In the study of Neo et al. (2013), gallic acid at different ratios was successfully encapsulated in the zein nanofibers by electrospinning. It was found that the incorporated gallic acid has retained its antioxidant activity. Gallic acid was also encapsulated into cellulose acetate (Phiriyawirut & Phaechamud, 2012) and poly(L-lactic acid) (Aytac, Kusku, Durgun, & Uyar, 2016; Chuysinuan, Chimnoi, Techasakul, & Supaphol, 2009) nanofibers by electrospinning method. β -carotene, a colorant and antioxidant molecule widely used in the food industry and the encapsulation of β -carotene into zein matrices was achieved by (Fernandez, Torres-Giner, & Lagaron, 2009) with using electrospinning. Since β -carotene is a light sensitive antioxidant molecule, stability test by UV-Vis irradiation was conducted. It was concluded that encapsulation of β -carotene in electrospun nanofiber significantly increased light

stability and protected against oxidation when exposed to UV–vis irradiation. Quercetin is another antioxidant agent showing fast photodegradation and Aytac, Kusku, Durgun, & Uyar (2016b) found that encapsulated quercetin into polyacrylic acid/ β -cyclodextrin inclusion complex electrospun nanofibers represented high antioxidant activity and photostability. Similarly, in the study of Aytac & Uyar (2016), electrospun polycaprolactone (PCL) nanofibers which encapsulated α -tocopherol (vitamin E) / β -cyclodextrin inclusion complex showed high oxidative stability and strong photostability. Table 1 represents examples of bioactive compounds encapsulated into different biopolymer-based matrices by electrospinning.

Table 1.1 *Examples of bioactive compounds encapsulated into different biopolymer-based matrices by electrospinning*

Bioactive compound	Polymer matrices	Polymer concentration	Solvent	References
Quercetin and ferulic acid	Amaranth protein isolate / pullulan	80:20 w/w	95% formic acid	(Aceituno-Medina, Mendoza, Rodríguez, Lagaron, & López-Rubio, 2014)
Curcumin	Gelatin (type B)	25% (w/v) gelatin	40% acetic aqueous solution	(Deng, Kang, Liu, Feng, & Zhang, 2017)
Vanillin	Polyvinyl alcohol/cyclodextrin inclusion complex	5% (w/w) PVA/32% (w/w) cyclodextrin	Water	(Kayaci & Uyar, 2012)
Folic acid	Amaranth protein isolate (API):pullulan	80:20 w/w	95% formic acid	(Aceituno-Medina, María Lagaron, & Lopez-Rubio, 2015)
Fish oil	Zein	20% (w/w)	Ethanol	(Moomand & Lim, 2014)
Perillaldehyde	Pullulan and β -cyclodextrin	20% (w/w) pullulan and 25% (w/w) β -cyclodextrin with respect to pullulan	Water	(Mascheroni et al., 2013)
Cinnamaldehyde	Chitosan/PEO	5%/5% (w/v)	50% acetic acid solution	(Rieger, Birch, & Schiffman, 2016)

Table 1.1 *Examples of bioactive compounds encapsulated into different biopolymer-based matrices by electrospinning (continued)*

Orange essential oil	Gelatin type A	15% w/w gelatin	Water	(Tavassoli-Kafrani, Goli, & Fathi, 2018)
Eugenol	Cyclodextrin (CD) derivatives (HP- β -CD, HP- γ -CD, and M- β -CD)	highly concentrated aqueous CD solutions (160% (w/v))	Water	(Celebioglu, Yildiz, & Uyar, 2018)
Allyl isothiocyanate	Soy protein isolate/poly(ethylene oxide)	15%/0.6% (w/w)	Water	(Vega-Lugo & Lim, 2009)

1.1.3.3. Food packaging

Packaging has a significant role in protecting foods from environmental factors during distribution and storage. The increase of petroleum-based polymers usage as packaging materials is one of the important threats for environmental pollution, global economy and world's climate change. Therefore, currently food industry has tried to replace the petroleum-based polymers by biopolymers obtained from natural resources to reduce plastic waste. The bio-based polymers can be derived from agricultural products (corn, potato, soybean), microorganisms or algae. Moreover, natural biopolymers are macromolecules found in nature which are proteins (e.g. gelatin, zein, collagen), polysaccharides (e.g. starch, chitosan, cellulose) and lipids (Hottle, Bilec, & Landis, 2013). In addition to tendency to the usage of biopolymers as packaging materials, in recent years, the use of electrospinning has taken attention in food packaging industry. Among the production methods (phase separation, self-assembly, extrusion, template synthesis), electrospinning generates a special interest in biomaterial based packaging materials due to being simple, cost effective, versatile method and producing large surface/volume nanofibers (Soares, Siqueira, Prabhakaram, & Ramakrishna, 2018). Although some biopolymers such as proteins are good oxygen barriers, they are not water resistant or some of them are vice versa. Moreover, when most of biopolymers are used as packaging material, rigidity is the common problem, so plasticizers are needed. There is no material showing all the

desired mechanical and barrier properties for packaging, so using multilayer systems have been advantageous because of combining properties of each biopolymers. However, during multilayer film development from incompatible materials, adhesion of layers is a common problem and a tie layer is needed for adhesion. In order to overcome this problem, using electrospinning can offer a good approach to produce multilayer films. In recent years, some of researches have investigated the effect of electrospun nanolayer on multilayer packaging systems. Fabra, Lopez-Rubio, & Lagaron (2013) produced multilayer film composed of polyhydroxybutyrate-co-valerate 12% (PHBV12) films and nanostructured electrospun interlayers of zein. Although the addition of electrospun zein layer did not result significant changes in in mechanical and optical film properties, oxygen barrier properties of multilayer films improved. In addition, incorporation of zein interlayer decreased water vapor permeability and D-Limonene permeability which used as a standard system to test aroma barrier. In the further study, Fabra, Lopez-rubio, & Lagaron (2014) incorporated electrospun zein mat between layers of polyhydroxyalkanoate (PHA) materials (a PHB homopolymer and a PHBV5 copolymer with 5% valerate content) and as a reference into a poly-lactide (PLA) and a polyethylene terephthalate (PET). It was stated that while the outer layer made of PHB based materials increased the water vapor permeability, the zein interlayer improved the oxygen and aroma barrier properties of multilayer films. Moreover, the added zein interlayer resulted in decrease in both limonene and oxygen permeability but did not decrease water vapor permeability. It was concluded that since the water vapor and oxygen barrier properties of zein incorporated PHA multilayer was similar to PET, using them instead of PET being petroleum material could be a good solution for plastic waste. In another study of Fabra, López-Rubio, & Lagaron (2014), examined the effect of addition of whey protein isolate, pullulan, zein blends with whey protein isolate and pullulan to polyhydroxyalkanoates material (PHBV3) on barrier properties of multilayer films. Due to having beaded structure, whey protein nanofibers did not improve oxygen and water barrier properties of multilayer films. However, zein and pullulan electrospun nanofiber addition provided a significant improvement of barrier properties of

multilayer films. Thus, zein and pullulan incorporated PHB multilayer system was suggested to be used as biobased food packaging material. To offer as an alternative to development of biopolymer packaging materials, wheat gluten films were covered with more hydrophobic electrospun polyhydroxyalkanoate layers (polyhydroxybutyrate (PHB) and a polyhydroxybutyrate-co- valerate copolymer with 3 % valerate content (PHBV3)(María José Fabra, López-Rubio, & Lagaron, 2015). Three-layer films prepared with PHBV3 had the lowest water vapor and oxygen permeability values. Biopolyester electrospun layer addition improved the mechanical properties of plasticized wheat gluten films, especially Young's modulus. In the continued study, the effect of film-processing conditions, relative humidity and ageing on wheat gluten films coated with electrospun polyhydroxyalkanoate was investigated (Maria Jose Fabra, Lopez-Rubio, & Lagaron, 2015). It was remarked that the improved barrier properties and stretchability of the developed multilayer systems remained over the storage time due to the excellent adhesion between layers provided by electrospinning process.

Active packaging is the name given to the packaging method. In addition to providing all the benefits of standard packaging, it also features the modification of packaging conditions throughout the whole shelf life with the purpose of increasing shelf life or ensuring product quality. By regarding to the aim of usage, oxygen scavengers, carbon dioxide emitters/absorbers, moisture absorbers, ethylene absorbers, time-temperature indicators, antioxidants and antimicrobial agents can be incorporated to packages (Ozdemir & Floros, 2008). Electrospinning is suitable to encapsulate heat sensitive compounds and electrospun nanofibers have large area to volume ratio, and higher release rate, so electrospinning has been suggested as promising method to produce active packaging material (Vega-Lugo & Lim, 2009). Antimicrobial packaging, a type of active packaging, involves the release of antimicrobial agents from packaging material to food surface and inhibits or retards microbial growth during storage. Numerous studies have been conducted to produce antimicrobial packaging nanofibers with optimizing electrospinning parameters and to examine its

applicability. Chitosan is one of the favorite antimicrobial packaging biomaterials due to its bactericide property. In the study of Torres-Giner, Ocio, & Lagaron (2009a), the inhibition effect of chitosan/zein blend nanofibers against to *Staphylococcus aureus* (< 1 Log CFU/mL) was reported. (Y. Wang, Zhang, Zhang, & Li, 2012) fabricated PVA nanofibers containing chitosan combined with nano-ZnO to increase its antimicrobial activity and significant synergistic antimicrobial efficiency on *E. coli* and *C. albicans* was observed. A great interest has gone to essential oils to be used as antimicrobial agent. In a recent study, cinnamon essential oil was incorporated in polyvinyl alcohol/ β -cyclodextrin electrospun nanofibers and the antimicrobial effect of electrospun films and casting films having the same composition were compared (Wen et al., 2016). It was found that electrospun films showed greater antimicrobial activity against *E. coli* and *S. aureus* than casting films and nano to sub-micron structure of film promoted the release of antimicrobial agent. In addition, to evaluate the efficiency of cinnamon loaded both electrospun and casting films, they were applied in strawberry preservation. After conducting weight loss, firmness and sensory analysis, it was indicated that strawberries packed with nanofilm had longer shelf-life than the control and those packed with casting film. It was also highlighted that nanofibers containing cinnamon maintained sensorial properties of strawberries during storage. The same research group reported the antimicrobial activity of cinnamon essential oil/ β -cyclodextrin inclusion complex (CEO/ β -CD-IC) into polylactic acid (PLA) nanofibers against both Gram-positive and Gram-negative bacteria (Wen et al., 2016). In this study, the PLA/CEO/ β -CD nanofilm was applied in the preservation of pork to evaluate its efficacy in food antimicrobial packaging and it was stated that nanofilms could effectively prolong the shelf-life of pork. Carvacrol is a major component of oregano and thyme oil and in the study of (Altan, Aytac, & Uyar, 2018a), highly volatile carvacrol was successfully encapsulated in electrospun zein and PLA fibers. It was demonstrated that nanofibers containing 20% carvacrol inhibited 99.6% and 91.3% of the growth of mold and yeast during storage of bread samples, respectively and usage of fabricated nanofibers were suggested to be used as antimicrobial packaging material. In addition to antimicrobial active package material

fabrication, electrospinning has been applied to produce antioxidant packaging materials. In the study of Neo et al. (2013) the applicability of gallic acid encapsulated zein electrospun nanofibers was evaluated as a potential active food packaging material. Approximately 90% gallic acid release was observed since electrospun nanofibers had large surface area that increased the mass transfer rate of gallic acid and the diffusion through nanofibers. In addition, it was also found that electrospun nanofibers remained thermally and chemically stable after 60 days and showed antimicrobial activity against bacteria and yeast cells. In this respect, gallic acid loaded electrospun zein nanofibers were suggested to be used as active packaging materials. In the study of Maria Jose Fabra, Lopez-Rubio, & Lagaron (2016), α -tocopherol was encapsulated in using different electrospun hydrocolloid matrices (whey protein isolate, zein and soy protein isolate). The one side of wheat gluten film was covered by these antioxidant loaded electrospun nanofibers. The encapsulation efficiency was found as up to 95% and after applying industrial sterilization process more than 70-85% α -tocopherol protection was observed. Therefore, it was stated that electrospinning is promising technology for producing active multilayer packaging material.

1.2. Objectives of the study

In recent years, electrospinning has gained more attention since it is simple, versatile and cost-effective method to produce nanofibers. Electrospun nanofibers have high surface area to volume ratio, light-weight and nanoporous structure. Although synthetic polymers have been widely used for the production of nanofiber, biopolymers derived from agricultural raw materials have been great interest in electrospinning research area because they are nontoxic, edible, digestible, biocompatible, biodegradable and renewable. However, fabrication of nanofibers from biopolymers is more difficult than synthetic polymers. To overcome the poor electrospinnability of biopolymers, mixing them with carrier synthetic polymers can be a good solution. Polyethyleneoxide (PEO) is one of the most common carrier polymers because of being nontoxic, biocompatible, water soluble and biodegradable.

Electrospun nanofibers have been attracted great interest for food packaging applications. Especially for active packaging material production, electrospinning is an efficient method to encapsulate bioactive compounds. Among biopolymers, Hydroxypropyl methylcellulose (HPMC) is a common cellulose derivative that can be used as film forming material due to its low flavor and aroma properties, high solubility in water and good barrier properties.

Legume flours which are composed of both protein and carbohydrate, combine the advantages of both of them and show good filming properties (e.g. lower water vapor permeability, higher tensile strength etc.). Therefore, lentil and pea flours are promising biopolymers to be used as packaging material. To produce active packaging material, gallic acid, which shows strong antioxidant activity, is a good choice as bioactive compound.

Although it is common to produce biopolymer based films by casting method, there is still significant literature gap on the production of biopolymer based electrospun nanofibers to be used as active packaging materials. In literature, there is no study about the applicability of legume flours and HPMC based active packaging materials produced by electrospinning as active packaging material. Moreover, the effect of gallic acid containing nanofibers on oxidation of foods has not been studied yet.

The main aim of this study is to produce biopolymer based (HPMC, lentil and pea flour) and gallic acid loaded active packaging materials by means of electrospinning. The effect of solution properties on the nanofiber formation and encapsulation efficiency was examined and the nanofibers were characterized in terms of thermal properties, water vapor permeability and chemical interaction. Moreover, the use of gallic acid loaded nanofibers on prevention of oxidation of walnuts during storage was investigated. In addition to active packaging material, the usage of electrospinning to produce PLA/nanofibers bilayer sheets with soy protein and HPMC was studied and the optical, thermal and permeability characteristics of sheets were analyzed.

CHAPTER 2

MATERIALS AND METHODS

2.1. Materials

HPMC which had a molecular weight of 86 kDa and PEO with molecular weight of 900 kDa were purchased from Sigma-Aldrich. Lentil flour containing 22.2% protein, 1.7% fat, 8.9% moisture and 3% ash was obtained from Smart Chemical Trading Co. Inc. (Turkey). Pea flour containing (weight basis) 55± 5% carbohydrate, 22± 2% protein, 2±2% fat, 7–10% moisture, 3±1% ash and 12±2% dietary fiber and soy protein isolate (95%) purchased from Molar Chemical Materials Trading Co. Inc. (Turkey). Polyoxyethylene sorbitan monooleate (Tween 80) (density: 1.064 g/cm³, viscosity: 400 - 620 cp at 25°C) as a surfactant and gallic acid with molar mass of 170.12 g/mol were bought from Merck (Darmstadt, Germany). PLA granules (NatureWorks LLC Ingeo™ 2003D) were provided from NatureWorks (MN, USA). PEG 400 was provided from Merck (Germany). Walnuts were bought from a local market in Turkey. Chloroform, acetic acid, potassium iodide (KI), 2-Thiobarbituric acid (2-TBA reagent), butanol, p-anisidine were purchased from Sigma-Aldrich.

2.2. Methods

2.2.1. Preparation of electrospinning solutions

2.2.1.1. HPMC solutions

PEO (1%, 1.5%, 2% w/v) was dissolved in water with magnetic stirrer (MaxTir 500, Daihan Scientific, Seoul, Korea) for 24 h. Then, different amount of HPMC (1%, 1.5%, 2%, 3%, 4%, 4.5%, 5% w/v) was added to PEO solutions and mixed with a high-speed homogenizer (IKA T25 Digital Ultra-Turrax, Staufen, Germany) at 9000 rpm. The surfactant (Tween 80) with a concentration of 2% (w/v) was added to the

solutions. The solution containing various combination concentrations of PEO and HPMC were stirred at room temperature with magnetic stirrer (MaxTir 500, Daihan Scientific, Seoul, Korea) for 18 hours to obtain homogeneous solutions. Properties of solutions having different amount of HPMC and PEO (HPMC/PEO (w/w); 4/2, 3/2, 2/2, 1/2, 4.5/1.5, 3/1.5, 2/1.5, 1.5/1.5, 5/1, 4/1, 2/1, 1/1) were determined and then all of them was subjected to electrospinning process.

2.2.1.2. HPMC/gallic acid solutions

PEO was dissolved in water with magnetic stirrer (MaxTir 500, Daihan Scientific, Seoul, Korea) for 24 hours to obtain 1% (w/v) concentration. Then, HPMC at concentration of 4% (w/v) and the surfactant (Tween 80) at 2% (w/v) were added to solution and mixed with a high-speed homogenizer (IKA T25 Digital Ultra-Turrax, Staufen, Germany) at 9000 rpm for 15 min. The solution was stirred at room temperature with magnetic stirrer (MaxTir 500, Daihan Scientific, Seoul, Korea) for 18 h to obtain homogeneous solutions. The gallic acid (0.1 g/ml) was dissolved in 80% ethanol aqueous solutions (ethanol–water = 4:1 w/w) and added to HPMC/PEO solution by adjusting gallic acid content to be 2%, 5%, and 10% of in solid fibers. The solution containing no gallic acid was defined as control.

2.2.1.3. Lentil flour/gallic acid solutions

PEO (3.5% w/v) was dissolved in water with magnetic stirrer (MaxTir 500, Daihan Scientific, Seoul, Korea) for 24 h. Lentil flour (5.25 w/v) was added to PEO solution and stirred with a high-speed homogenizer (IKA T25 Digital Ultra-Turrax, Staufen, Germany) at 10000 rpm. Then, the solution of pH was adjusted to 10 with 2 M NaOH solution and to pH 1 with HCl. Solutions were heated to 80°C in a water bath and kept 80°C with a magnetic stirrer at 1000 rpm for 2 h. When it was cooled to room temperature, the surfactant (Tween 80) with a concentration of 2% (w/v) was added and stirred with a magnetic stirrer at 750 rpm for 1 hour. The gallic acid (0.1 g/ml) was dissolved in 80% ethanol aqueous solutions (ethanol–water = 4:1 w/w) and added to lentil flour/PEO solution by adjusting gallic acid content to be 10% in solid fibers.

After gallic acid was added to solutions with pH 10, pH of solution decreased to about 3 so pH was again adjusted to pH 10 with 2 M NaOH solution. The solution containing no gallic acid was defined as control.

2.2.1.4. Pea flour/gallic acid solutions

PEO (3.5% w/v) was dissolved in water with magnetic stirrer (MaxTir 500, Daihan Scientific, Seoul, Korea). To complete dissolution, it was stirred about 24 h. Pea flour (5.25 w/v) was added to PEO solution and mixed with a high-speed homogenizer (IKA T25 Digital Ultra-Turrax, Staufen, Germany) at 10000 rpm. Then, pH of the solution was adjusted to 10 with 2 M NaOH solution. Solutions were heated to 80 °C in a water bath and kept at 80 °C with a magnetic stirrer at 1000 rpm for 2 h. After the temperature decreased up to room temperature, the surfactant (Tween 80) with a concentration of 2% (w/v) was added and stirred with a magnetic stirrer at 750 rpm for 1 h. Gallic acid (0.1 g/ml) was dissolved in 80% ethanol aqueous solutions (ethanol–water = 4:1 w/w) and added to pea flour/PEO solution by adjusting gallic acid content to be 5% and 10% in solid fibers. Addition of gallic acid decreased pH of solutions to about 3 so pH of solutions was adjusted to pH 10 with 2 M NaOH solution. The solution containing no gallic acid was used as control.

2.2.1.5. Soy protein solutions

PEO (3.5% w/v) was dissolved in water with magnetic stirrer (MaxTir 500, Daihan Scientific, Seoul, Korea) for 24 h. For soy protein solution, soy protein isolate (3.5 w/v) was added into PEO (3.5% w/v) solution and stirred with a high-speed homogenizer (IKA T25 Digital Ultra-Turrax, Staufen, Germany) at 10000 rpm. pH of the solution was adjusted to 12 with 2 M NaOH solution. Solutions were heated to 80°C in a water bath and kept at that temperature while being mixed with magnetic stirrer at 1000 rpm for 2 h. When it was cooled to room temperature, the surfactant (Tween 80) with a concentration of 2% (w/v) was added and stirred with a magnetic stirrer at 750 rpm for 1 h.

2.2.1.6. Soy Protein/HPMC solutions

HPMC at concentration of 3.5 % (w/v) and Tween 80 at concentration of 2 % (w/v) were added to soy protein 3.5% (w/v) / PEO 3.5% (w/v) solution and mixed with a high-speed homogenizer (IKA T25 Digital Ultra-Turrax, Staufen, Germany) at 10000 rpm. Then, solution was stirred at 750 rpm at room temperature for overnight using a magnetic stirrer to remove the air bubbles.

2.2.2. Characterization of solutions

2.2.2.1. Rheological properties

The rheological behavior of solutions was measured using a controlled strain rheometer (Kinexus dynamic rheometer, Malvern, UK) with a cone (4° cone angle) and plate (40 mm diameter) geometry. The sample was placed, and the edges were carefully trimmed with a spatula. For flow measurement, shear stress values were recorded with respect to shear rates varying between $0.1 \text{ s}^{-1} - 100 \text{ s}^{-1}$. The shear stress (τ) versus shear rate ($\dot{\gamma}$) data was fitted well to the Power Law Equation (1),

$$\tau = k (\dot{\gamma})^n \quad (1)$$

where, τ is the shear stress (Pa), $\dot{\gamma}$ is the shear rate (s^{-1}), k is the consistency index (Pa s^n) and n is the flow behavior index.

In dynamic oscillatory experiments, amplitude tests with varying strains of 0.01% - 100% were applied to samples at a fixed frequency of 1 Hz to measure the linear viscoelastic region of samples. Then, frequency sweep test from 0.1 to 10 Hz were conducted at 0.1% strain rate that was determined from the amplitude test and elastic (G') and loss (G'') modulus values were obtained.

The measurements were carried out in triplicate.

2.2.2.2. Electrical Conductivity

The electrical conductivities of solutions were measured using a conductometer (WTW LF95, Germany) at 25°C in duplicate.

2.2.2.3. Total phenolic content of lentil and pea flour solutions

Total phenolic content (TPC) of solutions was measured by the modified Folin–Ciocalteu method (Luca, Cilek, Hasirci, Sahin, & Sumnu, 2013). Solutions were diluted with 80% ethanol aqueous solution. Diluted sample of 1 mL was mixed with 0.2 N Folin-Ciocalteu reagent. After keeping it in dark place for 5 min, 2 mL of 75 g/L sodium carbonate solution was added to and mixed by vortex. Prepared solutions were stored in dark for 1 h. Then, the absorption of solutions was measured at 760 nm by using a spectrophotometer (UV 2450, Shamadzu, Columbia, USA). Calibration curve was prepared with different gallic acid concentrations and by using calibration curve total phenolic content of solutions were expressed as gallic acid equivalents (GAE) in milligrams per gram dry weight. The measurements were carried out in triplicate.

2.2.3. Electrospinning of solutions

The electrospinning process was carried out using electrospinning device (Nano-Web 103, Mersin, Turkey). Each solution was placed in a 5 mL syringe having metallic needle with 11.53 mm inner diameter and 21 gauge steel needle. The syringe was positioned horizontally on the syringe pump and connected to the positively charged electrode, which was powered by a direct current (DC) high voltage supplier. The solutions were fed through the metal collector which was connected to the negatively charged part and covered by aluminum foil at a flow rate of 0.6-0.8 mL/h. The distance between the collector and needle tip was fixed as 30 cm. The voltage was maintained at 12-15 kV. Experiments were performed at 25° C and 30-40 % relative humidity.

To obtain bilayer electrospun nanofibers and PLA active packaging materials, first of all PLA granules were mixed with PEG 400 (5% w/v) and kept at 40°C for 2 days and dissolved in chloroform at 60°C for 12 h using magnetic stirrer. The air bubbles formed during stirring were removed under vacuum. The PLA solution was manually casted on TLC plate coater (CAMAG, Muttenz, Switzerland) in sizes of 20×20 cm with the final thickness of 31±1 µm. The plates were dried at 75°C for 30 min. The dried PLA

sheets were removed from the plates and stored at 23 ± 2 °C until they were used as matrix for electrospinning. PLA sheets were set onto collector and the solutions were directly fed onto PLA layer which was connected to the negatively charged part.

2.2.4. Characterization of nanofibers

2.2.4.1. Morphological analysis

The morphological characterization of fibers was carried out using Field Emission Scanning Electron Microscopy (FESEM) (JEOL, Japan). Samples were stuck on metal stubs and then coated with gold palladium (10 nm). In order to measure fiber diameters for each sample, at least 100 fibers from each sample were randomly selected from SEM images and their diameters were measured by using Image J software (Maryland, USA).

2.2.4.2. Loading efficiency of gallic acid in HPMC based electrospun fiber

To determine loading efficiency of gallic acid in HPMC based nanofibers, the procedure in the study of Neo et al. (2013) was followed. The spectrum of gallic acid dissolved in 80% ethanol aqueous solution was taken by spectrophotometer at range of 150-800 nm and maximum absorbance was observed at 280 nm. Therefore, the obtained absorbance at 280 nm was directly related to gallic acid amount. Thus, the loading efficiency of gallic acid in the electrospun fibers was determined by first dissolving 10 mg of the electrospun fibers in 25 mL of 80% ethanol aqueous solutions. Then, suitable dilutions were made and the absorption values of solutions at wavelength of 280 nm were measured using a spectrophotometer (UV 2450, Shamadzu, Columbia, USA). The amount of gallic acid was determined against a predetermined gallic acid standard calibration curve. The loading efficiency (LE) of gallic acid was calculated as follows:

$$LE(\%) = \frac{\text{Calculated gallic acid concentration}}{\text{Theoretical gallic acid concentration}} \times 100 \quad (2)$$

The measurements were carried out in triplicate.

2.2.4.3. Loading efficiency of gallic acid in lentil and pea flour based electrospun fiber

To determine TPC of nanofibers, the modified Folin–Ciocalteu method was used (Luca, Cilek, Hasirci, Sahin, & Sumnu, 2013). About 0.1 g nanofiber was dissolved in ethanol-water solution (80:20). The same procedure of lentil and pea flour solutions was applied. The absorption of solutions was measured at 760 nm by using a spectrophotometer (UV 2450, Shamadzu, Columbia, USA). The loading efficiency (LE) of gallic acid was calculated as follows:

$$LE(\%) = \frac{TPC \text{ of gallic acid loaded nanofibers}}{TPC \text{ of gallic acid added solutions}} \times 100 \quad (3)$$

The measurements were carried out in triplicate.

2.2.4.4. Antioxidant capacity of electrospun fiber

The antioxidant activity of electrospun nanofibers was measured with the DPPH (2,2-diphenyl-1-picrylhydrazyl) method described by Luca, Cilek, Hasirci, Sahin, & Sumnu (2013) with some modifications. By considering absorbance value as smaller than 1, nanofibers were dissolved in 50 mL ethanol/water solution (80:20). From DPPH[•] radical solution with 25 ppm (2.5 mg DPPH[•] / 100 mL methanol) 3.9 mL was taken and it was mixed with 100 μ L of methanol. Absorption at 517 nm was measured (A_1) by using UV/VIS spectrophotometer (UV 2450, Shamadzu, Columbia, USA). Solutions of 100 μ l were mixed with 3.9 mL DPPH[•] radical solution and allowed to wait in the dark for 2 hours to complete reaction between DPPH solution and gallic acid. Then the absorptions of samples were measured spectrometrically (A_2). Methanol was used as blank. By using calibration curve, concentrations (C_1 and C_2) were found for A_1 and A_2 , respectively. Then, the antioxidant activities (AA) were calculated according to Eq. (4)

$$AA(mg \text{ DPPH} / g \text{ dry weight}) = \frac{C_1 - C_2}{W_{\text{sample}}} \times V \quad (4)$$

where C_1 is the concentration of DPPH \cdot immediately after the sample (ppm) and DPPH \cdot solution was mixed, C_2 is the concentration of DPPH \cdot 2 h after mixing (ppm), V is the volume of solution in L, W_{sample} is the amount of nanofiber in g.

Moreover, the antioxidant activity (%AA) of the electrospun fibers was expressed as followed Eq. (5)

$$AA (\%) = \frac{(A_{\text{control}} - A_{\text{sample}})}{A_{\text{control}}} \times 100 \quad (5)$$

where A_{control} and A_{sample} are the absorbance values of the DPPH solution without and with the presence of the sample solutions, respectively.

2.2.4.5. Water Vapor Permeability (WVP)

WVP of nanofibers were determined by using ASTM E96 method. Cups with 40 mm internal diameter were filled with distilled water to expose the nanofiber to 100 % RH inside the test cup. Nanofibers were mounted in the cups. The test cups containing nanofibers were placed into pre-equilibrated 20% RH desiccator cabinets. After steady state condition was obtained, cups were weighted at 2 hour intervals. Water vapor transmission rates of nanofibers were determined from the slope of weight loss versus time plots divided by the area of nanofibers exposed in the test cup. The WVP of nanofibers were calculated by Eq. 6;

$$WVP = \frac{(WVTR) \cdot (\Delta x)}{(P_1 - P_2)} \quad (6)$$

where WVTR is the water vapor transmission rate ($\text{g m}^{-2} \text{s}^{-1}$) and P_1 is the partial pressure of water vapor at the inner surface of the film inside the cup, P_2 is the partial pressure of water vapor at the outer surface of the film outside the cup (Pa) and Δx is the thickness of the film (m).

Measurements were performed in triplicates.

2.2.4.6. Thermogravimetric Analysis (TGA)

Thermogravimetric analyses were done with TGA 2950 (Exstar TG/DTA 6300, RTI Instruments, Inc., Woodland, USA) by using dry nitrogen purge. About 5 mg nanofibers, HPMC, PEO, lentil and pea flour, soy protein and gallic acid powder were heated from room temperature to 500°C at a rate of 10 °C/min and with nitrogen at a flow rate of 30 mL/ min. Analyses were performed in triplicates.

2.2.4.7. Differential Scanning Calorimetry (DSC)

The thermal analysis of gallic acid and electrospun nanofibers was carried out by using the DSC (Pyris 6 DSC, PerkinElmer, Massachusetts, USA), equipped with a cooler system with nitrogen. DSC was calibrated using an indium standard (melting point: 156.6 °C) and an empty sample pan was used as a reference. About 4-5 mg sample was placed in hermetically sealed aluminum pan and heated from room temperature to 250°C at a heating rate of 5°C/min. The area of the peak (normalized per unit weight of nanofiber) and Tg of samples were determined in DSC thermograms. The DSC measurements were performed in triplicate.

2.2.4.8. Fourier-transform infrared (FTIR) Analysis

FTIR analyses of electrospun nanofibers, HPMC, PEO, lentil and pea flour, soy protein and gallic acid were performed by using a FTIR spectrophotometer (IR-Affinity1, Shimadzu, Kyoto, Japan) in attenuated total reflectance (ATR) mode using a diamond ATR crystal. The infrared regions analysis was recorded with 32 scans over the wavenumber range of 600-4000 cm⁻¹.

2.2.4.9. Opacity

The light transmittance of the films was measured at 600 nm with a UV-vis spectrophotometer (UV-1700, Shimadzu, Kyoto, Japan) as described by Shiku et. al (2004). The opacity value of the films was calculated using the Eq. 7;

$$Opacity = \frac{A_{600}}{x} \quad (7)$$

Measurements were performed in triplicates.

2.2.5. Packaging of walnuts and accelerated oxidation test

Two types of packaging were designed to examine the effect of nanofibers as active packaging material.

Firstly, HPMC nanofibers containing 10% gallic acid due to having higher antioxidant activity were chosen as active packaging material. About 0.15 g nanofibers were fixed to the inner surface of polyamide/polyethylene (PA/PE) having thickness 90 μm by adhesive septum and walnuts (30 ± 0.5 g) were packaged in the packages that were sealed with constant heat sealer (Taiwan). For fast lipid oxidation, packages were stored in incubator at 40°C for 21 days. Packages containing no nanofiber were used as control.

Secondly, gallic acid loaded lentil flour based nanofibers prepared at pH 10 were chosen due to having homogenous structure. Gallic acid loaded lentil flour electrospun nanofibers were deposited directly onto PLA sheets. Walnuts (30 ± 0.5 gr) were placed between PLA sheets and they were sealed with constant heat sealer (Taiwan). For accelerated oxidation test, packages were stored in incubator set to 40°C for 21 days. Packages containing no nanofiber were used as control.

2.2.5.1. Oil extraction

Walnut kernel was ground with a coffee mill (Fakir, Germany). Ground walnut kernel and solvent mixture (10-fold hexane of oil content of walnut kernel) were mixed with magnetic stirrer (MaxTir 500, Daihan Scientific, Seoul, Korea) for 2 hours. Lipids containing hexane were processed by a centrifuge at 4000 rpm for 15 minutes. The fine walnut powder was separated by using filter paper (Whatman no.1). The hexane was removed from oil-hexane mixture by using rotary evaporator (Heidolph Laborota

4000 efficient, Schwabach, Germany) at 40 °C. The oil was transferred into 10 mL sample vials, capped with nitrogen, and stored at -80 °C until use.

2.2.5.2. Oxidation analyses

Peroxide values (PV) were determined by the following the AOAC method (AOAC, 1995). Oil of 5 g was dissolved in 30 mL of chloroform/acetic acid 2:3 (v/v). Saturated potassium iodide solution of 0.5 ml was added and mixed for 1 minutes. Then, 30 mL distilled water was added to solution. To be used as an indicator, 1 mL of starch solution (1 g/100 mL of water) was added, and the mixture was titrated with 0.01 N Na₂S₂O₃. The end point was determined by the disappearance of the purple color caused by the presence of starch and peroxide value was calculated according to the following Eq. 8;

$$\text{Peroxide value} \left(\frac{\text{milliequivalents peroxide}}{\text{kg sample}} \right) = \frac{(S-B) \times N \times 100}{W_s} \quad (8)$$

B was the volume (mL) of titrant for blank, S was the volume (mL) of titrant for sample, N was the normality (moles equivalent/L) of Na₂S₂O₃ solution, and W_s was the weight (g) of sample.

Thiobarbituric acid reactive substances (TBARS) values were determined according to the official AOCS (1998) method. The oil (50–100 mg) was weighed into a 25-mL volumetric flask and made up to volume with 1-butanol. Solution of 5 mL was mixed with 5 mL of 2-TBA reagent (500 mg 2-TBA in 250 mL 1-butanol). The solutions were heated in water bath at 95 °C. After 2 h, the samples were taken from the water bath and cooled in an ice bath. The absorbance was read at 532 nm by using UV/VIS spectrophotometer (UV 2450, Shamadzu, Columbia, USA). TBARS values were determined by the following Eq. (9);

$$\text{TBARS} \left(\frac{\text{mg Malondialdehyde}}{\text{g sample}} \right) = \frac{50 \times A_{532}}{m} \quad (9)$$

A₅₃₂ was the absorbance read at 532 and m was the weight (mg) of sample.

The p-anisidine value (AnV) was determined according to IUPAC method 2.504 (IUPAC, 1987). The walnut oil samples were dissolved in 25 ml isooctane and absorbance of this solution was measured at 350 nm using a spectrophotometer (UV-2450, Shimadzu, Columbia, USA). Solution of 5 ml was mixed with 1 ml 0.25% p-anisidine in acetic acid (w/v) and after 10 min waiting, absorbance was read at 350 nm using a spectrophotometer (UV-2450, Shimadzu, Columbia, USA). AnV was calculated according to the Eq. 10:

$$AnV = 25 \times (1.2 A_S - A_B)/m \quad (10)$$

where A_s was the absorbance of the fat solution after reaction with the p-anisidine reagent, A_b was the absorbance of the fat solution, m was the mass of oil (g) sample.

The totox value (TV) was defined as the sum of both values (peroxide and anisidine) to total oxidation:

$$\text{Totox value} = 2 \times \text{PV} + \text{AnV} \quad (11)$$

2.2.6. Statistical analysis

Analysis of variance (ANOVA) was conducted by MINITAB (version 16, State College, PA, USA). If significant differences were found, the Tukey's Multiple Comparison Test was used for comparisons ($p \leq 0.05$).

CHAPTER 3

RESULTS AND DISCUSSION

3.1. Fabrication of HPMC/PEO nanofibers by electrospinning

In the preliminary experiments, it was observed that at low concentrations of HPMC and PEO, droplets were observed in electrospinning since the viscosity of solutions were too low. In contrast, when the total concentration of HPMC/PEO was higher than 6% (w/v), the electrospinning process could not be achieved due to the high viscosity of the solution. The optimum amount of HPMC/PEO was determined to obtain fibers.

3.1.1. Physical properties of solutions

3.1.1.1. Rheological properties

Viscosity is the most important parameter for the electrospinning process because it directly affects the extent of the polymer molecule chain entanglement within the solution. In order to produce homogenous nanofibers, polymer molecules must be entangled. Otherwise, instead of fiber formation, beads or droplets are deposited on the collector. This is due to the low viscoelastic force which does not counterbalance the higher Coulombic stretching force that causes jet instability (Kriegel et al., 2008). The viscosity of solutions depends on the polymer type, concentration of polymer and solvent type. Four different concentration regions which are dilute, semidilute unentangled, semidilute entangled, and concentrated regions have been defined related to the concentration dependence of viscosity of polymers. Critical entanglement concentration (C_e) is the boundary concentration between the semi-dilute unentangled and semi-dilute entangled regimes at which entanglements between polymer chains form and start chain motions. The minimum polymer concentration to avoid beaded nanofibers depends on the C_e (McKee, Wilkes, Colby,

& Long, 2004). In order to determine C_e , specific viscosity of solutions (γ_{sp}) was firstly calculated by Eq. 12;

$$\gamma_{sp} = \frac{\gamma_0 - \gamma_s}{\gamma_s} \quad (12)$$

where γ_s is the solvent viscosity (Pa.s) and γ_0 is the zero shear viscosity (Pa.s).

Zero shear viscosities, γ_0 , were approximated from the flow curves by using the actual or extrapolated values for apparent viscosity at shear rate of 0.1 s^{-1} . The changes in the slope of the $\log \gamma_s$ vs $\log C$ graph represent the inception of the semidilute unentangled to semidilute entangled regime (McKee et al., 2004). C_e was determined from the intercept of the fitted lines in the semidilute unentangled and the semidilute entangled regimes (Kong & Ziegler, 2014). In general, for neutral, linear polymers in a good solvent, there is a relationship as $\gamma_s \sim C^{1.25}$ in the semidilute unentangled regime and $\gamma_s \sim C^{4.8}$ in the semidilute entangled regimes (McKee et al., 2004). In this study, the C_e was found to be 2.75% wt. Hence, the semidilute unentangled regime ($\gamma_s \sim C^{1.49}$) was in good agreement with the theoretical predictions of 1.25. In the study of Neo et al. (2012), the semidilute unentangled regime ($\gamma_s \sim C^{1.45}$) was defined for zein solution that was used to produce nanofibers. Moreover, the semidilute entangled regime showed slightly high concentration dependence ($\gamma_s \sim C^{5.5}$). This strong scaling dependence indicated that the polymer chains were associating in solution and polymers were entangled in the solution used for the electrospinning experiments. Similarly, in the study of Klossner et al. (2008), in semi-dilute entangled solution, concentration dependence was found to be $\gamma_s \sim C^{6.0}$ for chitosan solutions.

Table 3.1 shows the consistency index (k) and flow behavior index (n) of the solutions that contains different amounts of HPMC and PEO. All solutions obeyed the Power Law with a high coefficient of determination and the flow curves are shown in Figure 3.1. As shown in Figure 3.1, the apparent viscosity of the solutions decreased with increase in the shear rate that was defined as a Non-Newtonian shear thinning behavior. All solutions displayed n values (0.53-0.94) lower than 1 which represented shear thinning behavior. When the amount of HPMC increased, the solutions shifted

from Newtonian behavior to Non-Newtonian, with a decrease in n value. Table 3.1 indicates that as the HPMC concentration was increased, k values of solutions significantly increased ($p \leq 0.05$) (Table A.1). HPMC is a well-known mucoadhesive polymer and it swells quickly when in contact with water (Tort & Acartürk, 2016). Due to its high water holding capacity, HPMC increased the k values of solutions. A similar increase in viscosity of solutions was observed by Lim, Gwon, Pyo Jeun, & Nho (2010) by increasing HPMC amount.

Frequency sweep test was carried out. Storage (G') and loss modulus (G'') values of HPMC/PEO solutions are shown in Figure 3.2. In all samples, both G' and G'' values increased with angular frequency. While storage modulus represents elastic behavior, loss modulus shows the viscous behavior. Loss modulus was found to be higher than storage modulus, which indicated a liquid-like behavior of the solutions. It is well known that both G' and G'' are very sensitive to water. As can be seen from Figure 3.2, increasing the concentration of HPMC, resulted in higher storage and loss modulus values. Similar increase was observed in the study by Celebioglu & Uyar (2013) in which as the cyclodextrin concentration increased, G' and G'' values also increased.

Table 3.1 *Rheological properties and electrical conductivities of solutions, the morphology and average diameters of the HPMC/PEO fibers*

Solutions (HPMC/PEO)	k ($Pa\ s^n$)	n	Electrical Conductivity ($\mu S/cm$)	Fiber Morphology	Average Diameter (nm)
4/2	17.52±0.37 ^{ab}	0.65±0.01 ^d	209.00 ±1.00 ^{ab}	Homogenous	311±69 ^a
3/2	6.77±0.39 ^c	0.77±0.01 ^c	189.10±0.60 ^{cd}	Homogenous	279±61 ^b
2/2	2.55±0.20 ^d	0.86±0.01 ^b	180.65±1.15 ^d	Homogenous	235±64 ^c
1/2	0.65±0.01 ^d	0.93±0.01 ^a	154.20±0.90 ^e	Beaded	
4.5/1.5	20.33±0.64 ^a	0.63±0.01 ^d	220.00±3.00 ^a	Homogenous	317±56 ^a
3/1.5	5.94±0.39 ^c	0.73±0.02 ^c	200.00±1.00 ^{bc}	Homogenous	235±59 ^c
2/1.5	2.01±0.16 ^d	0.86±0.01 ^b	182.50±1.30 ^d	Homogenous	216±63 ^{cd}
1.5/1.5	1.08±0.09 ^d	0.89±0.01 ^{ab}	158.75±0.55 ^e	Less Beaded	
5/1	19.34±1.8 ^a	0.61±0.02 ^d	199.95±4.05 ^{bc}	Homogenous	322±60 ^a
4/1	15.50±0.62 ^b	0.53±0.02 ^e	191.40±3.10 ^{cd}	Homogenous	301±47 ^{ab}
2/1	1.35±0.05 ^d	0.86±0.01 ^b	147.60±5.40 ^e	Homogenous	205±50 ^d
1/1	0.35±0.01 ^d	0.94±0.02 ^a	128.55±2.45 ^f	Beaded	

*Columns having different letters are significantly different ($p \leq 0.05$).

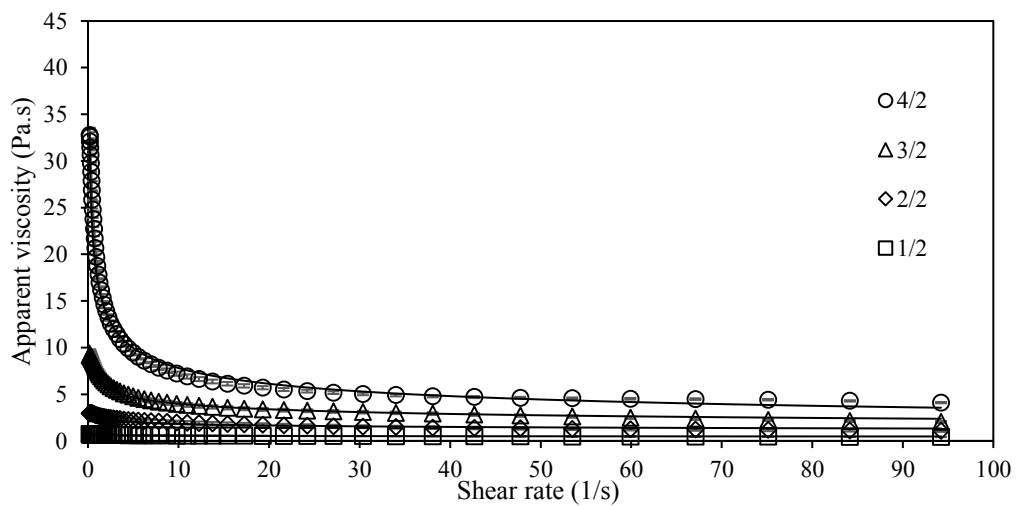
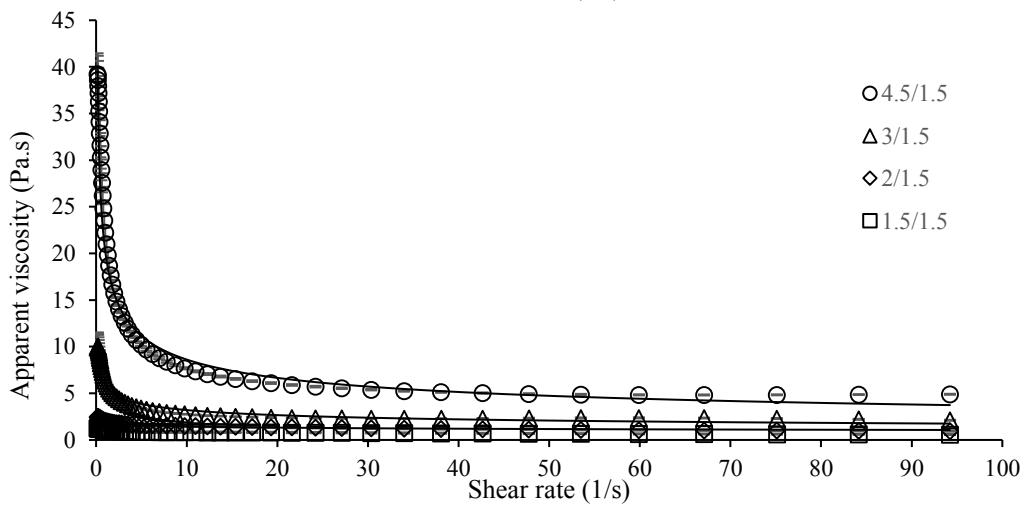
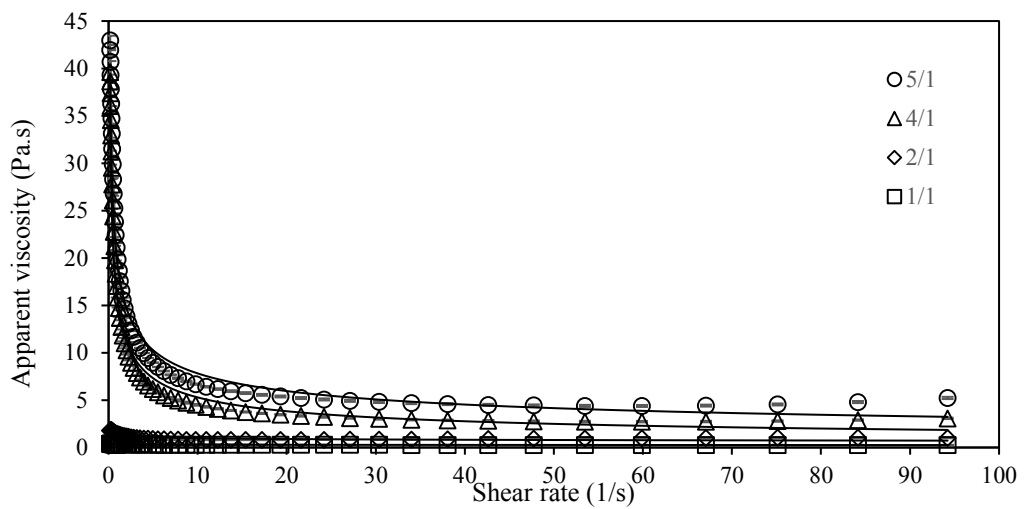


Figure 3.1 Flow curves of solutions containing different amount of HPMC/PEO

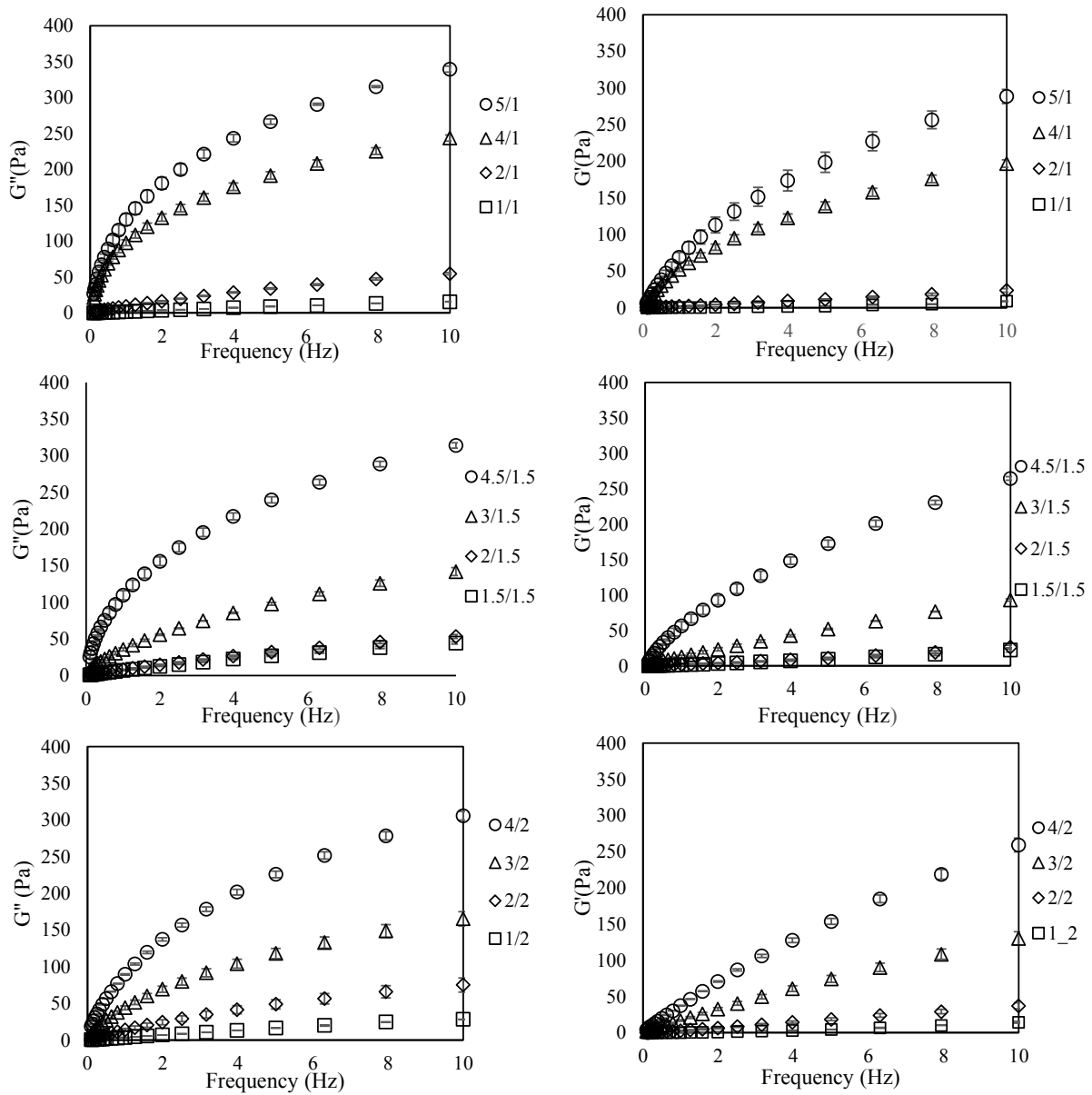


Figure 3.2 Variation of storage modulus (G') and loss modulus (G'') with frequency for solutions containing different amount of HPMC/PEO

3.1.1.2. Electrical Conductivity

Electrical conductivity is one of the important parameters that affect electrospun nanofiber formation and morphology. It shows the ability of charge to move, thereby affecting the electrostatic repulsion force which is critical to initiate jet formation. The solution should have adequate electrical conductivity for the establishment of repulsion force needed to overcome the surface tension of a droplet to form a fiber jet. However, at a certain point, due to the great transfer of surface charge to the spinning polymer jet, a high conductivity results in high electrostatic repulsion force, which can cause bending instability and stretching (Vega-Lugo & Lim, 2012, S. Wang, Marcone, Barbut, & Lim, 2013). Thus, in order to produce homogeneous nanofibers, electrical conductivity should be at an optimum level. Solution conductivity mainly depends on the polymer type, solvent used, and the availability of ionisable salts. The conductivity values of solutions that were used for nanofiber production are shown in Table 3.1. In a two-phase blend polymeric matrix, all conducting particles affect the formation of electrical conductivity. The conductivity is the inverse of resistivity, which is the sum of resistance of both polymers. Thus, the conductivity change, which is related to the composite ratio, is not linear (Colín-Orozco, Zapata-Torres, Rodríguez-Gattorno, & Pedroza-Islas, 2015).

It was clear that as the PEO and HPMC concentrations increased, the conductivity of solutions significantly increased, too ($p \leq 0.05$). Although both PEO and HPMC are non-ionic polymers, an increase in electrical conductivity of solutions was observed. The reason could be the interaction between the surfactant (Tween 80) and polymers. Normally, at low concentrations, most of the surfactant molecules behave as free monomers. However, micelles begin to form above a certain concentration, known as critical micelle concentration (CMC) (Sardar & Kamil, 2012). In the study of Ćirin, Poša, Krstonošić, & Lj Milanović (2012), which considered CMC values, Tween 80 showed the strongest synergistic effect with the lowest CMC amongst the polysorbate surfactants. Micelles generate a network-like structure, which results in a hydrodynamic resistance to ion mobility and therefore, lowering the electrical

conductivity (Wang, Wei, Chen, & Tsao, 2004). As the concentration of polymers increased, the interaction between polymers and surfactant decreased. Thus, the formation of micelles reduced, and ion mobility increased that led to higher conductivity.

3.1.2. Characterization of nanofibers

3.1.2.1. Fiber morphology

In order to decrease surface tension of solutions, Tween 80 was added as a surfactant. Surfactants are amphiphilic molecules and the hydrocarbon chains provide the hydrophobic nature of the Tween 80 while the hydrophilic nature is provided by the ethylene oxide subunits (Nidhi, Indrajeet, Khushboo, Gauri, & Sen, 2011). The HLB (hydrophilic–lipophilic balance) value of Tween 80 is 15 that means it is a hydrophilic surfactant (W. Liu, Sun, Li, Liu, & Xu, 2006). Tween 80 dissolved in water and readily absorbed at the surfaces of the medium and decreases the surface tension. Surface tension should be low enough to be overcome by the electrical field. Therefore, adding Tween 80 improved the spinnability of solutions.

Nonhomogenous beaded nanofibers were obtained when solution containing pure HPMC was electrospun. Therefore, to increase electrospinnability of HPMC, PEO was added to the HPMC solution at different ratios. In general, in order to overcome the poor electrospinnability of biopolymers, blending them with carrier synthetic polymers can be a good solution. PEO is one of the most commonly used carrier polymers, being nontoxic, biocompatible, water soluble and biodegradable (Safi, Morshed, Hosseini Ravandi, & Ghiaci, 2007). By blending HPMC with PEO, the viscosity of the solution is modified, which makes the electrospinning process successful. Due to the strong repulsive force between biopolymer molecules, sufficient chain entanglement cannot occur. Adding PEO reduces the repelling force between molecules, hence nanofiber formation is promoted (Lu, Zhu, Guo, Hu, & Yu, 2006). There are numerous studies that reported the successes recorded with the addition of PEO in order to obtain homogeneous nanofibers. For example, in the study

of Huang, Nagapudi, Apkarian, & Chaikof (2001), pure collagen electrospun nanofibers could not be formed but with the addition of PEO, homogenous nanofibers derived from collagen were obtained. Similarly, Alborzi, Lim, & Kakuda (2010) were able to produce alginate/pectin nanofibers by adding PEO to the solutions.

In this study, processing parameters and ambient conditions were kept constant. Therefore, the composition of the solutions was the only parameter that affected the fiber morphology and diameter. Fibers obtained from the solutions containing HPMC and PEO at a ratio of 1/2 and 1/1 had beaded morphology. Moreover, the 1.5/1.5 nanofiber showed few beads (Figures were not shown). The other nanofibers were bead-free. Figures 3.3 & 3.4 show the SEM images and the average diameters of the electrospun HPMC/PEO fibers with different ratios. The SEM images of nanofibers containing 1.5% PEO and 4.5, 3 & 2% HPMC were not given but they showed similar images and diameter distribution with Figures 3.3 & 3.4. It was observed that the morphology of fibers changed from the highly beaded structure to a uniform structure as the solution concentration was increased, which was related to the rheological properties of solutions. In this study, with regards to the total polymer concentration, the entanglement concentration (C_e) was found to be 2.75% (w/v). As can be seen in Figure 3.3, polymer solutions that were electrospun from solutions below C_e , resulted in bead formation. Below C_e , there are no entanglements or topological constraint, and the jet cannot withstand the force of the electric field and surface tension of the solution. Thus, instead of a stable Taylor cone, jets broke into droplets (Klossner et al., 2008). Similar result was obtained by McKee et al. (2004). In their study, polymer droplets was observed by using solutions below C_e value. With regards to the k value, increasing HPMC and PEO concentrations in the solution increased, the k values of the solutions that led to the formation of fibers without beads. Similar trend was observed in the study by Jia et al. (2007) that produced chitosan/PVA electrospun nanofibers at different concentrations. It was stated that as the concentration of the solution was increased, beaded nanofibers transformed into uniform beadless structure. Moreover, in the study of Geng, Kwon, & Jang (2005), it was found that the

morphology of the fibers changed gradually from the highly beaded structure to the uniform fiber structure with increasing concentration of the solution.

Fiber diameter plays a key role on the final properties of the electrospun networks. The diameter distributions with average fiber diameter and standard deviation are shown in Figures 3.3 and 3.4. The average diameters of the nanofibers ranged almost between 200 to 300 nm with standard deviation of between 47-69 nm. With regards to the narrow distribution and small standard deviations of nanofiber, it suffices to state that uniform nanofibers were obtained by electrospinning process. The properties of the solutions, especially the rheological properties and electrical conductivity directly affect the diameter of nanofibers. The results indicated that the diameter of fibers increased by increasing polymer concentration, which was directly proportional to the viscosity of the solutions. As the k values of solutions increased, nanofibers having larger diameters were obtained. However, as the HPMC and PEO concentration increased, the distributions of fiber diameter shifted to the right (to higher diameters). The reason of this trend was explained by Ramakrishna et al. (2005). It was stated that having high viscosity, prevents the instability of bending and reduced jet path. Due to the low stretching of the solutions, reduced the jet path resulted in high diameters. The same trend was found by Neo et al. (2012) in which increasing viscosity due to higher zein concentration led to an increase in fiber diameter. The effect of viscosity on the fiber diameter was reported by many researchers (Jia et al., 2007, Ramji & Shah, 2014, Yao, Li, & Song, 2006). Viscoelastic behavior of solutions also affects the morphology of nanofibers. As the solution concentration increased, G' and G'' of the solutions also increased. In this study, it was found that nanofibers produced from solutions with high modulus values, showed high diameter. The study of Gupta, Jassal, & Agrawal (2015) confirmed the present result, in which diameter of nanofibers was directly proportional to elasticity of the solutions. In general, while the viscosity shows increasing effects, the increase in conductivity decreases the diameter, which is in accordance with the observations of other researchers (Hardiansyah, Tanadi, Yang, & Liu, 2015; Lu et al., 2006; Pakravan,

Heuzey, & Ajji, 2011). However, in this study, the rheological properties of the solutions were found to be a more significant factor that controls the fiber diameter, rather than the electrical conductivity.

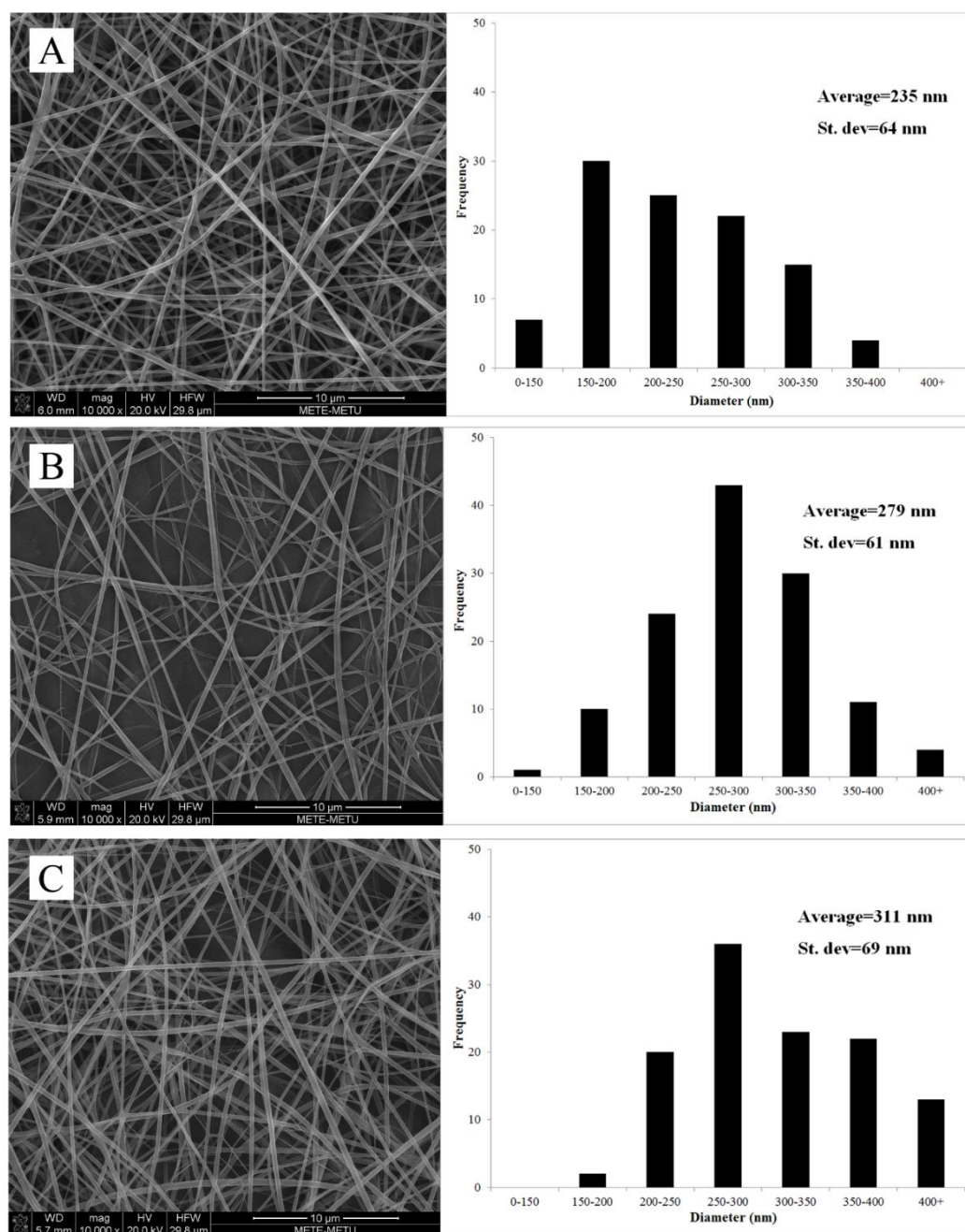


Figure 3.3 SEM images of electrospun fibers containing 2% PEO with different HPMC contents: A: 2%, B: 3%, C: 4%.

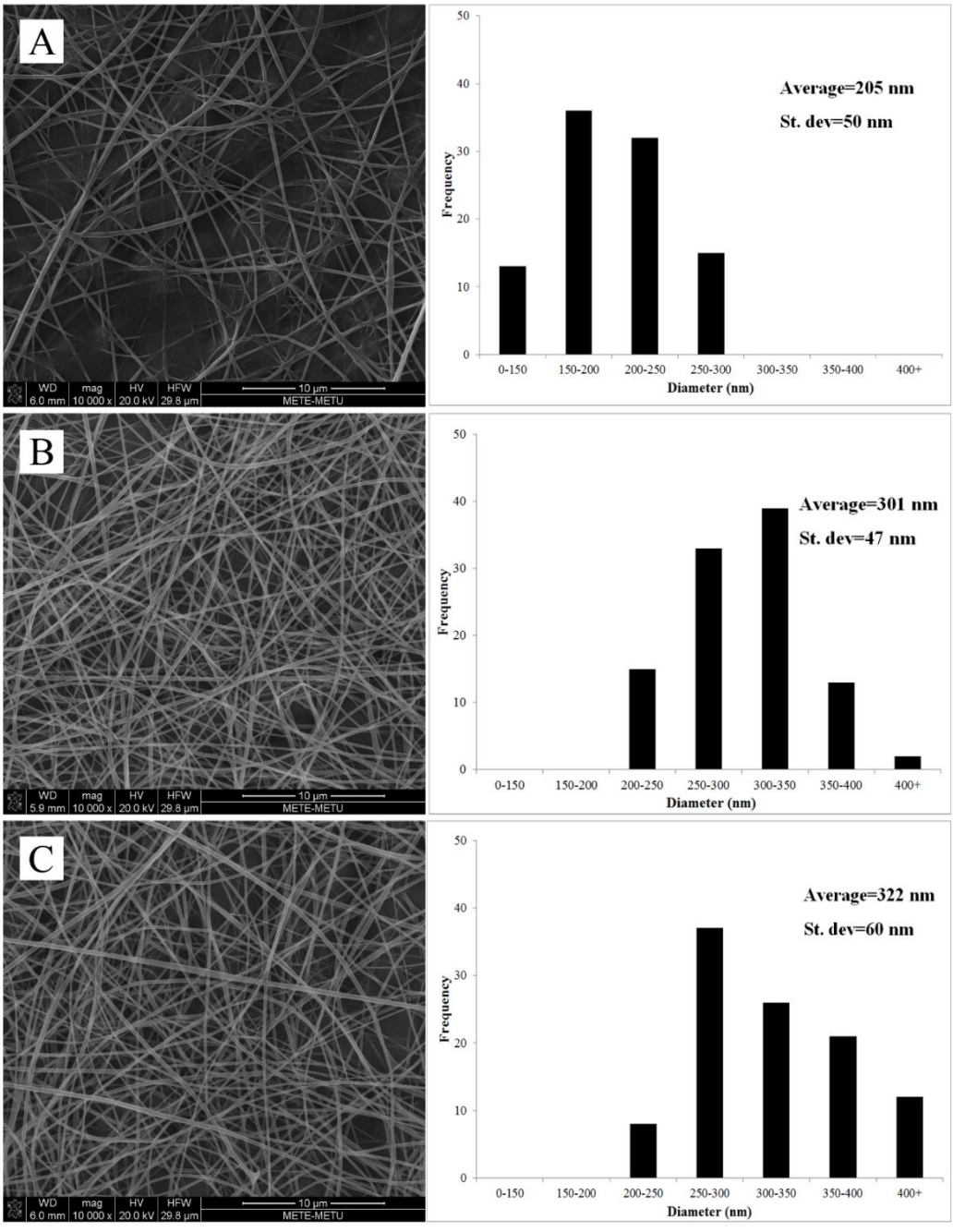


Figure 3.4 SEM images of electrospun fibers containing 1% PEO with different HPMC contents: A: 2%, B: 4%, C: 5%.

3.1.2.2. Water Vapor Permeability (WVP)

WVP is a critical property for food packaging materials, since it is directly related to the ability of the materials to control moisture transfer between the environment and the food. In general, materials with minimum WVP values are preferred as food packaging materials. However, the problem of biopolymer films is their high WVP. Therefore, in order to improve WVP of biopolymer-based films, the use of nanoscience can be a good approach. The WVP values electrospun HPMC/PEO nanofibers ranged between $7.4\text{-}12 \times 10^{-11} \text{ g m}^{-1} \text{ s}^{-1} \text{ Pa}^{-1}$ (Table 3.2). In several studies, the WVP properties of HPMC films produced by casting method were found in the range between $6\text{-}9 \times 10^{-10} \text{ g m}^{-1} \text{ s}^{-1} \text{ Pa}^{-1}$ (Akhtar et al., 2013a). Since PEO is a hydrophilic material, it is expected that the addition of PEO increases the WVP values of the films. However, electrospun nanofibers had lower WVP than HPMC films prepared by casting method. As can be seen from the Table 3.1, electrospun films have fiber structure at nano size. This tightly linked to three dimensional network decreased the migration of water through the film. Thus, electrospun nanofibers can be used to decrease the WVP of films that can be used as packaging material. In the study by Fabra, Lopez-rubio, & Lagaron (2014), zein nanofibers were directly collected onto films from polyhydroxyalkanoates (PHA) polymers and it was found that by the addition of electrospun zein nanofibers, water permeabilities of PHA films were significantly decreased. Similarly, as the composition time of electrospun zein nanofibers on the Poly(3-hydroxybutyrate) (PHB) films was increased, the WVP values decreased.

Nanofibers with HPMC/PEO ratios of: 4/2, 4.5/1.5 and 5/1 had the lowest WVP values ($p \leq 0.05$). As the total polymer content in the solutions increased, the WVP values of the nanofibers decreased. The porosity of nanofibers can affect the WVP values. As shown in Table 3.1, nanofibers with high amount of polymer had significantly high diameter. Due to the higher fiber junctions, as the fiber diameter increased, the porosity of electrospun mat decreased (Liu, Guo, Shen, Wang, & Shi, 2009). Similarly, in the study of Guo, Zhou, & Lv (2013), it was found that the porosity

decreased with an increase in the nanofiber diameter. Moreover, Ayrancı, Ukta, & Cetin (1997) stated that permeability of HPMC films decreased with increasing molecular weight of the component since, the mobility of the molecule decreased with increasing molecular weight and thus, its contribution to water vapor transfer became less. Similarly, as the polymer concentration was increased, the mobility of molecules decreased due to the higher viscosity. Thus, in this study, fibers having high total polymer content showed high viscosity and less water vapor transfer.

Table 3.2 *WVP and thermal properties of fibers*

Fibers (HPMC/PEO)	$WVP \times 10^{-11}$ ($g\ m^{-1}\ s^{-1}\ Pa^{-1}$)	T_g ($^{\circ}C$)	T_m ($^{\circ}C$)	ΔH_m (J/g)
4/2	7.429±0.488 ^c	181.4±1.1 ^a	55.66±0.01 ^{ab}	14.53±1.19 ^{bc}
2/2	8.422±0.153 ^{bc}	136.6±0.3 ^e	56.13±0.01 ^a	23.33±0.35 ^a
4.5/1.5	7.532±0.154 ^c	179.1±0.5 ^a	54.51±0.17 ^{bc}	10.49±0.37 ^d
2/1.5	10.206±0.195 ^{ab}	144.1±1.0 ^d	54.07±0.27 ^{cd}	23.09±0.95 ^a
5/1	7.832±0.722 ^c	168.8±0.6 ^b	55.03±0.23 ^{bc}	13.95±0.87 ^c
2/1	12.008±0.326 ^a	160.3±0.5 ^c	53.06±0.11 ^d	18.42±1.06 ^b

*Columns with different superscript letters are significantly different ($p \leq 0.05$).

3.1.2.3. FTIR Analysis

FTIR spectrum provides information of the functional groups present in the sample, it is needed to examine the interaction between the components in the electrospun fibers. Figure 3.5 shows the FTIR spectra of HPMC/PEO electrospun nanofibers with different compositions and also obtained from pure HPMC and PEO. It is worth mentioning that the peak at $2900\ cm^{-1}$, corresponds to CH_2 stretching (methylene stretching) (Y. J. Lee et al., 2007). FTIR spectra of pure HPMC powder shows a small peak at this wavelength when compared to PEO. Thus, as the HPMC content increased, this peak disappeared. Therefore, as PEO concentration in the electrospun nanofibers was increased, the absorbance intensity of CH_2 stretching increased. Similar results were found by Kriegel, Kit, McClements, & Weiss (2009). In this

study, with the addition of PEO, absorbance intensity of CH₂ stretching at 2885 cm⁻¹ increased in the FTIR spectrum of chitosan/PEO electrospun nanofibers. As shown in Figure 3.5, the FTIR spectrum of HPMC powder, exhibited absorption bands at 1060, 2900 and 3400 cm⁻¹, which attributed to the stretching vibration of C-O, C-H and O-H groups, respectively. Similar FTIR spectrum of HPMC was found by Ding, Zhang, & Li (2015). The region between 1500 cm⁻¹ to 750 cm⁻¹ shows the fingerprint region that usually consists of bending vibrations within the molecule. In this region, each component produces its own unique pattern of peaks. A closer look to the fingerprint region of pure PEO, PEO displays a triplet absorbance (1058, 1095 and 1145) with a maximum at 1100 cm⁻¹, which corresponded to its crystalline phase. This peak was shown to correspond to the stretching vibrations of the ether bond or C-O-C complex (Vega-Lugo & Lim, 2012). PEO is a semicrystalline polymer (Furlan et al., 2012). The changes in the intensity, shape and wavelength of the C-O-C stretching is related to the interaction between PEO and HPMC. Nanofibers containing mainly HPMC, showed a maximum absorbance that was shifted to left when compared with the PEO. Moreover, when PEO was blended with HPMC, instead of the triplet absorbance, just a peak around 1100 cm⁻¹, was observed. That means that, the crystallinity of PEO was depressed by blending with HPMC. The reason could be related to the regular structure of chains during crystallization, being interrupted by HPMC chains when they were miscible. Furthermore, the quick solvent evaporation in electrospinning can be another reason, disrupting the crystalline structure of nanofibers (X. Xu, Jiang, Zhou, Wu, & Wang, 2012). Similar results have been observed for blends of PEO/soy protein/lignin nanofibers, indicating the disappearance of crystallinity of the PEO in the blends (Salas, Ago, Lucia, & Rojas, 2014). The other peaks at fingerprint region of PEO are around 1280, 1340 and 1467 cm⁻¹, which are characteristics of CH₂ twisting, CH₂ wagging and CH₂ scissoring, respectively. Furthermore, peaks at around 840 and 960 cm⁻¹ are as a result of the C-O stretching and CH₂ rocking (Pielichowski & Flejtuch, 2005). Moreover, as stated in Liu et al. (2015) study, Tween 80 showed peaks at 2900 (CH₂), 1738 (C=O), 1648 (-HC=CH-), 1100 (C-O-C), 946 & 855 cm⁻¹

(CH₂). Nanofibers also showed the same peaks at these wavelengths except 1738 & 1648 cm⁻¹ due to the most probably low amount of Tween 80.

In general, if the polymers in the composite films are not compatible, each polymer shows its own pure peak positions and absorbance in the composite films of their FTIR spectra. In contrast, when the polymers are miscible, due to the possible chemical interactions between polymers, there can be shifts in the wavelength. In this study, the FTIR spectra of HPMC/PEO nanofibers were different from that of the pure polymers and it was an evidence of miscibility of HPMC/PEO blends.

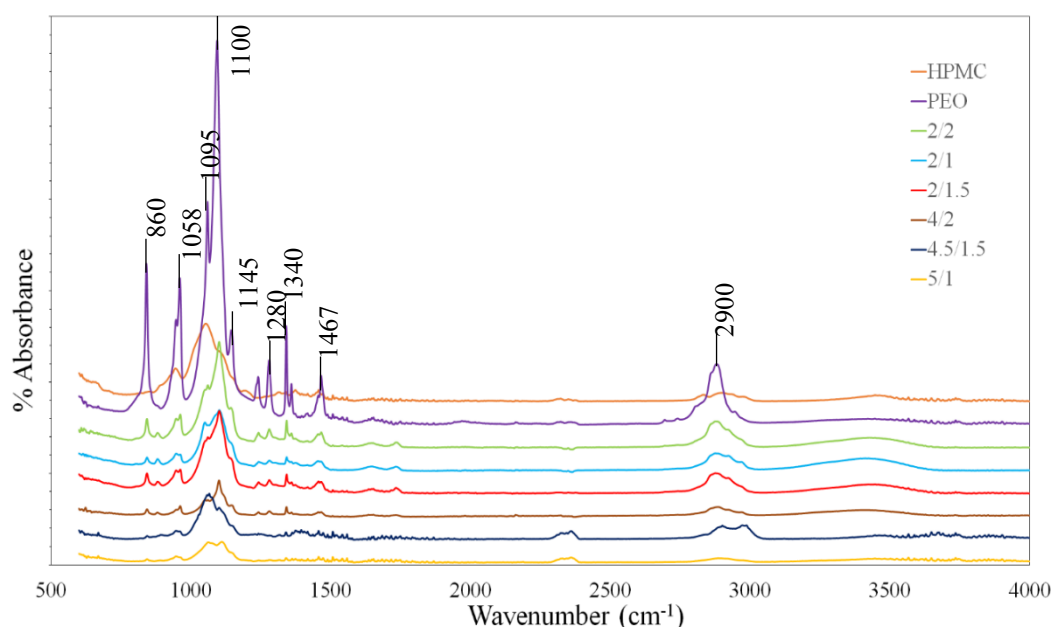


Figure 3.5 FTIR spectra of nanofibers containing different amounts of HPMC and PEO.

3.1.2.4. Thermo-gravimetric Analysis (TGA)

TGA examines the mass change as a function of temperature or time and it is used to determine the residues in a sample after it has been thermally degraded as well as to evaluate thermal stability (Ding et al., 2015). The TGA curves are shown in Figure 3.6. Pure PEO represents only a single stage degradation that began at onset temperature (T_{onset}) of $\sim 400^{\circ}\text{C}$ and the weight loss at the end of this stage was found to be 95%. Pielichowski & Flejtuch (2005) conducted a TGA experiment, with the

TGA coupled to an FTIR spectrophotometer in order to characterize the chemical composition of PEO after thermal degradation and it was found that the main decomposition products were: ethyl alcohol, methyl alcohol, alkenes, non-cyclic ethers (ethoxy-methane, ethoxyethane and methoxymethane), formaldehyde, acetic aldehyde, ethylene oxide, water, CO and CO₂. As can be seen from derivative thermogravimetric (DTG) curve in Figure 3.6, pure HPMC exhibits also, a one stage degradation pattern. However, before thermal degradation, due to the vaporization of moisture, at 55°C a small step change was observed. The main stage of degradation began at almost 350 °C (T_{onset}), which was related to cellulose ethers degradation, that included the parallel processes of dehydration and demethoxylation (Yin, Luo, Chen, & Khutoryanskiy, 2006). Also, T_{onset} of thermal degradation of pure HPMC was lower than T_{onset} of pure PEO. That means, PEO had a higher stability towards thermal degradation when compared to pure HPMC. The degradation behavior of HPMC/PEO nanofibers was intermediate between that of the pure components. Similar to HPMC, nanofibers lost unbound water at around 50 °C. The second change was the most important in the total weight loss. Nanofibers showed a weight loss of between % 90-95 after degradation temperature. T_{onset} of thermal degradation of HPMC/PEO nanofibers ranged between 340-370 °C. Figure 3.6 indicates the fact that as the PEO content of nanofibers was increased, T_{onset} of thermal degradation also increased. Therefore, it must be noted that the thermal stability of the nanofibers improved with the addition of PEO.

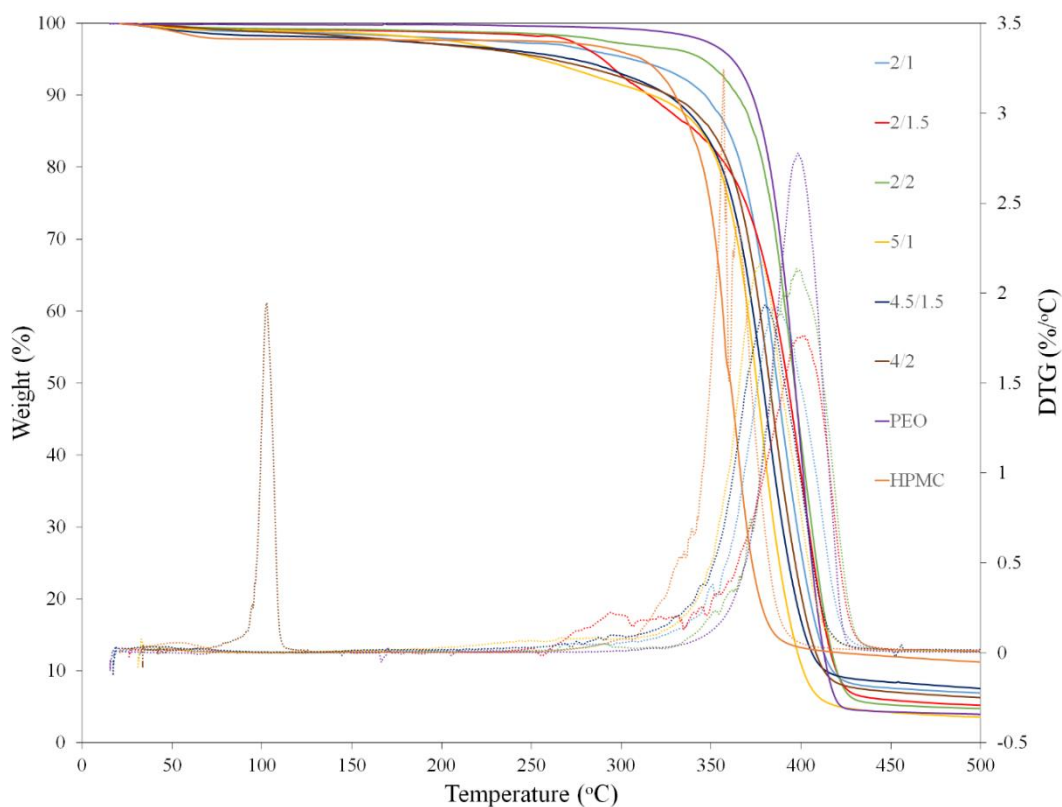


Figure 3.6 Thermo-gravimetric curves of nanofibers containing different amounts of HPMC and PEO.

3.1.2.5. DSC Analysis

DSC analysis gives information about the possible interactions between compounds in the matrix and the stability and applicability of the biopolymer (Pelissari, Andrade-Mahecha, Sobral, & Menegalli, 2013). Table 3.2 shows the glass transition temperature (T_g), the melting temperature (T_m) and enthalpy change (ΔH_m). T_m is a temperature of melting of the crystalline phase occurring. When the thermal analysis of pure PEO was conducted, the melting point of PEO was found to be 68 °C. However, the melting points of the nanofibers were between 53-56 °C. The reason of decrease in melting point could be related to the disruption of the crystalline structure of PEO with interaction between PEO and HPMC. FTIR results also confirm the destruction of the crystalline structure of PEO. In the study of Kriegel, Kit, McClements, & Weiss (2009a), pure PEO had higher T_m than chitosan/PEO

electrospun nanofibers due to the interactions between PEO and chitosan chains obstructing the crystallization of PEO. Moreover, the rapid solidification process of the stretched chains during electrospinning changed the crystalline structure of nanofibers (Islam & Karim, 2010). At constant HPMC content, the T_m value of nanofiber with HPMC/PEO ratio of 2/2 was higher than 2/1 one. The higher amount of PEO content had more regular crystalline structure. In a similar study, the T_m value of poly(bisphenol A-co-epichlorohydrin) (PBE)/PEO blend decreased as the PEO content was increased. It was concluded that this melting point depression in the polymer blends could be an evidence of miscibility of blends (Rocco, Moreira, & Pereira, 2003). Thus, in this study, it can also be said that PEO and HPMC were miscible in the electrospun nanofibers. Lee et al. (2007) similarly reported that due to the formation of a miscible phase with sodium alginate (SA) and PVA, the T_m of SA/PVA component was depressed to lower temperatures with the addition of SA. The endothermic peaks observed in the DSC curves were associated to the melting of the crystalline phase of the blend. The enthalpy of the melting (ΔH_m) of nanofibers decreased with increasing amount of HPMC. The reason could be again the same with T_m depression which was disruption of crystalline structure. A similar decrease was observed by (Kriegel et al., 2009b), where the blend of chitosan/PEO had significantly lower ΔH_m when compared to pure PEO. Moreover, in the study by (Rocco et al., 2003), it was reported that with the addition of PBE to PEO, a drastic decrease in the area of the endothermic peak was observed.

The glass transition temperature (T_g) is the parameter that is related to the softening point from glassy state to rubbery state, in which the polymer can exhibit a thermoplastic character. Having both T_m and T_g values, indicates the semicrystalline structure of electrospun nanofibers having both amorphous and crystalline regions. The glass transition is a property of only the amorphous portion of a semi-crystalline solid (Jimenez, Fabra, Talens, & Chiralt, 2012). T_g values of nanofibers were in the wide range of between 136 °C to 181 °C (Table 3.2). In the study of Kararli, Hurlbut, & Needham (1990), it was reported that T_g of HPMC films, varied between 157°C to

180°C. Moreover, Ford (1999) conducted thermal analysis of HPMC powder and found that the T_g of HPMC was 180 °C. Thus, T_g values were similar to pure HPMC which was an amorphous polymer. It was clear that higher amount of HPMC led to an increase in the T_g of the electrospun nanofibers, which was possibly responsible for the minimal chain mobility of polymers. Similarly, Guirguis & Moselhey (2012) found that with increasing hydroxypropyl cellulose (HPC) amounts, the T_g values of the PVA/HPC blends increased.

3.2. Fabrication of gallic acid loaded HPMC/PEO nanofibers with electrospinning

In this part, it was aimed to encapsulate gallic acid into HPMC/PEO nanofibers. The ratio of HPMC/PEO solution was chosen as 4/1 with regard to results obtained in Section 3.1.

3.2.1. Physical properties of solutions

3.2.1.1. Rheological properties

Table 3.3 shows k and n values of the solutions that contains different amounts of gallic acid. The flow curves are shown in Figure 3.7 and all solutions obeyed the Power Law with a high coefficient of determination ($r^2=0.995-0.998$). As can be seen from Figure 3.7, solutions displayed Non-Newtonian shear thinning behavior meaning that the apparent viscosity of the solutions decreased with increase in the shear rate. n values of solutions which were lower than 1 also confirmed the shear thinning behavior. HPMC/PEO solution containing no gallic acid had the highest k and lowest n value. Gallic acid was added to HPMC/PEO solutions by dissolving ethanol/water solution. As the amount of gallic acid was increased, the amount of ethanol/water in solution increased, too. Therefore, the solution became less viscous and n values of solutions increased to be closer Newtonian behavior. When the gallic acid amount of solutions increased, k values significantly decreased ($p \leq 0.05$). Solutions contained the same amount of HPMC and PEO, so the k value difference was caused by the addition of gallic acid with ethanol/water solution.

Table 3.3 Rheological properties and electrical conductivities of solutions and average diameter of nanofibers

Solutions with different gallic acid concentration (%)	k ($Pa\ s^n$)	n	Electrical Conductivity ($\mu S/cm$)	Average Diameter (nm)
Control	15.50 ± 0.62^a	0.53 ± 0.02^c	191.40 ± 3.10^b	301 ± 47^a
2	11.60 ± 0.27^b	0.61 ± 0.01^b	438.33 ± 2.33^a	285 ± 30^b
5	7.96 ± 0.53^c	0.65 ± 0.02^{ab}	410.00 ± 2.18^a	278 ± 42^{bc}
10	7.00 ± 0.14^c	0.66 ± 0.01^a	410.00 ± 3.78^a	267 ± 42^c

*Columns having different letters are significantly different ($p \leq 0.05$).

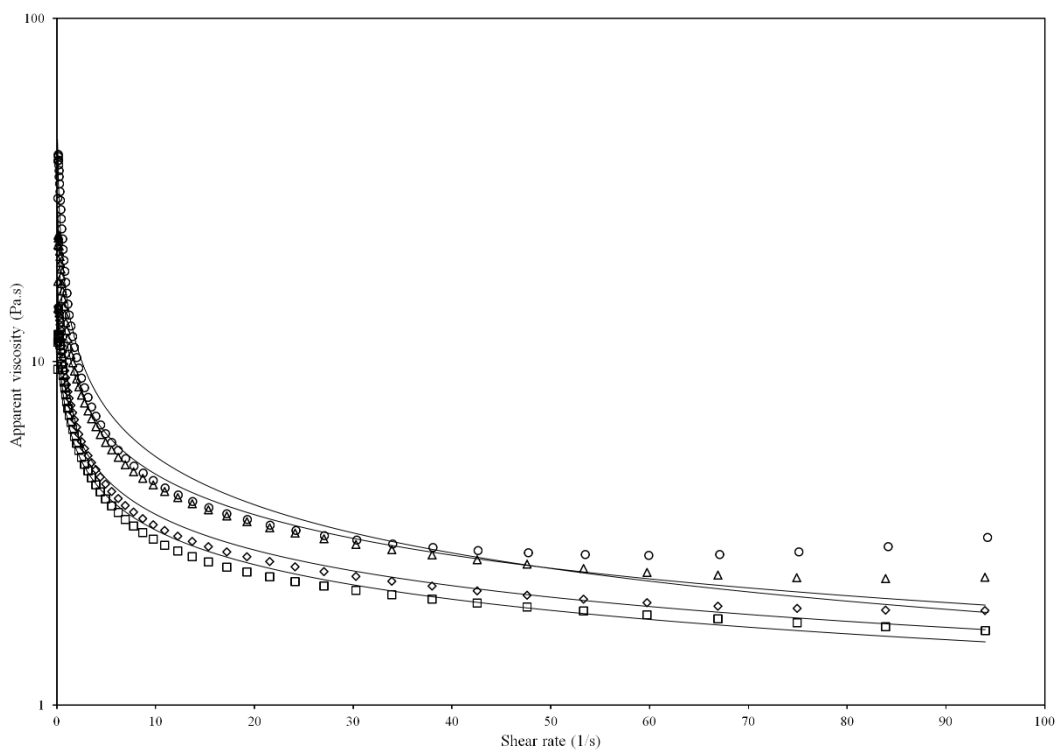


Figure 3.7 Flow curves of solutions containing different gallic acid concentration: \circ : control, Δ : 2%, \diamond : 5%, \square : 10%.

3.2.1.2. Electrical Conductivity

The electrical conductivity values of solutions are shown in Table 3.3. As the gallic acid concentration in the solutions increased, the electrical conductivity values of solutions did not change significantly ($p > 0.05$). However, the control HPMC/PEO solution had significantly lower electrical conductivity value compared to solution containing gallic acid. As stated in the study of Chuysinuan, Chimnoi, Techasakul, & Supaphol (2009), the increase in electrical conductivity of solution by adding gallic acid was explained as the dissociation of gallic acid into ionic species.

3.2.2. Characterization of electrospun nanofibers

3.2.2.1. Fiber Morphology

The SEM images and the average diameters of the electrospun nanofibers with different gallic acid amount are shown in Figure 3.8. The only parameter that affected the fiber morphology and diameter distribution was the composition of nanofibers because the processing parameters and ambient conditions were kept constant. In this study, all obtained sheets were bead free homogenous nanofibers. That was the evidence that the encapsulation of gallic acid in HPMC/PEO nanofibers did not destroy the structure of nanofibers. Gallic acid was incorporated well within the fibers. The diameter distributions with average fiber diameter and standard deviation are shown in Table 3.3 and Figure 3.8. The rheological properties and electrical conductivity of solutions directly affected the diameter of nanofibers. HPMC/PEO nanofibers with 2% gallic acid had the highest nanofiber diameter which was directly proportional with the viscosity of solutions. Higher k values of solutions caused nanofibers having larger diameters due to the increased molecular entanglement in the solution (Neo et al., 2013). The high viscosity was found to be the dominant factor to affect fiber diameter. The same trend was found by Phiriyawirut & Phaechamud (2012) in which increasing viscosity of solutions led to an increase in fiber diameter. Similarly, in the study of Blanco-Padilla, López-Rubio, Loarca-Piña, Gómez-Mascaraque, & Mendoza (2015), viscosity of solutions was found to affect nanofiber

diameter and as the viscosity of solutions increased, fiber diameter increased, too. As expected, the control HPMC/PEO nanofiber had the highest diameter value due to having the highest viscosity and the lowest electrical conductivity value. As shown in Figure 3.8, nanofibers had narrow diameter distribution and small standard deviations of diameter. Thus, it can be concluded that uniform gallic acid loaded electrospun nanofibers were obtained.

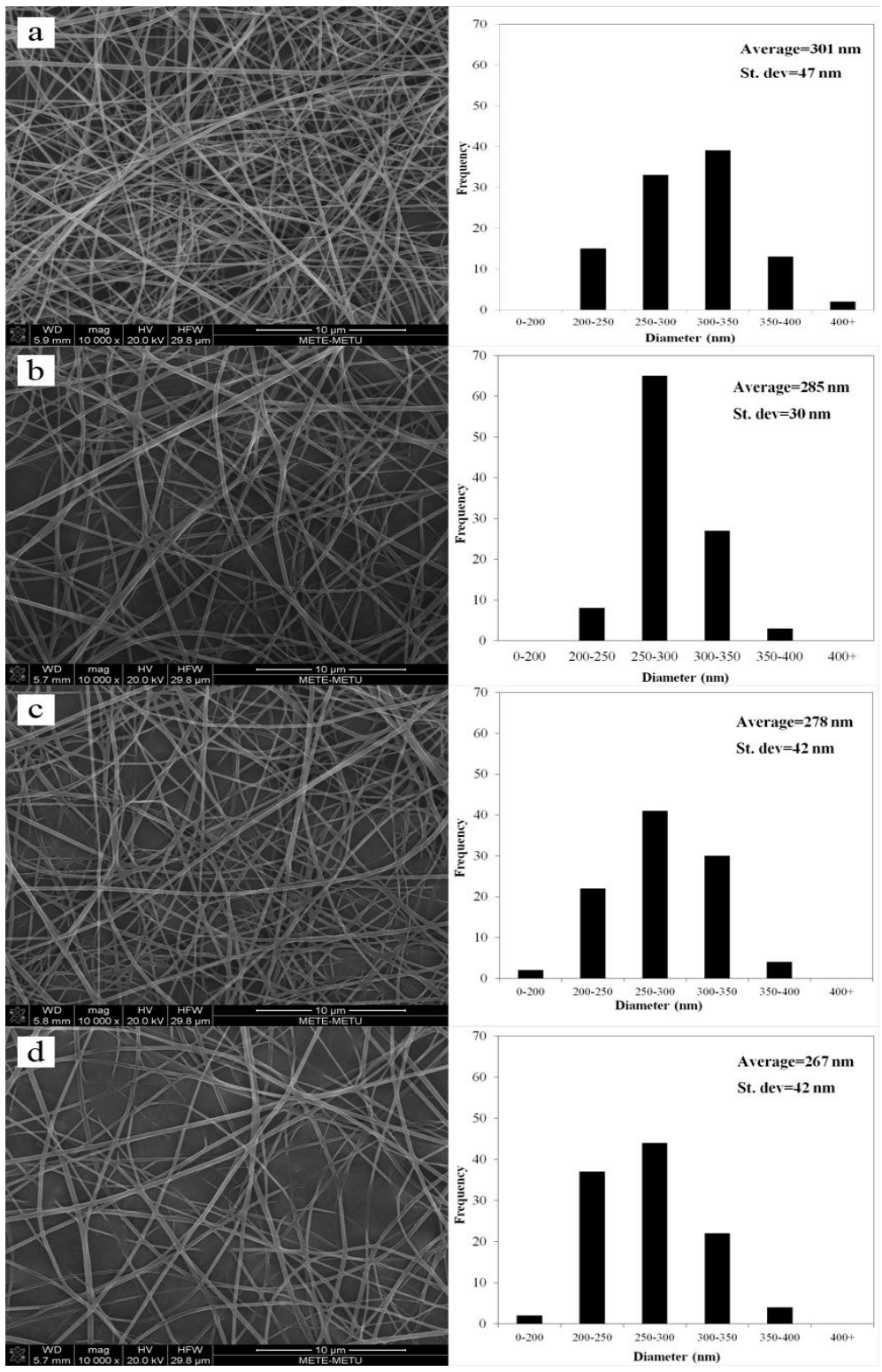


Figure 3.8 SEM images of electrospun nanofibers with different gallic acid concentration: a: control, b: 2%, c: 5%, d: 10%.

3.2.2.2. Loading efficiency and antioxidant activity of gallic acid in HPMC/PEO electrospun fiber

The loading efficiency of gallic acid within nanofibers is shown in Table 3.4. Nanofibers containing 10% gallic acid had significantly higher loading efficiency ($p \leq 0.05$). Gallic acid is a heat-sensitive antioxidant. Therefore, when encapsulating gallic acid, the most important criteria is the temperature of applied process. In the study of Robert, García, Reyes, Chávez, & Santos (2012), gallic acid was encapsulated with the native starch by spray drying and encapsulation efficiency ranged from 26.7% to 49.5% by changing gallic acid/starch ratio and process temperature. In another study, gallic acid extracted from blackberry was encapsulated by lyophilization in matrixes of β -cyclodextrin, chitosan, xanthan and hydrogel and encapsulation efficiencies were determined as 52, 75, 46 and 66 %, respectively (Cleonice Gonçalves Da Rosa et al., 2014). Although, lyophilization operates at low temperatures, again loss of gallic acid was observed depending on the coating material. Electrospinning is operated at room temperature so it is advantageous to encapsulate heat-sensitive bioactive compounds. In this study, by using electrospinning, gallic acid was successfully encapsulated in HPMC nanofibers by encapsulation. In the study of Tampau, González-Martinez, & Chiralt (2017), carvacrol was encapsulated in starch and poly- ϵ -caprolactone, at different concentrations by electrospinning and it was found that as the polymer concentration increased, the encapsulation efficiency increased, too. Therefore, higher polymer concentration (4/1, HPMC/PEO) was chosen to provide higher encapsulation efficiency of gallic acid.

Gallic acid has trihydroxyl groups and phenolic hydroxyl groups are important in showing a potential radical scavenging effect. The OH group at the para position to the carboxylic group is especially effective for antioxidant activity (Kim, 2007) . Therefore, gallic acid showed strong antioxidant activity. Total antioxidant activities of gallic acid loaded electrospun nanofibers are shown in Table 3.4. Gallic acid loaded HPMC/PEO nanofibers showed antioxidant activity that was the evidence of successful encapsulation with electrospinning. Moreover, as the gallic content of

nanofibers increased, the total antioxidant activities of nanofibers increased significantly ($p \leq 0.05$).

Table 3.4. *Loading efficiency and total antioxidant activities of gallic acid loaded HPMC/PEO electrospun nanofibers*

Nanofibers with different gallic acid concentration (%)	Gallic acid loading efficiency (%)	Antioxidant activity (mg DPPH/g dry weight)	
		AA (%)	
2	61.6±0.6 ^b	4.97±0.06 ^c	21.70±0.28 ^c
5	62.2±0.4 ^b	12.36±0.05 ^b	29.71±0.13 ^b
10	69.0±0.3 ^a	24.74±0.48 ^a	50.35±0.98 ^a

*Columns having different letters are significantly different ($p \leq 0.05$).

3.2.2.3. Thermo-gravimetric Analysis (TGA)

The weight loss curves of gallic acid, the control and gallic acid loaded HPMC/PEO fibers are shown in Figure 3.9. The control nanofibers showed one stage degradation that began at the onset temperature (T_{onset}) of 352 °C. It was found that T_{onset} of thermal degradation of HPMC/PEO nanofibers ranged between 340-370 °C (Figure 3.6). The T_{onset} of nanofibers depends on the ratio of HPMC and PEO. Nanofibers with 2% gallic acid had similar behavior with the control nanofiber having T_{onset} as 351°C. As the gallic amount in the nanofiber increased, the curve had shifted from one stage to two stage degradation. The first weight loss can be ascribed to degradation of gallic acid. Gallic acid exhibited two stage degradation that began at T_{onset} of 210°C and 320 °C which corresponded to the decomposition of gallic acid. Similarly, in the study of Aytac, Kusku, Durgun, & Uyar (2016), gallic acid showed two steps of weight loss, between 210 °C and 325 °C which corresponded to the decomposition of gallic acid. The temperature which gives the highest rate of weight loss in the derivative thermogravimetry (DTG) thermogram can be expressed as degradation temperature (T_d) of the component. The DTG curve showed that T_d of gallic acid was approximately 275°C that corresponded to melting temperature of a crystalline region.

When the DTG curve of nanofiber with 10% gallic acid was interpreted, it was observed that T_d value of gallic acid had shifted from 275 °C to around 250 °C. Due to the disrupted crystalline structure of gallic acid, T_d shifted to a lower temperature. The same result was found in the study of Neo et al. (2013) in which when the gallic acid was loaded in zein nanofibers, the T_d values interpreted from DTG curve decreased from 275 °C to 231 °C. The results obtained from TGA was the evidence of successful loading of gallic acid into HPMC/PEO electrospun nanofibers.

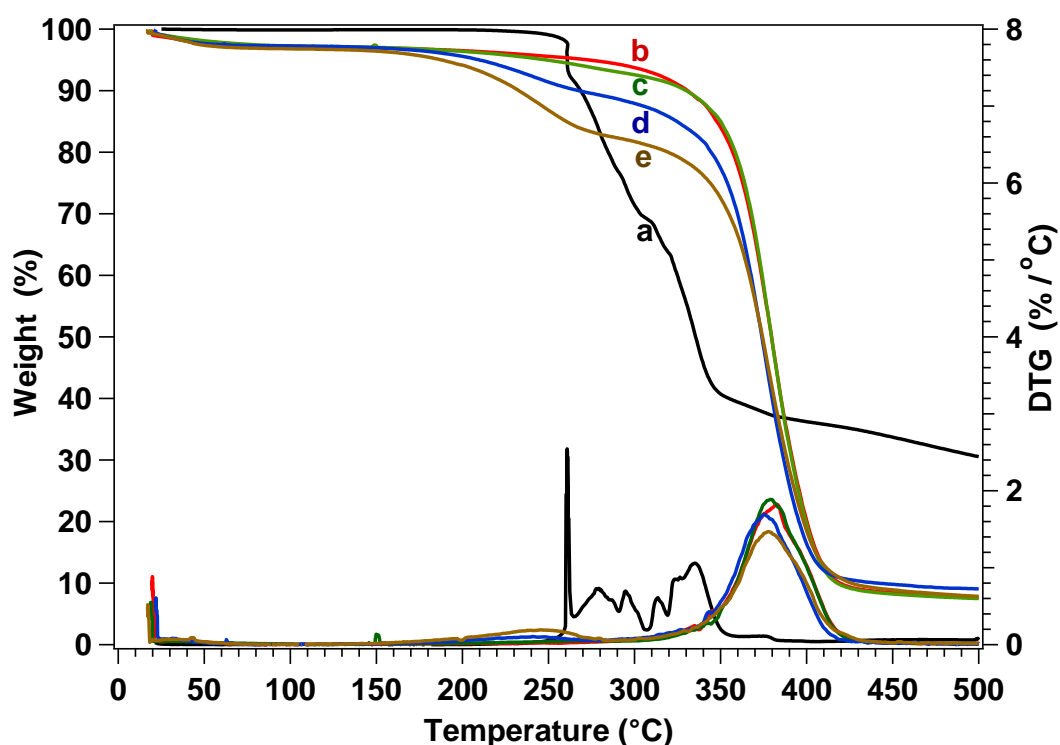


Figure 3.9 Thermo-gravimetric curves of gallic acid and electrospun nanofibers with different gallic acid concentration: a: gallic acid, b: control, c: 2%, d: 5%, e: 10%.

3.2.2.4. DSC Analysis

The DSC thermograms of gallic acid, the control and gallic acid loaded electrospun fibers are shown in Figure 3.10. Gallic acid demonstrated a sharp endothermic peak at 274°C which is attributed to melting point of crystal form of gallic acid. Similarly, in the study of Olga, Styliani, & Ioannis (2015), the melting point of crystal structure of gallic acid was stated as 267°C in DSC curve. The control and gallic acid capsulated

HPMC/PEO nanofibers exhibited endothermic peak at around 55°C which corresponds to the melting point of PEO. The melting point of pure PEO was found as 68 °C as stated in Section 3.1.2.5 but due to the disruption of the crystalline structure of PEO by interaction between PEO and HPMC, melting point of PEO might be depressed. Although gallic acid showed a characteristic peak at 274°C, this peak almost disappeared in DSC curves of gallic acid loaded nanofibers. This indicated that the incorporated gallic acid had lost its original crystalline structure and consequent encapsulation of gallic acid. In similar studies, the disappearance of melting endotherm peak of gallic acid were indicative of true inclusion complex and amorphization that was related to efficient loading (Cleonice Goncalves da Rosa et al., 2013; Olga et al., 2015).

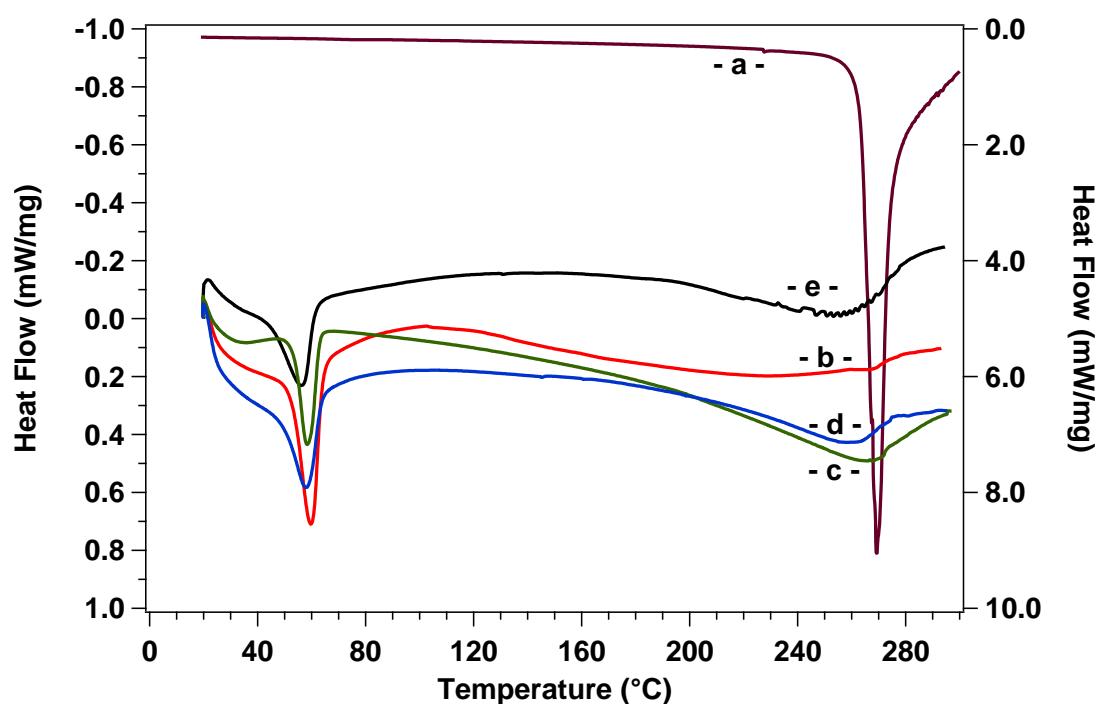


Figure 3.10 DSC curves of gallic acid and electrospun nanofibers with different gallic acid concentration: a: gallic acid, b: control, c: 2%, d: 5%, e: 10%.

3.2.2.5. FTIR Analysis

The ATR-FTIR spectra of gallic acid, control and gallic acid loaded HPMC/PEO nanofibers are presented in Figure 3.11. In Figure 3.11.e, several bands from

3300 cm^{-1} to 3800 cm^{-1} can be ascribed to $-\text{OH}$ stretching and hydrogen bonds between phenolic hydroxyl groups (Aceituno-Medina, Mendoza, Lagaron, & López-Rubio, 2015). The band at 1625 cm^{-1} corresponds to $\text{C}=\text{O}$ stretch of conjugated acids (Cleonic Goncalves da Rosa et al., 2013). The stretching and bending vibrations of aromatic ring are assigned by bands in the 1533 cm^{-1} and 1429 cm^{-1} . The bending vibrations of $\text{C}-\text{H}$ in the ring and $\text{O}-\text{H}$ of the phenol alcohol are mainly characterized by bands in the 1320-1022 cm^{-1} (Neo et al., 2013). These FTIR spectrum of gallic acid is consistent with those obtained by Olga et al. (2015) and Li, Kim, Chen, & Park (2016). Figure 3.11. a, b, c and d provides information of the functional groups present in the control and gallic acid loaded HPMC/PEO nanofibers. The whole nanofibers showed peak at 3460 cm^{-1} and 2885 cm^{-1} which corresponds to $-\text{OH}$ stretching and CH_2 stretching (methylene stretching), respectively (Lee et al., 2007). Aromatic ring stretching is observed at 1460 cm^{-1} commonly in all of the nanofibers. Moreover, nanofibers showed peak at 1100 cm^{-1} which the stretching vibrations of the $\text{C}-\text{O}-\text{C}$ complex and the crystallinity of PEO and peaks at around 844 cm^{-1} and 950 cm^{-1} are as a result of the $\text{C}-\text{O}$ stretching and CH_2 rocking, respectively (Pielichowski & Flejtuch, 2005). The spectra of nanofibers with 5% and 10% gallic acid indicated the additional bands due to the association with the gallic acid. The band at 1317 cm^{-1} in gallic acid spectrum were observed to shift to 1344 cm^{-1} for 5 % and 10% gallic acid containing nanofibers which could result from formation of gallic acid dimers or oligomers. As the gallic acid amount increased, new bands were observed in spectrum of nanofiber with 10% gallic acid. The additional bands at 1610 and 1703 cm^{-1} correspond to the $\text{C}=\text{O}$ stretch of conjugated acids that belongs to gallic acid. The obtained results confirm the interactions between gallic acid and HPMC/PEO nanofibers at molecular level which indicates the stability of gallic acid in nanofiber. Similarly, in the study of Neo et al. (2013), new bands and band shifting were observed in gallic acid loaded zein nanofibers as the evidence of successful encapsulation.

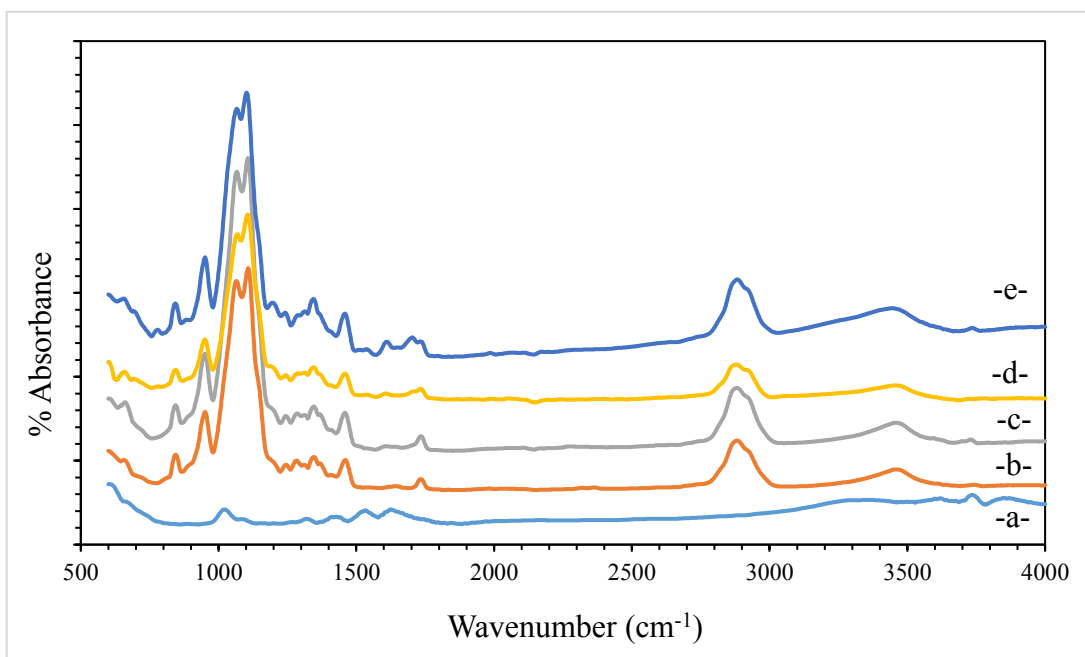


Figure 3.11 FTIR spectra of gallic acid and electrospun nanofibers with different gallic acid concentration: a: gallic acid, b: control, c: 2%, d: 5%, e: 10%.

3.2.3. Application of HPMC based nanofibers for packaging of walnuts

Walnut kernels have a lipid content of 65% (Vanhanen & Savage, 2006) of which 73% consists of polyunsaturated fatty acids (PUFA) (Crews et al., 2005). Due to having high amount of PUFA, walnuts were highly prone to oxidation. Therefore, prevention of oxidation is an important issue to increase shelf life of walnuts. Gallic acid loaded electrospun nanofibers can be an alternative to be used as active packaging material. To pack walnut, 10% gallic acid containing nanofibers were chosen due to higher loading efficiency and antioxidant activity (Figure 3.12). The peroxide, p-anisidin, totox and TBARS values of walnuts that were packed in polyamide/polyethylene packages without nanofiber and 10% gallic acid loaded nanofiber were shown in Table 3.5. Peroxide value is the measure of peroxides and hydroperoxides formed in the initial stages of lipid oxidation that is commonly used for the measurement of oxidative rancidity in oils and fats (Y. Zhang et al., 2010). As can be seen from the Table 3.5, peroxide value of control walnut was significantly

higher than walnut packed with nanofiber. Similarly, p-anisidin value of control one was significantly higher ($p \leq 0.05$). While the anisidine value was used as a measure of secondary oxidation products, while the totox value was an indication of overall oxidative stability (Pereira de Abreu, Paseiro Losada, Maroto, & Cruz, 2011). Walnuts packed in nanofiber containing packages had lower totox value than the control one. The TBARS value is an index of lipid oxidation measuring malondialdehyde (MDA) content (Zhang et al., 2010). Similarly, TBARS value of walnut that was stored in nanofiber containing packages was not significantly lower than the control walnut ($p > 0.05$). The oxidation analyses showed that gallic acid loaded nanofibers decreased the oxidation reaction occurred during storage when it was used as active packaging material. Gallic acid has strong antioxidant activity and prevents oxidation of oils and fats by displaying free radical scavenger (Kim, 2007). In this study, gallic acid was successfully incorporated into HPMC/PEO nanofiber by electrospinning and they showed antioxidant activity (Table 3.4). Thus, the usage of nanofibers as an active package material was found to be effective to prevent oxidation.

Table 3.5 Peroxide, p-anisidin, Totox and TBARS values of walnuts that packed in gallic acid loaded nanofibers containing packages

Package	<i>Peroxide value (PV)</i>	<i>p-anisidin (AnV)</i>	<i>Totox</i>	<i>TBARS</i>
Control	1.35±0.05 ^a	2.407±0.103 ^a	5.107 ^a	0.094±0.000 ^a
Package containing nanofiber	0.57±0.05 ^b	0.636±0.112 ^b	1.776 ^b	0.088±0.000 ^a

*Columns having different letters are significantly different ($p \leq 0.05$).



Figure 3.12 The packaged walnuts: A: packaged with 10% gallic acid loaded nanofibers, B&C: control

3.3. Fabrication of gallic acid loaded lentil flour/PEO nanofibers with electrospinning

3.3.1. Physical properties of solutions

Upon preliminary experiments, to encapsulate gallic acid into lentil flour based nanofibers, lentil flour/PEO ratio was chosen as 5.25/3.5 (w/v).

3.3.1.1. Rheological properties

Consistency index (k) and flow behavior index (n) values of solutions are shown in Table 3.6. All solutions containing gallic acid prepared at different pH values obeyed the Power Law with a high coefficient of determination ($r^2=0.998-0.999$). Lentil flour contained about 22% protein which was enough to be affected by pH. Molecular net charge of proteins depends on pH of solutions and at isoelectric point, there is no net charge on the proteins. The isoelectric point (pI) of lentil protein was pH 4.5 (Bamdad, Goli, & Kadivar, 2006). Above and below isoelectric point, proteins carry negative and positive charges, respectively. In general, the solubility of proteins depends on the net charges that are related to pH of solutions. Protein represents minimum solubility at pH adjusted to pI. As the net charge of proteins increases, proteins become more unfolded and solubility of proteins increased, too (Pelegri & Gasparetto, 2005). Therefore, rheological properties of solutions strongly depend on pH values. As can be seen in Table 3.6, n ranged between 0.89 and 0.95 which were smaller than 1. It

could be inferred that the solutions showed pseudo-plastic (shear-thinning) behavior. With increasing pH, n values of solutions decreased indicating more non-Newtonian-like behavior. Similarly, in the study of Xu, Carson, & Kim (2015), as the pH of wheat protein isolate solutions increased, solutions shifted from Newtonian behavior to Non-Newtonian, with a decrease in n value. In this study, to increase solubility of lentil flour proteins, pH was adjusted to acidic and alkaline conditions. It can be observed that k values of alkaline solutions were significantly higher than that of acidic solutions ($p \leq 0.05$). This could be related to the degree of unfolding of flour protein being greater at alkaline than at the acidic pH values (Ahmed, Mohamed Ahmed, Eltayeb, Ahmed, & Babiker, 2011). As going far away from pI values, the solubility of protein, and also viscosity of solutions increased. In the study of Oguz, Tam, Aydogdu, Sumnu, & Sahin (2018), the solutions prepared at alkaline conditions showed higher viscosity values than the neutral ones. The addition of gallic acid to acidic solutions did not change k values of solutions. However, in alkaline solutions, addition of gallic acid decreased k values. After gallic acid was added to solutions, pH of solutions decreased to about pH 3, and it was necessary to adjust it again to alkaline value before electrospinning process. Dilution effect of NaOH solution caused the decrease in k values of solutions. Another reason could be explained as the addition of gallic acid might reduce the intra and intermolecular forces between PEO and lentil flour polymer blending to a certain extent. Similar results were obtained when gallic acid was incorporated into the chitosan gallates. It was recorded that higher amount of gallic acid was more detrimental for basic chitosan linkages and resulted in lower k values (Wu et al., 2016).

3.3.1.2. Electrical conductivity

The electrical conductivity values of solutions prepared at different pH values are shown in Table 3.6. Gallic acid addition to solutions increased electrical conductivity values of solutions significantly ($p \leq 0.05$). In the study of Chuysinuan et al. (2009) an increase in electrical conductivity of solutions was observed with the addition of gallic acid to Poly(L-lactic acid) solutions and the reason was associated with the

dissociation of gallic acid into ionic species. Moreover, due to dilution effect of gallic acid, viscosity of solutions decreased, and mobility of ions could be easier which could cause an increase in electrical conductivity. pH was the important parameter that affected the electrical conductivity. As mentioned before, as the pH of solutions was moved away from pI of solutions, the net charge of solutions increased so electrical conductivity of solutions increased, too. There are some studies that confirm this relation. In the study of Tam, Oguz, Aydogdu, Sumnu, & Sahin (2017), pH of lentil flour solutions was adjusted to alkaline conditions and it was observed that they had higher electrical conductivity than neutral pH which was close to isoelectric point of lentil protein. Likewise, Sullivan, Tang, Kennedy, Talwar, & Khan (2014) prepared whey protein isolate based solutions at pH 7.5 and 2, and it was stated that conductivity of solutions increased with decreased pH. Moreover, as can be seen from Table 3.6, acidic solutions had higher conductivity values than alkaline solutions ($p \leq 0.05$). This can be related to the difference between viscosity of solutions. Lower viscosity enabled to the movement of charges faster and easier so resulted higher electrical conductivity.

Table 3.6 *Rheological properties, electrical conductivities, and TPC of solutions and average diameter of nanofibers*

Gallic acid (%)	pH	k ($Pa s^n$)	n	Electrical Conductivity ($\mu S/cm$)	TPC of solutions (mg gallic acid equivalence (GAE) / g dry matter)	Average Diameter (nm)
0	10	2.12±0.05 ^a	0.89 ±0.02 ^c	1800±8 ^d	4.99±0.32 ^c	208±49 ^c
10	10	1.03±0.03 ^b	0.92±0.01 ^b	5185±35 ^c	34.68±1.49 ^b	184±52 ^d
0	1	0.72±0.02 ^c	0.95±0.02 ^a	24300±100 ^b	5.31±0.11 ^c	334±61 ^a
10	1	0.63±0.01 ^c	0.95±0.01 ^a	28550±150 ^a	143.74±3.42 ^a	307±74 ^b

*Columns having different letters are significantly different ($p \leq 0.05$).

3.3.2. Characterization of electrospun nanofibers

3.3.2.1. Fiber morphology

Based on preliminary experiments, when the solution containing pure lentil flour was electrospun, beaded nanofibers were obtained. Therefore, PEO was mixed with lentil flour in order to increase electrospinnability of solutions. Lentil flour contains lysine and arginine (Aydogdu, Kirtil, Sumnu, Oztop, & Aydogdu, 2018) and PEO has electron-rich oxygen in the backbone polymer chain and it could interact with positively charged lysine and arginine (Ramji & Shah, 2014). These interaction between PEO and amino acids increases the electrospinnability of solutions.

The SEM images, the average diameters and size distribution of the electrospun nanofibers are shown in Figure 3.13. Besides the other polymers, the electrospinnability of protein solutions strongly depends on whether the proteins are dissolved in solutions or not. Ramji & Shah (2014) investigated the electrospinnability of soy proteins and it was concluded that unfolding of proteins played critical role on bead free nanofiber formation and the more the number of unfolded protein chains induced the easier formation of continuous fibers during the electrospinning process. All nanofibers had bead free structure. As mentioned before, pH of solutions was adjusted far away from its isoelectric point to increase not only the solubility of proteins in lentil flour but also electrospinnability of the solutions. In the study of Tam et al. (2017), structure with beads was observed when solutions were at pH 7 but alkaline pH values (10 and 12) resulted in perfect homogenous structure. Similarly, Cho, Nnadi, Netravali, & Joo (2010) reported that at pH 7 soy protein based homogenous nanofibers could not be obtained but when the pH of soy protein solutions was increased to 12, bead formation decreased, and homogenous nanofibers could be produced. By considering these results, in this study pH was adjusted to acidic and alkaline values. However, although nanofibers prepared at pH 1 had bead free structure, the fibers got stuck to each other at some points. In electrospinning process, the solvent of solution must be evaporated by the electrical field. When the

solvent does not evaporate completely, the nanofibers can stick to each other. The reason of insufficient evaporation could be related to higher electrical conductivity values of solutions at pH 1 (Table 3.6). Solutions with higher conductivity experienced higher attractive force through the collector. When solution travels faster from tip of the nozzle to the collector, time required for evaporation of solvent becomes insufficient. This causes fusion of fibers and leads to higher diameters (Bhardwaj & Kundu, 2010). Increasing fiber diameter with conductivity was also observed in inclusion of tannin acid Fe^{+3} complexes into cellulose acetate fibers. Increasing concentration of complex from 1% to 2% in formulation also increased conductivity of solutions but led to a change in fiber diameter from 281 ± 131 nm to 343 ± 142 nm (Yang et al., 2017). Moreover, nanofibers at pH 1 had broad range in fiber diameter distribution compared to fibers obtained by spinning of solutions at pH 10, which might be due to the bending instability of highly conductive solutions under electric field (Bhardwaj & Kundu, 2010). When the effect of gallic acid addition was examined, a significant decrease was observed in average diameter at the same pH value. The reason could be related to viscosity and electrical conductivity values of solutions. While gallic acid addition decreased the viscosity of solutions, electrical conductivity of solutions increased (Table 3.6). Solutions with higher viscosity showed lower stretching and shorter jet path that resulted in higher diameters of nanofibers (Ramakrishna, Fujihara, Teo, Lim, & Ma, 2005b). The same trend was observed in Section 3.1.2.1 in which increasing viscosity due to higher HPMC concentration led to an increase in fiber diameter. Furthermore, up to a certain point, higher conductivity was interpreted as thinner fiber formation. In the study of Kriegel et al. (2009b), when the solutions having higher electrical conductivity values was used, nanofibers with smaller diameter were obtained. Gallic acid addition increased the electrical conductivity of solution and this synergistic effect of both decreasing viscosity and increasing electrical conductivity with the addition of gallic acid was the reason of decreasing fiber diameter.

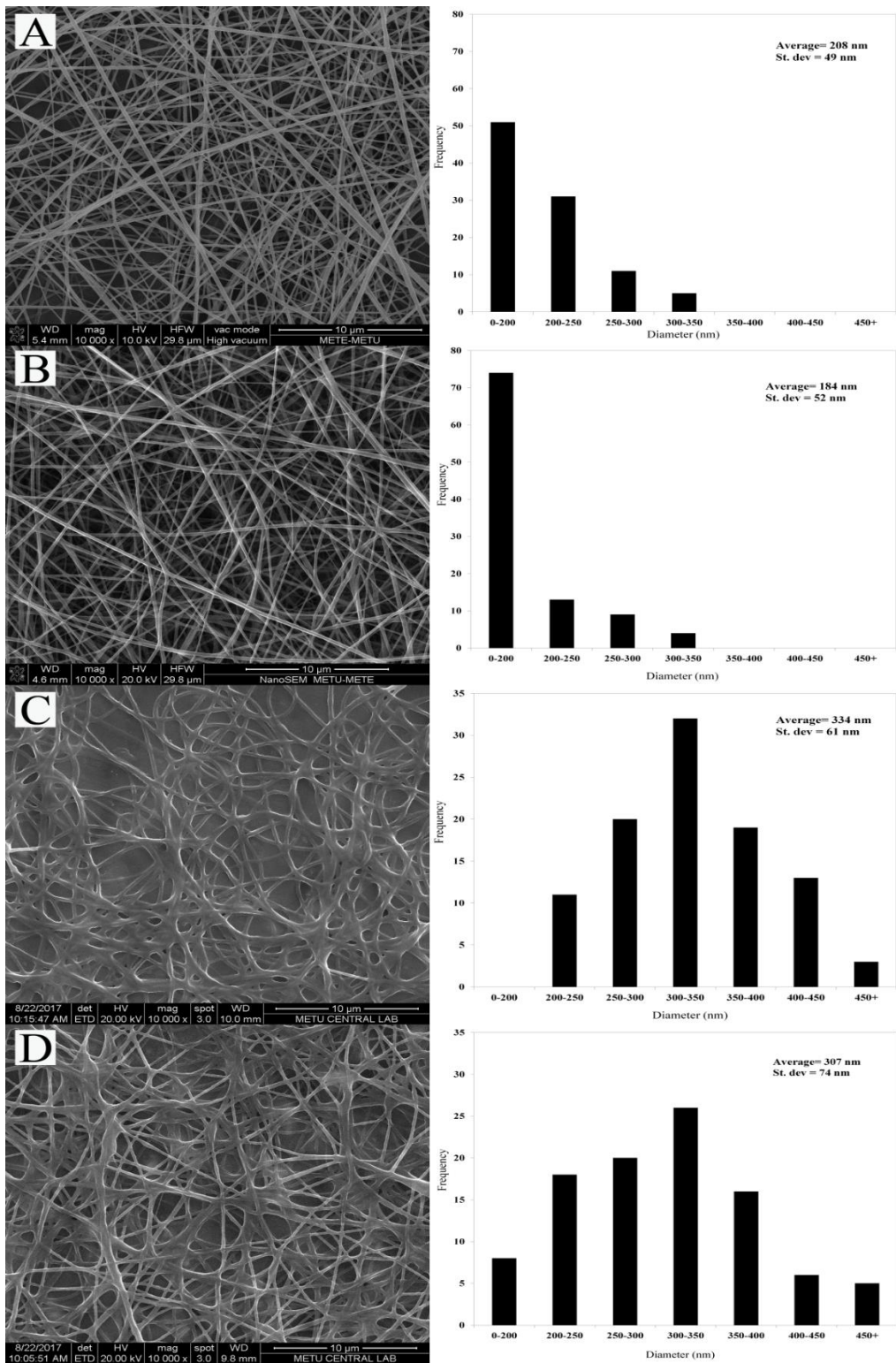


Figure 3.13 SEM images of electrospun nanofibers, A: pH10_nogallicacid, B: pH10_gallic acid. C: pH1_nogallicacid, D: pH1_gallic acid.

3.3.2.2. Total phenolic content (TPC) and antioxidant activity of solutions and nanofibers

TPC of lentil flour solutions before and after gallic acid addition at different pH values are shown in Table 3.6. TPC of lentil flour solutions at acidic and alkaline pH values was about 4.99 and 5.31 mg GAE / g dry matter, respectively. This was indication of the fact that lentil flour contained phenolic compounds. Protocatechuic acid, gentisic acid, p-coumaric acid were some of the phenolic compounds in lentil flour (Bartolomeo, Estrella, & Hernandez, 1997). Gallic acid (3,4,5-trihydroxybenzoic acid) is a natural phenolic compound (Phiriyawirut & Phaechamud, 2012). Therefore, when gallic acid was added to solutions, TPC values of solutions increased significantly. However, as can be seen from Table 3.6, although the same amount of gallic acid was added to lentil flour solutions, at different pH values TPC value of acidic solution was much higher than that of the alkaline solutions. In the study of Friedman & Jü (2000), the effect of pH on stability of phenolic compounds was examined and it was found that caffeic, chlorogenic and gallic acids were not stable at high pH values and the destruction was irreversible. Gallic acid like caffeic and chlorogenic acids has phenolic -OH groups and no carbon-carbon double bond conjugated to the benzene ring. The degradation was associated with this common structure properties (Friedman & Jü, 2000). Similarly, in this study gallic acid was destructed due to high pH of alkaline solutions. The solutions at different pH was used in electrospinning process and the TPC values of nanofibers are shown in Table 3.7. Nanofibers at acidic pH values had higher TPC values than alkaline ones. The reason could be explained by the difference between TPC values of the solutions. As stated before, acidic solutions had higher TPC than alkaline solutions. That's why, although the process conditions were the same, TPC values of nanofibers were significantly different. Gallic acid is unstable at high temperatures and in the presence of oxygen and light. Therefore, the temperature of encapsulation process is the significant parameter that must be considered (Cleonic Goncalves da Rosa et al., 2013). Electrospinning is operated at room temperature, so it is an effective way to encapsulate heat-sensitive compounds.

In this study, gallic acid was successfully encapsulated into lentil flour-based nanofibers. The results of loading efficiency of gallic acid into nanofibers are shown in Table 3.7. Loading efficiency of gallic acid prepared at acidic conditions were significantly higher than the ones prepared at alkaline conditions ($p \leq 0.05$). It could again be related to initial gallic acid concentration of solutions. Alkaline pH values destroyed the gallic acid in solutions so the total loading efficiency of it was lower. Gallic acid has OH group at the para position to the carboxylic group and due to having this specific property, it shows antioxidant activity (Kim, 2007). Table 3.7 represents antioxidant activity of gallic acid loaded nanofibers. As can be seen, nanofibers at pH 1 showed higher antioxidant activity than the nanofibers at pH 10. This was directly correlated with gallic acid content of nanofibers. Since alkaline pH destructed the gallic acid, nanofibers prepared at acidic pH value had higher amount of gallic acid than alkaline ones. Although there was a decrease in antioxidant activity of nanofibers at pH 10, both nanofibers showed antioxidant activity (Table 3.7). This was the evidence of successful encapsulation of gallic acid with electrospinning technique. Similar antioxidant values of active agent encapsulated nanofibers were obtained by electrospinning. In the study of Hosseini, Nahvi, & Zandi (2019), antioxidant peptide was encapsulated into chitosan/PVA electrospun nanofibers and it was reported that with using different amount of peptide the antioxidant activities of nanofibers were found in the range of 20-60%.

Table 3.7 Loading efficiency and total antioxidant activities of gallic acid loaded lentil flour based electrospun nanofibers prepared at different pH values

pH	TPC of nanofibers (mg gallic acid equivalence (GAE) / g dry matter)	Gallic acid loading efficiency (%)	Antioxidant activity (mg DPPH/g dry weight)	AA (%)
1	89.49±6.82 ^a	62.2±4.7 ^a	20.93±0.79 ^b	74.24±1.04 ^a
10	7.01±0.35 ^b	20.6±0.8 ^b	1.63±0.11 ^a	34.03±0.48 ^b

*Columns having different letters are significantly different ($p \leq 0.05$).

3.3.2.3. Thermo-gravimetric analysis (TGA)

The weight loss versus temperature curves of nanofibers and gallic acid are shown in Figure 3.14. All electrospun nanofibers showed two stage degradation. The onset temperatures of first degradation (T_{onset}) were in the range of 200-300 °C. The first weight loss corresponded to the decomposition of the polysaccharide. Similarly, in the study of Dick et al. (2015), edible films were produced from chia seed mucilage and in TGA experiment, weight loss above 250°C was correlated to the decomposition of the polysaccharide. When the nanofibers prepared at acidic and alkaline conditions were compared, it was observed that T_{onset} of acidic nanofibers was lower than alkaline ones. It can be stated that nanofibers prepared at pH 10 had a higher stability towards thermal degradation than nanofibers prepared at pH 1. That was the indication of having weaker intermolecular forces between protein molecules at acidic pH. The T_{onset} of second degradation of nanofibers was about 400 °C. In fact, in the study of (Aydogdu et al., 2018), the main T_{onset} of lentil flour films was found as about 280 °C. Therefore, the second additional weight loss step change at 400 °C belongs to degradation of PEO. Nanofibers were composed of both lentil flour and PEO so they had two stage degradation and showed the same second degradation pattern without pH effect. Moreover, gallic acid represented two stage degradation with T_{onset} of 210 °C and 320 °C which corresponded to the decomposition of gallic acid. When the gallic acid were added to nanofibers prepared at acidic and alkaline conditions, T_{onset} of nanofibers decreased. This could be related to decrease in the number of protein–protein bonds which resulted in lower thermal stability of these samples in the presence of gallic acid (Marina Patricia Arrieta, Parres, López, & Jiménez, 2013) . The reduction in thermal stability was the evidence of successful loading of gallic acid into lentil flour based electrospun nanofibers.

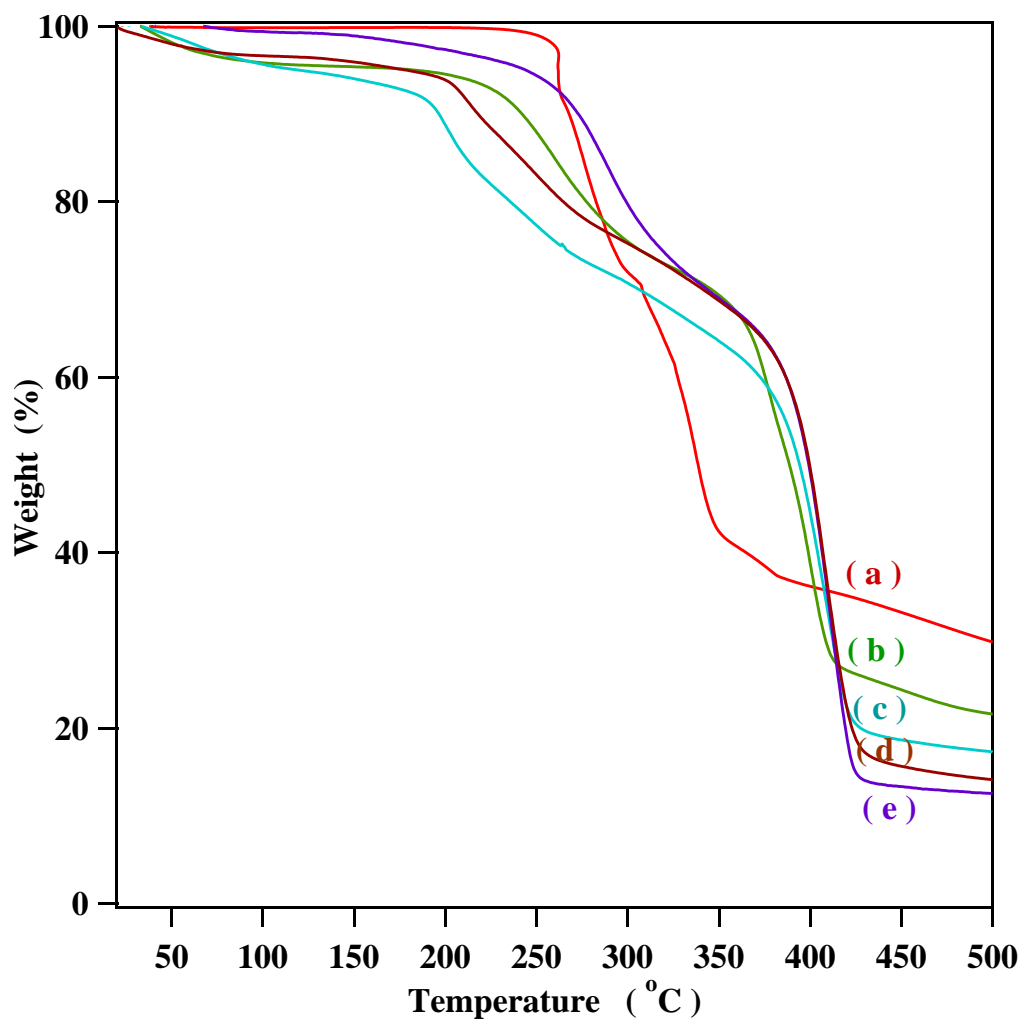


Figure 3.14 Thermo-gravimetric curves of gallic acid and electrospun nanofibers: a: gallic acid, c: pH10_gallicacid, d: pH1_gallicacid. e: pH1_nogallicacid, f: pH10_nogallicacid.

3.3.2.4. Differential scanning calorimetry (DSC) analysis

The DSC thermograms of nanofibers and gallic acid are shown in Figure 3.15. It was obviously seen that gallic acid had an endothermic peak at 275 °C which was melting point of crystal form of gallic acid. Similarly, in the study of (Singh, Singh Maniyari Rawat, Semalty, & Semalty, 2011), the melting point of gallic acid was reported as 263 °C. When the DSC curves of gallic acid loaded nanofibers were examined, no

enthalpic peak related to gallic acid was observed. This indicated that gallic acid lost its original crystalline structure. In similar study, da Rosa et al. (2013), gallic acid encapsulated into chitosan, β -cyclodextrin and xanthan and it was observed that the melting peak of gallic acid disappeared as an evidence of the amorphization and encapsulation of gallic acid. In the encapsulation study by (Pralhad & Rajendrakumar, 2004), quercetin demonstrated enthalpic peak at 322 °C but when it is encapsulated into polymers, the characteristic peak disappeared due to interaction between components. It could be taken as an indication of quercetin inclusion complex and successful encapsulation. The phenomenon was valid to this study and the disappearance of endothermic peak was related to amorphization of gallic acid and evidence of encapsulation. Nanofibers showed another peak at about 62°C corresponding to melting point of PEO. In fact, the melting point of pure PEO was found as 68 °C. That was indication of depressed melting point of PEO. The decrease in melting temperature of PEO could be related to disruption of the crystalline structure of PEO due to interaction between PEO and lentil flour and also gallic acid. Nanofiber composed of both PEO and lentil flour. In fact, the gelatinization temperature of lentil flour was between 63 and 67 °C (Barbana & Boye, 2013). However, during preparation the lentil flour solutions heated up to 80°C and starch gelatinization completed. Therefore, the gelatinization peak could not be seen in DSC curves.

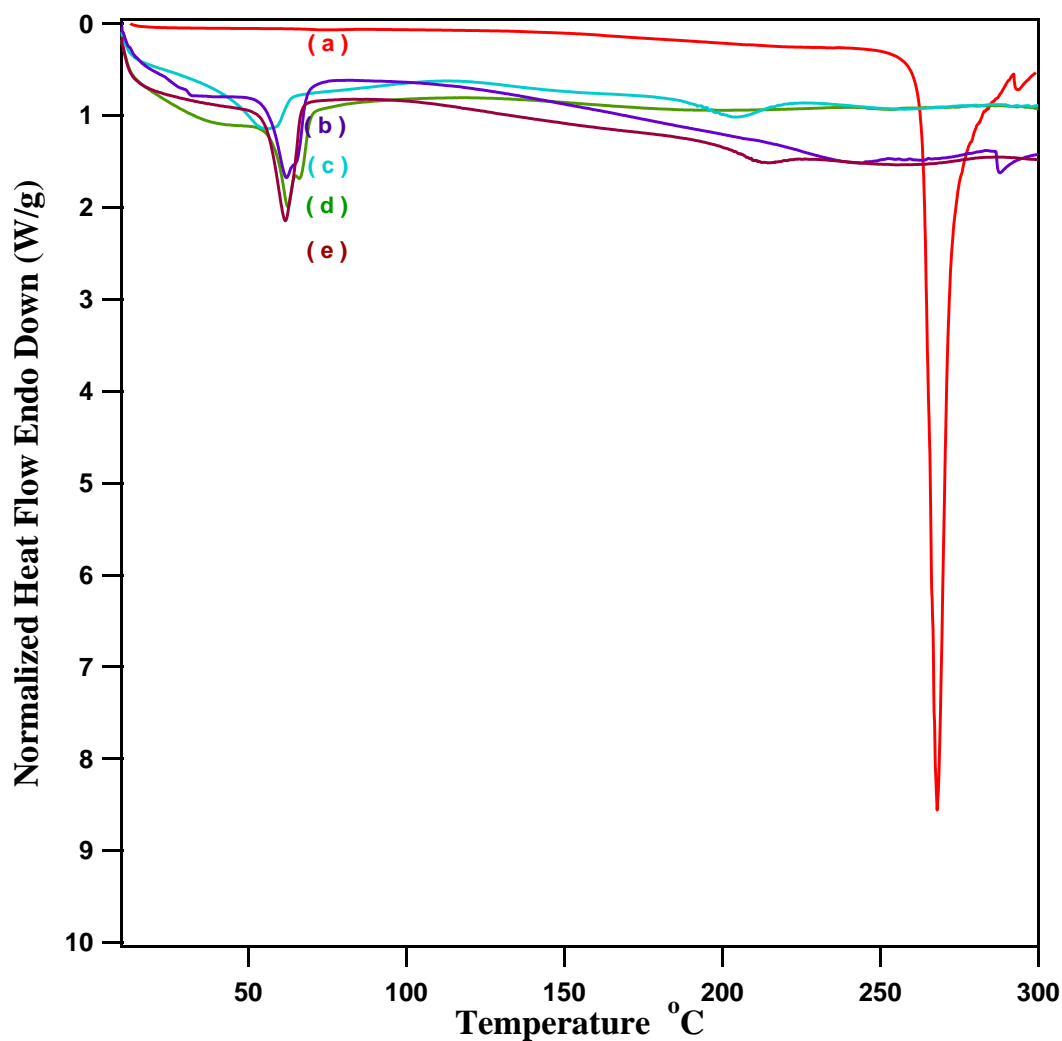


Figure 3.15 DSC curves of gallic acid and electrospun nanofibers, a: gallic acid, b: pH10_nogallicacid, c: pH1_gallicacid, d: pH10_gallicacid, e: pH1_nogallicacid.

3.3.2.5. FTIR analysis

The ATR-FTIR spectra of nanofibers, lentil flour and gallic acid are presented in Figure 3.16. In general, it was defined as $800\text{-}1600\text{ cm}^{-1}$ (the fingerprint region), the region between 2800 and 3000 cm^{-1} (C-H stretch region), and finally the region between 3000 and 3600 cm^{-1} (O-H stretch region). Lentil flour was composed of starch and proteins. That's why, nanofibers represented characteristics of both starch and protein. Nanofibers showed peak at 1460 cm^{-1} which was attributed to the CH_2

deformation and $1342\text{-}1360\text{ cm}^{-1}$ due to the bending modes of C-H (Kizil, Irudayaraj, And, & Seetharaman, 2002). The bands were located at $1240\text{-}1280\text{ cm}^{-1}$ associated with CH_2OH related deformation that was characteristic of the V-form amylose (Cael, Koenig, & Blackwell, 1975). The peaks at $960\text{-}990\text{ cm}^{-1}$ in the spectra of both lentil flour and nanofibers were attributed to the vibrations originating from the C-O-C of $\alpha\text{-}1,4$ glycosidic linkages (Kizil et al., 2002). Similarly, in the study of Pelissari et al. (2013), the bands at 926 cm^{-1} were observed in the spectrum of banana flour and starch film. The location differences of this band might be due to the presence of amylopectin $\alpha\text{-}1,6$ bonds as stated by Pelissari et al. (2013). The peaks were observed at 1643 and 1543 cm^{-1} in lentil flour spectra and they were associated with the Amide I and Amide II groups of proteins particularly to the C=O stretching, respectively (Valenzuela, Abugoch, Tapia, & Gamboa, 2013). Lentil flour films characterized in the study of Aydogdu, Kirtil, et al. (2018) had similar FTIR spectrum (bands at 1613 , 1430 , 1300 , 925) which were associated with protein and starch composition of lentil flour. Nanofibers were composed of not only lentil flour but also PEO, so all nanofibers had the characteristic peaks of PEO. As defined in Section 3.1.2.3, a triplet peaks at 1058 , 1095 and 1145 cm^{-1} were seen in the fingerprint region of pure PEO and it was correlated to the stretching vibrations of the ether bond or C-O-C complex. In Figure 3.16, the spectrum of nanofibers exhibited to max absorption at 1100 cm^{-1} and relatively small peaks at about 1058 and 1147 cm^{-1} . As stated before, the changes in the intensity and wavelength of C-O-C stretching was related to destruction of crystalline structure of PEO by the interaction between PEO and lentil flour. Moreover, the peak at 840 cm^{-1} just seen in nanofiber spectrums was attributed to C-O stretching, C-C stretching, CH_2 rocking of PEO (Pielichowski & Flejtuch, 2005) and the peak at 2900 cm^{-1} corresponded to CH_2 stretching (methylene stretching) (Lee et al., 2007). It is worth mentioning that the peaks observed in the region 3000 and 3500 cm^{-1} and centered around 3300 cm^{-1} were assigned to the stretching of the -OH groups due to the presence of hydrogen bonds in the studied specimen (Chen, Mo, & Qing, 2007). The intensity of that peak at 3300 cm^{-1} was higher for nanofibers prepared at acidic pH value. This could be due to the fact that at pH below the

isoelectric point of proteins (pH 4.5), the proteins could be highly protonated and so could exhibit more hydrogen bonding (Sullivan et al., 2014). A closer look to the gallic acid spectrum, the peaks were observed at 1024 and 1320 cm^{-1} . In the study of (Neo et al., 2013), bands at 1320-1022 cm^{-1} were attributed to the bending vibrations of C–H in the ring and O–H of the phenol alcohol. When the spectrum of gallic acid loaded and unloaded nanofibers were compared, gallic acid loaded nanofibers represented peaks at 1022 and 1330 cm^{-1} that were associated with the presence of gallic acid. Thus, this was the evidence of successful encapsulation. The shifting of peaks could be resulted from formation of gallic acid dimers or oligomers (Neo et al., 2013). Moreover, the intensity of peaks associated to gallic acid was lower in nanofibers prepared at alkaline condition. As stated before, gallic acid was not stable at alkaline conditions so the amount of gallic acid was lower in nanofibers at pH 10.

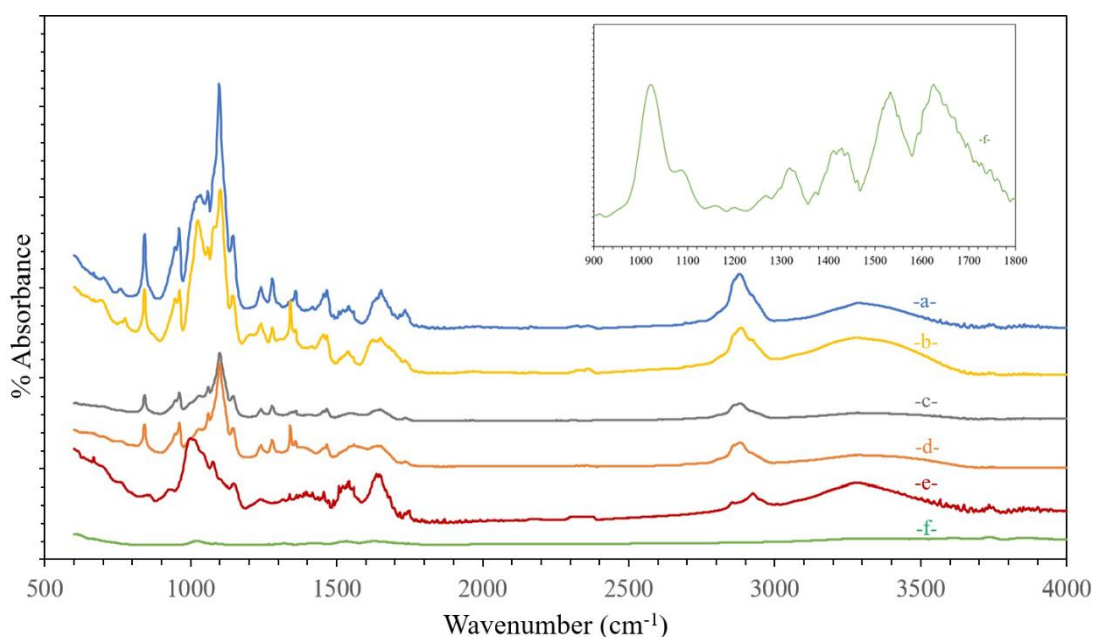


Figure 3.16 FTIR spectra of electrospun nanofibers, gallic acid and lentil flour, A: pH1_nogallicacid, B: pH1_gallicacid. C: pH10_nogallicacid, D: pH10_gallicacid, E: lentil flour, F: gallic acid

3.3.3. Application of lentil flour based nanofibers for packaging of walnuts

To be used as an active packaging material, in this study gallic acid loaded nanofibers prepared at alkaline pH was chosen. Although nanofibers at acidic pH had higher

antioxidant activity, when the morphology was examined, the fibers stuck to each other at some points due to solvent evaporation problem (Figure 3.13). Therefore, to pack walnuts alkaline nanofibers having homogeneous and smooth structure were used. Nanofibers were directly electrospun on PLA sheets and walnuts were packed in these sheets having nanofibers on the inner side for food contact (Figure 3.17). The peroxide, p-anisidine, Totox and TBARS values of walnuts that were packed in packages containing no nanofiber and gallic acid loaded nanofiber were shown in Table 3.8. Peroxides are the primer products of lipid oxidation and peroxide value is a measure of the concentration of peroxides and hydroperoxides (Zhang et al., 2010). Determination of peroxide value has been used for the measurement of oxidative rancidity in fats and oils. While peroxide value of walnuts packed in nanofibers had 1.3 meq O₂/kg walnut oil, the control walnuts had significantly higher peroxide value with 2.3 meq O₂/kg walnut oil (Table 3.8). It is worth to note that the oxidation of walnuts packed without gallic acid loaded nanofibers had higher than the walnuts packed by using nanofibers. In the study of (Cozmuta et al., 2018), peroxide values which are below the value of 2 meq O₂/kg are considered as the average of acceptable quality range. In that study, it was also reported that when TiO₂ and Ag was used as active agent, the oxidation level of walnuts during storage was kept below acceptable level. Similarly, in the study of de Moraes Crizel et al. (2018), microparticles of olive pomace flour in chitosan-based film was found to be effective in minimizing oxidation of walnuts during storage. Table 3 also shows p-anisidine values of walnuts. The p-anisidine measures the content of aldehydes (mainly 2-alkenals and 2,4-dienals) that are formed due to breakdown of hydroperoxides (Nawab, Alam, Haq, Lutfi, & Hasnain, 2018). At a certain point, determination of p-anisidine value gives an idea of the oxidation of oil. p-Anisidine value of control walnuts was found to be significantly higher (p≤0.05). It was deduced that gallic acid loaded nanofibers showed significant protective effect against to secondary lipid oxidation. In a similar study, carnosic acid represented inhibitory effects on p-anisidine value as antioxidant compound (Zhang et al., 2010). While p-anisidine value is a measure of secondary oxidation products, Totox value is used an indication of overall stability of oxidation (Pereira de Abreu et

al., 2011). As can be seen in Table 3.8, Totox value of control walnuts was significantly higher than walnuts packed with active packaging method ($p \leq 0.05$). Pereira de Abreu et al. (2011) extracted phenolic compounds from barley husks and used them to prepare the active packaging by a coating of blue sharks. It was observed that phenolic compounds showed antioxidant activity and coated samples had lower Totox value. However, in the same study, no significant differences between the TBARS values after storage was observed. TBARS value is another sign of lipid oxidation measuring malondialdehyde (MDA) content but there was no difference between walnut samples. As stated before gallic acid had strong antioxidant activity and it prevented oxidation of fats and oils acting as free radical scavenger (Kim, 2007). Therefore, it was found that the usage of gallic acid loaded nanofibers as active packaging material played an important role to reduce oxidation during storage.

Table 3.8 Peroxide, *p*-anisidine, Totox and TBARS values of walnuts that packed in gallic acid loaded nanofibers containing packages

Package	Peroxide value (PV) (meq O ₂ /kg walnut oil)	<i>p</i> -anisidine (AnV)	Totox	TBARS
Control	2.3±0.1 ^a	2.101±0.230 ^a	6.701 ^a	0.118±0.004 ^a
Package containing nanofiber	1.3±0.1 ^b	1.075±0.112 ^b	3.675 ^b	0.104±0.001 ^a



Figure 3.17 The packaged walnuts: A: control and B: packaged with gallic acid loaded nanofibers on PLA sheets.

3.4. Fabrication of gallic acid loaded pea flour/PEO nanofibers with electrospinning

With regarding to preliminary experiments, to encapsulate gallic acid into pea flour based nanofibers, lentil flour/PEO ratio was chosen as 5.25/3.5 (w/v).

3.4.1. Physical properties of solutions

3.4.1.1. Rheological properties

The rheological properties of solutions are shown in Table 3.9. The viscosity of solutions depends on the polymer type, concentration of polymer and solvent type. In this study, solutions contained the same amount of pea flour and PEO and gallic acid concentration was the only changing parameter. As can be seen from Table 3.9, both control solution and solutions containing gallic acid represented Non-Newtonian shear thinning behavior ($n < 1$). That is apparent viscosity of the solutions decreased with increase in the shear rate. Moreover, all the solutions obeyed the Power Law with a high coefficient of determination ($r^2 = 0.997-0.999$). Pea flour/PEO solution containing no gallic acid had the highest k value. When the gallic acid was added to the solutions, the k values of solutions decreased, significantly. Although all the solutions had the same amount of polymer concentration, the apparent viscosity of gallic acid added

solutions was lower. Gallic acid was dissolved in ethanol/water solution and this solution was added to polymer solution. Therefore, the decrease in k value can be explained by the dilution effect of gallic acid solution.

Table 3.9 *Rheological properties, electrical conductivities, TPC of solutions and average diameter of nanofibers*

Gallic acid (%)	k ($Pa s^n$)	n	Electrical Conductivity ($\mu S/cm$)	Average Diameter (nm)	TPC of solutions (mg gallic acid equivalence (GAE) / g dry matter)
0	2.66±0.01 ^a	0.85±0.01 ^b	1419±3 ^c	297±68 ^a	9.42±0.49 ^c
5	2.29±0.06 ^b	0.88 ±0.02 ^a	13700±126 ^b	219±48 ^b	14.48±0.27 ^b
10	1.52±0.03 ^c	0.89±0.01 ^a	38433±466 ^a	191±38 ^c	36.46±0.03 ^a

Columns having different letters are significantly different ($p \leq 0.05$).

3.4.1.2. Electrical conductivity

The electrical conductivity values of solutions with or without gallic acid are shown in Table 3.9. It was clear that gallic acid addition increased electrical conductivity of solutions drastically. Moreover, as the gallic acid concentration of solution increased, the electrical conductivity increased too. Phenolic compounds possess electron and/or hydrogen donor ability (Aytac et al., 2016a) and the reason of the increase in electrical conductivity of solution could be related to -OH group as being an electron-donating group. Similarly, in the study of Tavassoli-Kafrani, Goli, & Fathi (2017), addition of phenolic compounds (tannic, gallic, ferulic and caffeic acids) increased the electrical conductivities of solutions. In this study, even the higher electrical conductivity of solutions containing 10% gallic acid did not result jet instability. Homogenous fibers were obtained from solutions containing 10% gallic acid (Figure 3.18)

3.4.2. Characterization of electrospun nanofibers

3.4.2.1. Fiber morphology

Pea flour contains about 22% protein. The isoelectric point of pea protein is 4.5. It is well known that when pH of proteins is equal to their pI, protein starts to aggregate,

and their solubility is minimum. In alkaline conditions, proteins become more unfolded by breaking of the hydrogen bonds and dissociation of hydrogen from carboxylic and sulphate groups. This resulted in higher chain entanglements between pea protein and PEO and possibility of homogenous nanofiber productions (Oguz et al., 2018, Lin, Breene, & Sargent, 1990). Therefore, pH of solutions was adjusted to alkaline condition. It can be seen from Figure 3.18 that all nanofibers prepared with different gallic acid concentration had homogenous structure. Similarly, in the study of Oguz et al. (2018), the production of pea flour based nanofibers was aimed. Although nanofibers could not be obtained at neutral pH, when pH of solutions was adjusted to alkaline, homogenous nanofibers were produced. As can be seen from Figure 3.18, gallic acid addition did not damage nanofiber structure. This was an indication of successful gallic acid encapsulation by electrospinning. The average diameters and diameter distribution of the electrospun nanofibers are also shown in Figure 3.18. In this study, the process parameters and ambient conditions were kept constant so the only parameter that affected the diameter of nanofibers was the solution characteristics. The rheological properties and electrical conductivity were important solution properties that could affect nanofiber morphology directly. Although, all solutions had the same polymer concentration, the gallic acid addition decreased the apparent viscosity and increased electrical conductivity of solutions (Table 3.9). The average diameters of the nanofibers ranged almost between 190–300 nm with standard deviation of between 38 and 68 nm. The narrow distributions and small standard deviations of nanofibers were the evidence of obtaining uniform nanofibers by electrospinning process. As explained before having high viscosity eliminated the instability of bending and reduced jet path. When jet path was low, stretching of the solutions was also low and it resulted in larger diameters. The solution without gallic acid had the highest k value and the lowest electrical conductivity and as a consequence nanofibers containing no gallic acid had the highest average diameter.

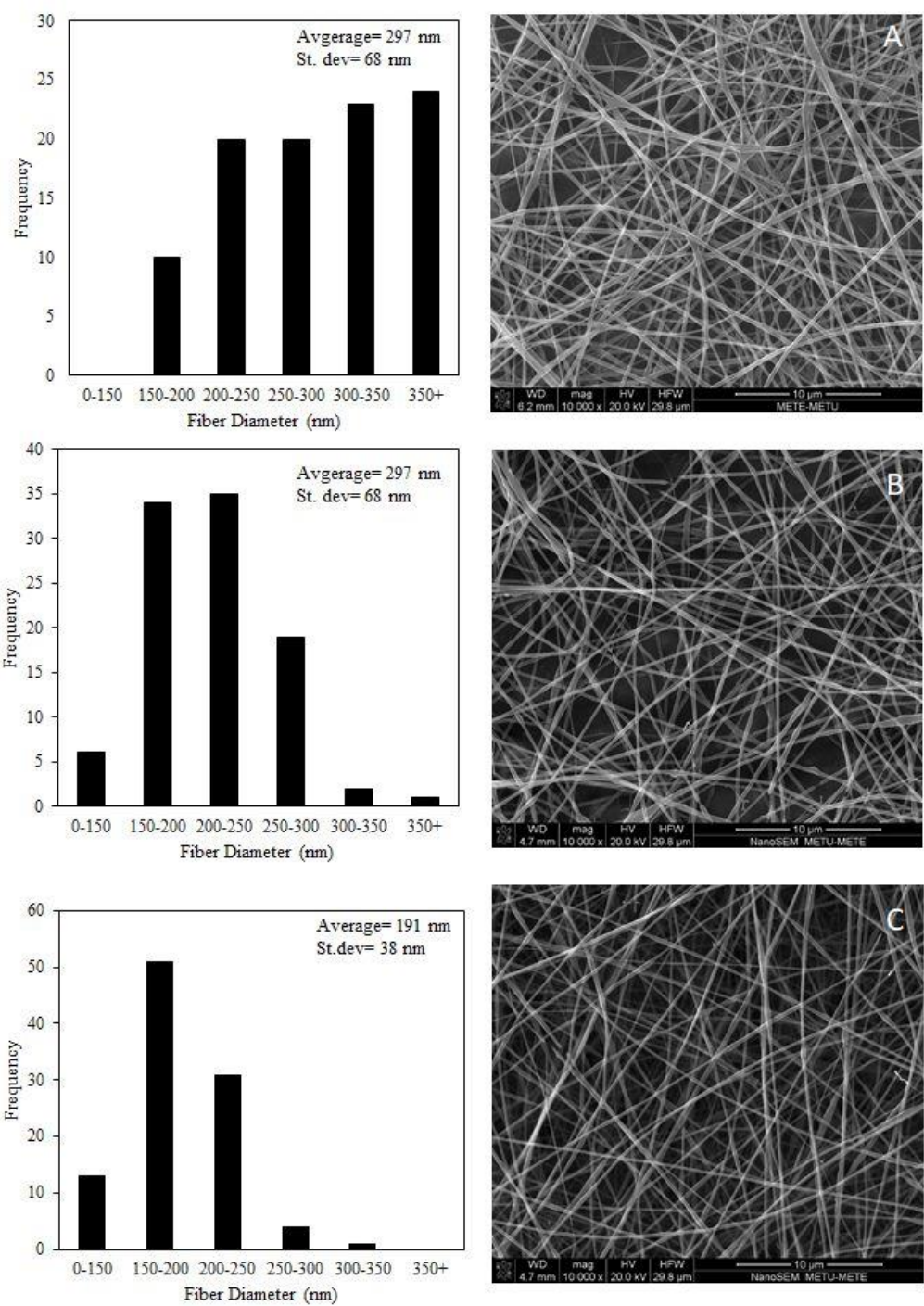


Figure 3.18 SEM images of electrospun nanofibers with different gallic acid concentration: a: control, b: 5%, c: 10%.

3.4.2.2. Total phenolic content (TPC) and antioxidant activity of solutions and nanofibers

TPC values of solutions with and without gallic acid are shown in Table 3.9. Pea flour contains several phenolic compounds which are protocatechuic acid, p-hydroxybenzoic acid, vanillic acid and p-coumaric acid (Lopez-Amoros, Hernandez, & Estrella, 2006). Therefore, before gallic acid addition, pea flour solutions already showed TPC values. As expected, when the gallic acid was added to solutions, TPC of solutions increased significantly. Gallic acid is one of the known natural phenolic acids (Friedman & Jü, 2000). Gallic acid is a heat sensitive active compound, so it is important to take process temperature into the consideration. Thus, electrospinning is an advantageous process for encapsulation of heat-labile compounds as it is operated at ambient temperature. As can be seen Table 3.10, nanofibers with gallic acid had higher TPC values. It is worth mentioning that gallic acid was successfully encapsulated in pea flour-based nanofibers by encapsulation. The loading efficiency of gallic acid within nanofibers is also shown in Table 3.10. The loading efficiency of gallic acid were about 92% and 74% which were the evidence of highly efficient encapsulation. In the study of Aceituno-Medina, Mendoza, Rodríguez, Lagaron, & López-Rubio (2014), quercetin and ferulic acid were encapsulated into amaranth protein isolate/ pullulan nanofibers by electrospinning with a high loading efficiency value (94% and 84%). In other study, proanthocyanidins was also encapsulated into zein fibers with a loading efficiency close to 100% (Hualin Wang et al., 2016) . They also reported the advantages of electrospinning for encapsulation. When the gallic acid amount increased, loading efficiency decreased. This difference could be related to gallic acid precipitation. In a similar manner, in the study of Blanco-Padilla et al. (2015), it was observed that as the curcumin amount increased, the encapsulation efficiency after electrospinning decreased. In the structure of gallic acid, three -OH groups ortho position bond to aromatic ring which is effective for showing antioxidant activity (Ghitescu, Popa, Popa, Rossi, & Fortunato, 2015). Table 3.10 represents the antioxidant activity of gallic acid loaded nanofibers. It demonstrated that loaded gallic

acid preserved its phenolic character and antioxidant activity after electrospinning. However, as the gallic acid amount increased, the antioxidant activity of nanofibers did not increase significantly ($p \leq 0.05$). This could be related to having lower loading efficiency of that nanofibers.

Table 3.10 *Loading efficiency and total antioxidant activities of gallic acid loaded pea flour/PEO electrospun nanofibers*

Gallic acid (%)	TPC of nanofibers (mg gallic acid equivalence (GAE) / g dry matter)	Gallic acid loading efficiency (%)	Antioxidant activity (mg DPPH/g dry weight)
5	13.42±0.45 ^b	92.6±3.1 ^a	5.29±0.24 ^a
10	27.15±0.75 ^a	74.4±2.0 ^b	5.72±0.33 ^a

*Columns having different letters are significantly different ($p \leq 0.05$).

3.4.2.3. Thermo-gravimetric analysis (TGA)

Weight loss curves as a function of the temperature are shown in Figure 3.19. Both control and gallic acid loaded nanofibers showed two stage degradation. The first degradation of control nanofiber began at the onset temperature T_{onset} of 264 °C. However, T_{onset} of gallic acid loaded nanofibers were determined as about 232 °C. Gallic acid addition to nanofibers decreased T_{onset} of nanofibers so the thermal stability of gallic acid loaded nanofibers was lower than control. Adding gallic acid to pea flour-based nanofibers decreased protein-protein bonds and interrupted interaction between molecules which reduced thermal stability of nanofibers. This was also the evidence of incorporation of gallic acid into nanofibers. Due to the same reason, Arrieta et al. (2013) observed that incorporation of carvacrol in sodium caseinate films resulted in lower thermal stability. However, increasing gallic acid amount did not affect thermal degradation profile of pea-flour based nanofibers significantly with having almost the same T_{onset} values. Similarly, in the study of Altan, Aytac, & Uyar, (2018), when the carvacrol amount increased in zein nanofibers, similar thermal degradation profile was observed. When the TGA curves of nanofibers were examined, the first weight losses were associated with decomposition of polysaccharides. In the study of Cano et al. (2015), the main degradation of pea starch

film was observed at T_{onset} of 310 °C. In this study, the first thermal degradation was related to pea flour. The reason of decrease in T_{onset} value could be the interaction between pea flour and PEO. The second degradation indicated thermal behavior of PEO. In fact, PEO had one stage thermal degradation with T_{onset} of 400 °C (Figure 3.6) . Although the second degradation of nanofibers showed the same characteristic behavior with pure PEO, T_{onset} values decreased to 384-393 °C. PEO had semi-crystalline polymer and blending PEO with another polymer depressed the crystallinity of PEO and decreased the thermal stability. Similarly, as stated in Section 3.1.2.4, when PEO was mixed with hydroxypropyl methylcellulose, obtained nanofibers represented lower thermal stability with lower T_{onset} values than pure PEO. Due to the same reason, gallic acid addition decreased T_{onset} of control nanofibers from 393 °C to 384 °C. This was also the indication of loading of gallic acid by electrospinning successfully.

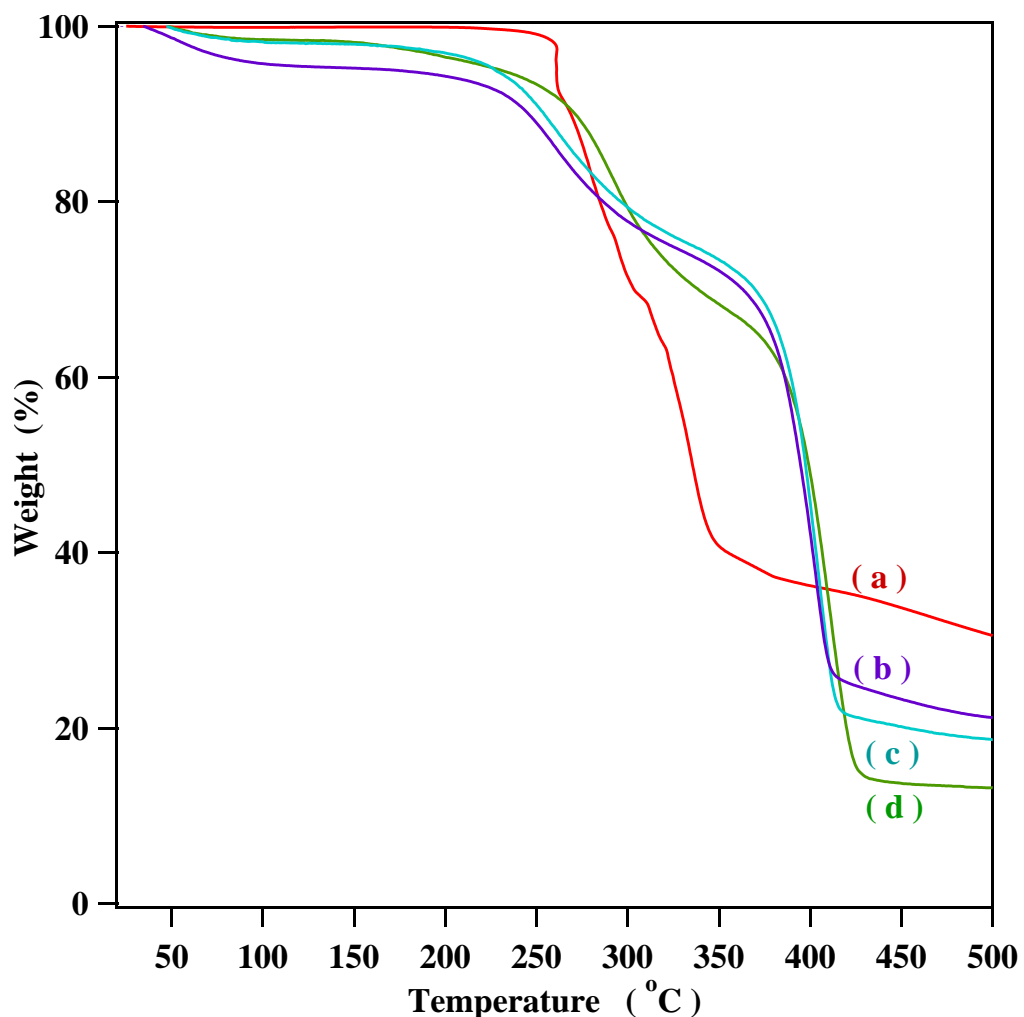


Figure 3.19 Thermo-gravimetric curves of gallic acid and electrospun nanofibers with different gallic acid concentration: a: gallic acid, b: 10%, c: 5%, d: control.

3.4.2.4. Differential Scanning Calorimetry (DSC) Analysis

DSC curves of control, gallic acid loaded nanofibers and gallic acid are shown in Figure 3.20. Nanofibers were composed of both pea flour and PEO. The endothermic peak at about 62 °C which was associated to melting point of PEO. As defined in Section 3.1.2.5, the melting point of pure PEO was reported as 68 °C. The depression of melting point of PEO was related to the disruption of the crystalline structure of PEO with interaction between PEO and pea flour and gallic acid that was also approved by TGA analysis. Pea flour is composed of starch and protein. The

gelatinization temperature of pea flour was reported as 62 °C (Chung, Liu, Hoover, Warkentin, & Vandenberg, 2008) and denaturation temperature of proteins was found as 84 °C (Shevkani, Singh, Kaur, & Rana, 2015). While preparing solutions, to increase electrospinnability, solutions were heated up 80 °C and their pH values were arranged to acidic pH value. The acid and heat treatment resulted in completed denaturation and gelatinization. That's why, no endothermic peak related to gelatinization and denaturation was observed in thermograms of nanofibers. When the thermograms of gallic acid was examined, it was obviously seen that there was an endothermic peak at 270 °C. This peak was related to melting transition of crystal form of gallic acid (Phiriyawirut & Phaechamud, 2012). However, this peak disappeared in gallic acid loaded nanofibers. Likewise, Neo et al. (2013) found that while gallic acid had characteristic peak at 260 °C, gallic acid loaded zein nanofibers did not represent any melting peaks of gallic acid due to loss of its original crystalline structure. Therefore, in that study, it was stated that gallic acid was incorporated into electrospun zein nanofibers.

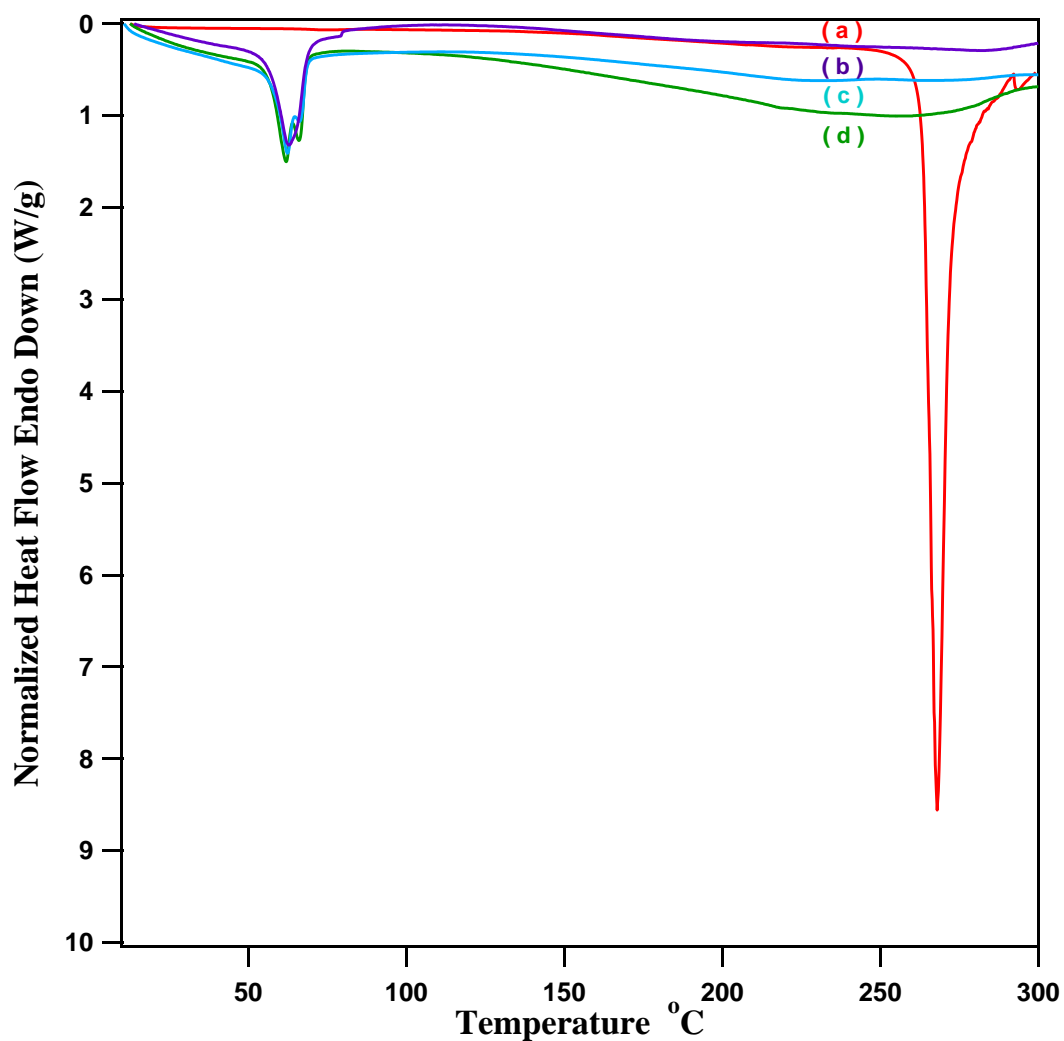


Figure 3.20 DSC curves of gallic acid and electrospun nanofibers with different gallic acid concentration: a: gallic acid, b: control, c: 10%, d: 5%.

3.4.2.5. FTIR analysis

The FTIR spectra of nanofibers, pea flour and gallic acid are illustrated in Figure 3.21. When the FTIR spectra of nanofibers was examined, the peak at around 2900 cm^{-1} was attributed to C-H stretching (Fortunati et al., 2013). The region between 1600 cm^{-1} to 800 cm^{-1} represents finger print region and in this region each of component shows its own unique pattern of peaks. A closer look to the fingerprint region of nanofibers,

a triplet absorbance (1058, 1110 and 1148) with a maximum at 1100 cm^{-1} was observed. This peak was correlated with crystalline phase of PEO. In the Section 3.1.2.3, triplet absorbance at 1058, 1095 and 1145 cm^{-1} corresponded to the stretching vibrations of the ether bond or C-O-C complex and indication of semi crystalline structure of PEO. Nanofibers represented peak at 1460 cm^{-1} associated with CH_2 deformation and peaks at 1342 and 1360 was assigned to the bending modes of C-H (Pielichowski & Flejtuch, 2005) . Peaks located at 1240 cm^{-1} and 1280 cm^{-1} were attributed to CH_2OH related mode which was characteristic of the V-form amylose (Kizil et al., 2002). Moreover, the peaks of nanofibers at around 840 cm^{-1} and 960 cm^{-1} were characteristics of the C-O stretching and CH_2 rocking (Sim, Gan, Chan, & Yahya, 2010). Pea flour was composed of starch and proteins. When compared to gallic acid loaded and control nanofibers, it was observed that gallic acid loaded nanofibers had peak at around 1550 cm^{-1} and similar peak at 1540 cm^{-1} was observed in the spectra of pure gallic acid. The other peaks (1024, 1319 and 1423 cm^{-1}) belonging to gallic acid coincided with other bands of PEO and pea flour.

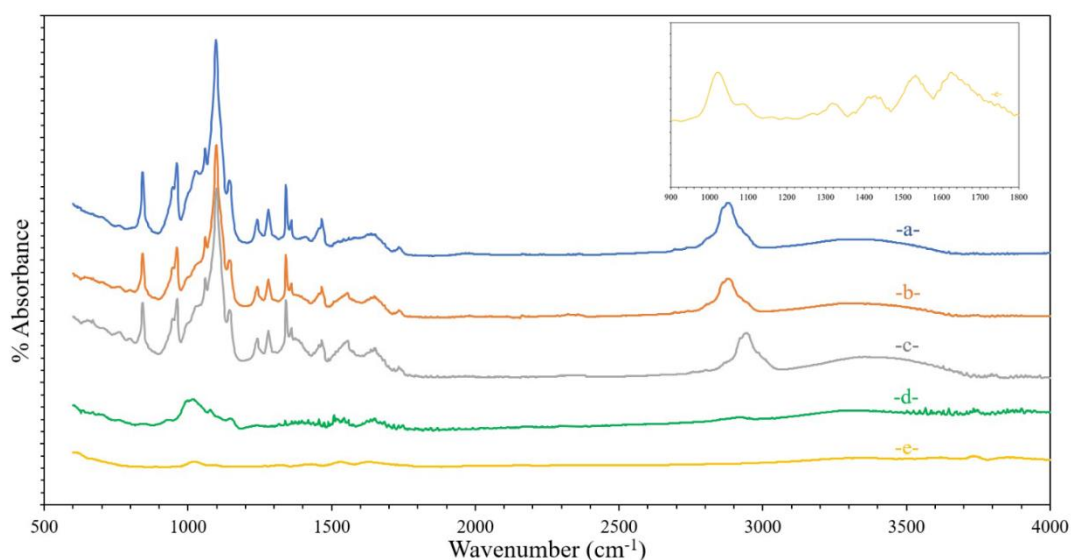


Figure 3.21 FTIR spectra of gallic acid, pea flour and electrospun nanofibers with different gallic acid concentration: a: control, b: 5%, c: 10%, d: pea flour, e: gallic acid.

3.5. Fabrication of Poly(lactic acid)/Soy Protein/HPMC nanofibers with electrospinning

PLA (polylactic acid) has a great potential as a raw material due to its good mechanical properties, biocompatibility, and easy processable characteristic. It is a completely biodegradable and hydrophobic linear polyester manufactured from renewable resources. Due to its remarkable features, PLA is a good competitor against fossil-based polymers. Therefore, to be used as packaging material, it was aimed to produce bilayer PLA/nanofiber sheets.

3.5.1. Physical properties of solutions

3.5.1.1. Rheological properties

k and n values of solutions prepared by PEO, HPMC and soy protein with different combinations are shown in Table 3.11. All solutions obeyed the Power Law with a high coefficient of determination and the flow curves are shown in Figure 3.22. As can be seen from Table 3.11, the solution containing just soy protein showed almost Newtonian behavior ($n=0.99$). Apparent viscosity change with respect to shear rate was represented in Figure 3.22. As seen, there was no significant change in apparent viscosity with respect to shear rate like Newtonian fluids. HPMC containing solutions shifted from Newtonian behavior to Non-Newtonian, with a decrease in n value and decreasing in apparent viscosity change with increasing shear rate (Figure 3.22). Lower n value is generally interpreted as high entanglement of molecules which is an essential requirement to obtain nano fiber through electrospinning (Kriegel et al., 2009a). Polymer solution prepared by PEO and HPMC had the highest k but the lowest n value (Table 3.11). k value is a degree of thickening of polymer solution which is correlated with the viscosity. The highest k represented the highest entanglement which shows how strongest the interaction between PEO and HPMC at molecular level. It was investigated that primary hydroxyl group of cellulose and methyl cellulose could make a hydrogen bonding with ether oxygen of the PEO. Analogous interactions might come true between PEO and HPMC (Fuller, MacRae, Walther, &

Cameron, 2001). This might explain the analogy behind the flow behavior of PEO and HPMC solution. HPMC is a well-known mucoadhesive polymer so when HPMC is contacted with water, it swells quickly (Tort & Acartürk, 2016) and k values of solutions increase.

Electrospinning of proteins is difficult due to hydrophobic interactions, complex structure and network, low charge density (Nieuwland et al., 2013). Soy proteins have strong intermolecular interactions such as electrostatic and covalent (disulphide) bonds. However, there are many factors that influence the interaction between molecules. For example, ionic environments have decreasing effect on electrostatic ones present within the protein molecules. Furthermore, enzymatic and alkaline hydrolysis have an impact on bond strength between molecules (Kumar, Kaur, & Bhatia, 2017). In this study, to make proteins more soluble by promoting new bonds between structure and aqueous medium, pH of environment was increased. To accelerate denaturation of proteins and promote new bonds, heat treatment was also applied to the system. Similarly in the study of Oguz et al. (2018)] to obtain fiber by electrospinning, pea protein, has also been treated in alkaline medium to make it unfolded by cleavage of the hydrogen bonds. This led to the improvement of interaction between pea protein and PEO.

As seen in the Table 3.11, both heat treatment and pH adjustment had an impact on the flow behavior of polymer blends. All treatments improved unfolding of proteins and entanglements of proteins with polymers which made proteins more spinnable. However, these newly created bonds were not as strong as the ones between PEO and HPMC. While k values of solutions decreased under these disturbances, n values had a tendency to increase. k values of solution containing PEO/ HPMC/ soy protein was lower than that of only PEO/ soy protein polymer solution. This might be due to newly constructed bonds between PEO and HPMC which might show extra resistance to pH and thermal treatment.

Table 3.11 Rheological properties and electrical conductivities of solutions.

Solutions (HPMC/Soy/PEO)	k ($Pa\ s^n$)	n	Electrical Conductivity ($\mu S/cm$)
3.5/0/3.5	24.07±0.12 ^a	0.71±0.00 ^c	394.5±4.5 ^c
0/3.5/3.5	0.27±0.02 ^c	0.99±0.00 ^a	3535.0±15.0 ^a
3.5/3.5/3.5	6.43±0.20 ^b	0.85±0.00 ^b	3400.0±10.0 ^b

Columns having different letters are significantly different ($p \leq 0.05$).

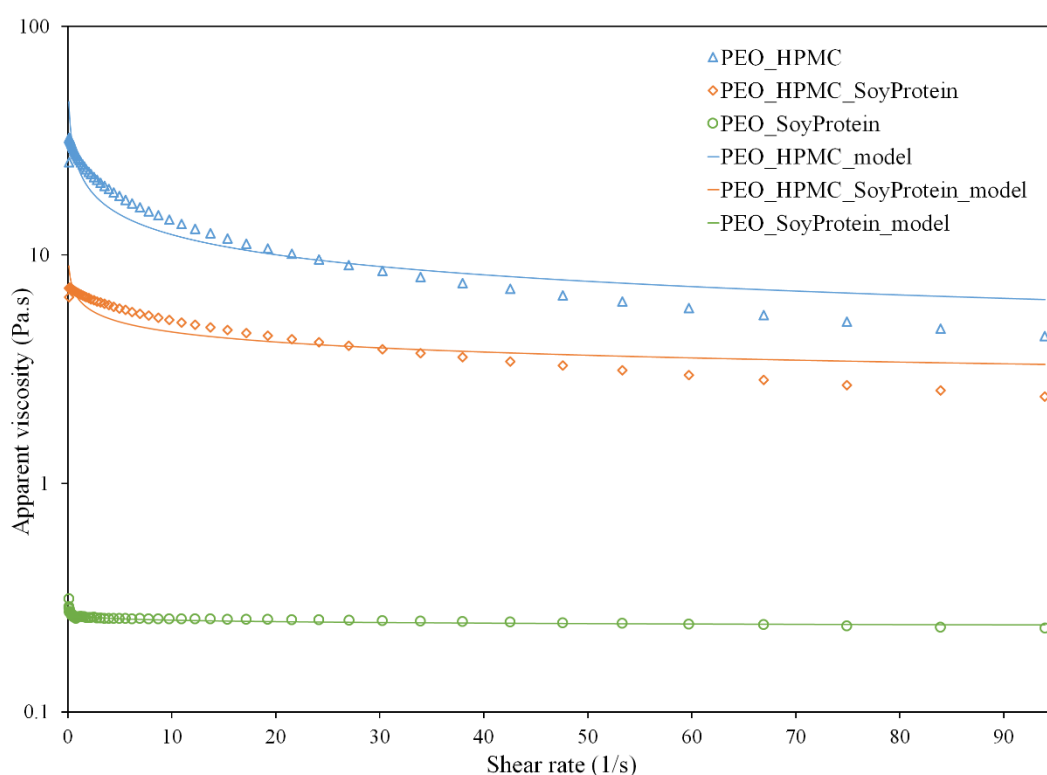


Figure 3.22 Flow curves of solutions that used in electrospinning process: \circ : PEO_Soy Protein, Δ : PEO_HPMC, \diamond : PEO_HPMC_Soy Protein.

3.5.1.2. Electrical Conductivity

Conductivity results of polymer solution were shown in Table 3.11. Dielectric constant is the indicator of polarity of solvent. Furthermore, it was recorded that higher

dielectric constant meant higher charge density of the polymer solution (Son et al., 2004) . Electrical conductivity is an indicator for the charge density of the solution (Tan, Inai, Kotaki, & Ramakrishna, 2005) . Therefore, although the PEO and HPMC are nonpolar polymers, due to high polarity of water, enough conductivity for homogenous fiber formation is provided. On the other hand, polymer solution with soy protein had higher conductivity values. The reason behind this result might be both addition of protein and changing pH of solution. Isoelectric point of soy protein is 4.5-5 pH at which protein has zero net charge (Cho, Netravali, & Joo, 2012). Altering the pH of the protein containing solution to a value which is different from the isoelectric point of the protein, number of charged molecule increased. This caused a direct change in electrical conductivity (Tam et al., 2017). Therefore, adjusting solution pH to 12 increased number of charged molecules in the solution and electrical conductivity. Furthermore, in a study, electrical conductivity values of whey protein/PEO solutions prepared at both acidic and basic pH values were measured. It was shown that solution having higher pH value had higher conductivity than the one with lower pH. It was interpreted that presence of Na^+ and OH^- ions were the reasons of higher conductivity (Vega-Lugo & Lim, 2012). In another study, lentil flour with 22.2 % protein blended with HPMC and pH value was adjusted to 7, 10 or 12. It was recorded that as the distance from the isoelectric point increased, the conductivity values of the solutions increased (Tam et al., 2017) .

Although pH adjustment was also applied to the PEO, HPMC, soy protein containing sample it had still lower conductivity than the PEO and soy protein containing solution. This might be related to viscosity results since HPMC/ soy protein /PEO containing sample had higher viscosity than the soy protein/PEO sample. Charge density is affected from amount of electrolyte, dielectric permittivity of solvent and mobility of ions. Correlation coefficient between viscosity and conductivity was determined as -0.997 ($p=0.001$). Therefore, higher viscosity might reduce mobility of ions which led to lower conductivity. Similarly, it was stated that if polymer had ionic

characteristics, conductivity became more concentration dependent (Okutan, Terzi, & Altay, 2014).

3.5.2. Characterization of Nanofibers

3.5.2.1. Fiber Morphology

The pH values of soy protein containing solutions were arranged to alkaline condition. The isoelectric point (pI) of soy protein was pH 4.5 (Elizalde, Bartholomai, & Pilosof, 1996). In general, solubility of proteins depends on the net charges of solutions and proteins have negative and positive charges above and below isoelectric point, respectively. Therefore, the solubility of proteins increases when pH is far away from pI (Pelegri & Gasparetto, 2005). Thus, the protein solubility increased by pH treatment and prevented bead formation due to solubility problem of proteins. Moreover, heat treatment was applied to solutions containing proteins to denature proteins. The denaturation of proteins is a process of major conformational changes and results in having higher protein-protein interaction and protein-polymer interaction (Boy, Maness, & Kotek, 2016). It means that denaturation increases the solubility of proteins and interaction between polymer. Therefore, to increase spinnability of solution, heat treatment was applied. In this study, all the nanofibers had homogenous and bead free structure (Figure 3.23), so it suffices to state that suitable electrospinning conditions were achieved. Moreover, from cross sectional images, bilayer film structure can be observed. As seen in Table 3.12, HPMC/PEO nanofibers had the highest mean fiber diameter because of their highest viscosity values. Similar behavior was also observed when cellulose nano fibrils was added to poly (3-hydroxybutyrate-co-3-hydroxyvalerate) (PHBV) solutions. It was recorded that addition of nano fibrils increased viscosity which was correlated with mean fiber diameter (Vega-Lugo & Lim, 2012). Electrical conductivity is one of important solution properties that affect the nanofiber size. Solution having higher conductivity resulted in longer elongation and thinner fiber due to experiencing stronger elongation forces. This result was correlated with charge density of solutions (Son et al., 2004).

Soy protein/PEO solution had the lowest viscosity values but its electrical conductivity was the highest one. As expected, soy protein/PEO containing solution had the lowest fiber diameter. When the diameter distributions of all nanofibers were examined, narrow distribution and small standard deviations were observed (Figure 3.24). Therefore, it might be concluded that electrospinning technique can be used to produce nanofibers with uniform diameters.

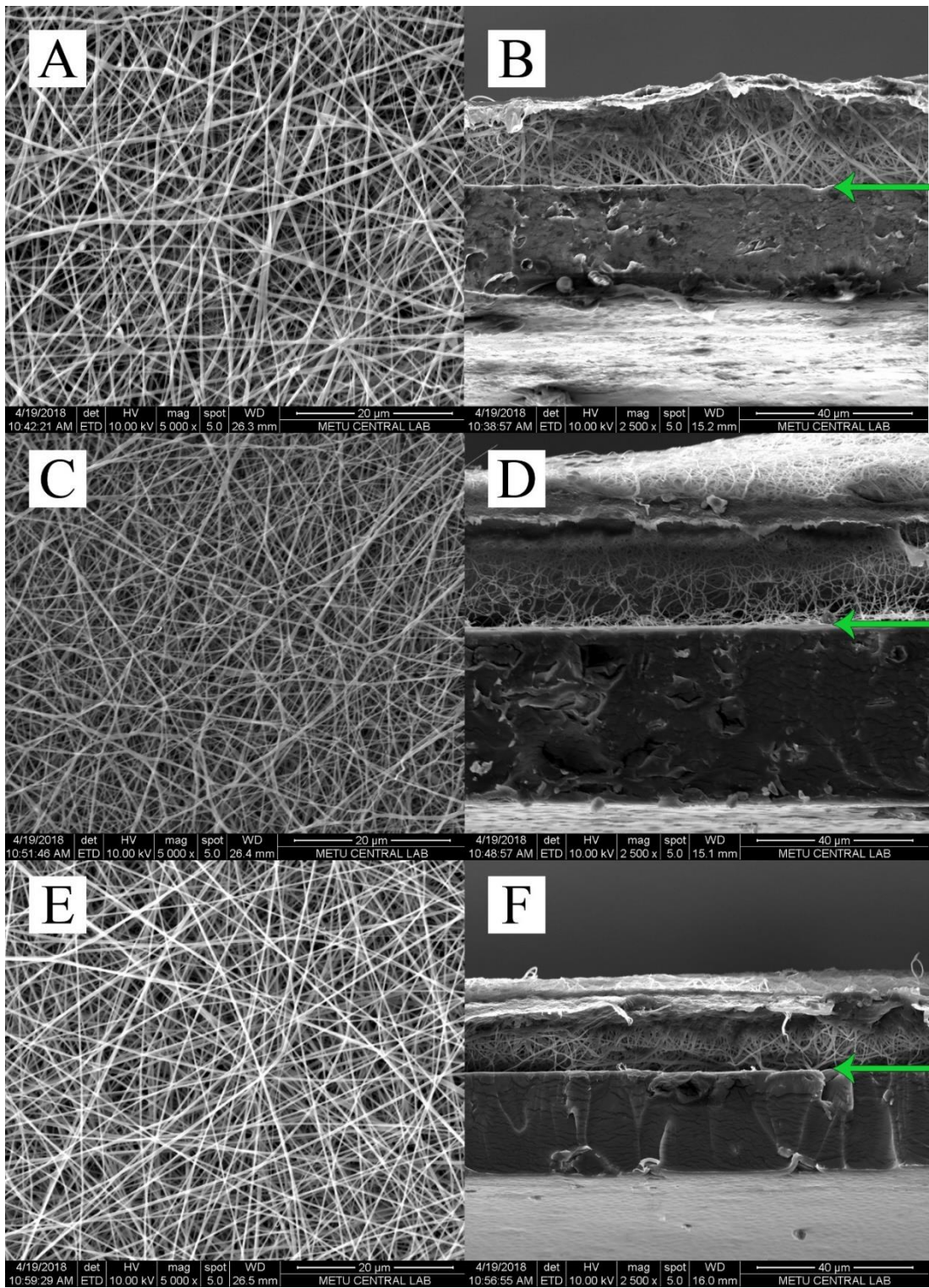


Figure 3.23 Surface (5000x magnification) and cross-section (2500x magnification) SEM images of nanofibers A-B PEO_HPMC, C-D: PEO_SoyProtein, E-F: PEO_HPMC_SoyProtein

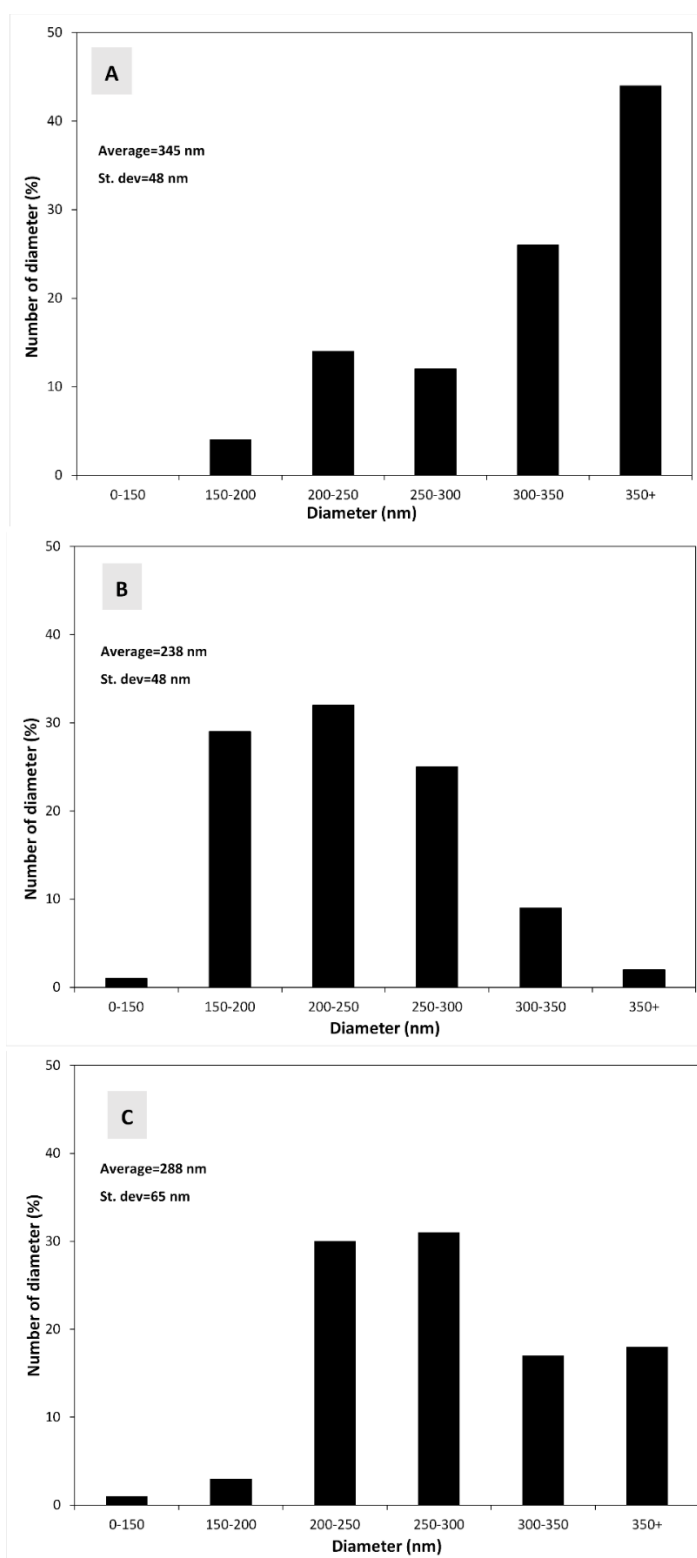


Figure 3.24 Diameter distributions of nanofibers A: PEO_HPMC, B: PEO_SoyProtein, C: PEO_HPMC_SoyProtein

Table 3.12 Average diameter, opacity and water vapor permeability of sheets

Nanofibers on PLA (HPMC/Soy/PEO)	Average		$WVP \times 10^{-11}$ ($g\ m^{-1}\ s^{-1}\ Pa^{-1}$)
	Diameter (nm)	Opacity	
3.5/0/3.5	345±48 ^a	39.72±0.37 ^b	5.899±0.084 ^a
0/3.5/3.5	238±48 ^c	43.67±1.92 ^a	6.225±0.313 ^a
3.5/3.5/3.5	288±65 ^b	42.39±1.25 ^{ab}	4.869±0.482 ^a
PLA	X	7.62±0.47 ^c	2.602±0.061 ^b

Columns having different letters are significantly different ($p \leq 0.05$).

3.5.2.2. Opacity

Film opacity is an important parameter for the food packaging application, especially if it is used as surface coating. For this reason, films were also characterized in terms of their optical characteristics. Opacity of films were shown in Table 3.12. As seen PLA film was more transparent compared to double layer films. Transparency strongly depended on internal structure and surface characteristic. Tortuosity in the structure influenced the light transmission, as a result of transparency/opacity ratio. More crystalline arrangement of molecules decreased transparency due to different refractive index of crystalline part (María José Fabra et al., 2013). As can be seen in DSC analysis, produced bilayer sheets had semi crystalline structure. Therefore, crystalline structure of nanofibers might cause the higher opacity of multi-layer film. Nanofiber obtained from soy protein and PEO was more opaque than the others. Due to higher protein ratio in overall and more crystalline structure formation might be the reason. Furthermore, nanofiber structure was not as compact as PLA film which was produced by casting. The small air gaps between nanofibers caused tortuosity and increased opacity of films. Refractive index difference, between nanofibers and air, might be another reason for higher opacity of double layer films. This hypothesis was supported by the study of Urbina et al. (2016). Bacterial cellulose films obtained by casting method resulted in more opaque structure due to crystal structure of cellulose

and air interstices between cellulose fiber. However, it was also recorded that addition of poly lactic acid – poly ethylene glycol mixture to the formulation improved transparency. Removing air gaps led to more uniform light diffraction (Rhim, Lee, & Ng, 2007). Another study showed that processing methods of films were also responsible from opacity. Film obtained by two different methods were analyzed. It was concluded that transparent films were obtained by solution casting, highly thin films produced by electrospinning had whitish color, and high opacity (Okutan et al., 2014). Therefore, electrospinning technique, crystal structure of nanofiber, and finally small air gap between fibers were mainly responsible from the opacity of the bilayer films.

3.5.2.3. Water Vapor Permeability (WVP)

WVP is a crucial property while choosing packaging material to control moisture transfer between environment and food. In general, packaging material having lower WVP values are preferred to pack foods. In this study, the effect of nanofibers having different composition on the WVP of PLA sheets were examined and shown in Table 3.12. However, it was seen that two layers PLA-nanofiber sheets had higher WVP values than PLA sheet ($p \leq 0.05$). The reason could be the hydrophilicity of nanofibers. In the study of (McHugh, Avenabustillos, & Krochta, 1993), it was stated that ideal polymeric films did not exhibit thickness effect on WVP but WVP values of most hydrophilic films increased proportionally with increasing thickness of films. Therefore, as the thickness of hydrophilic films increased, WVP values also increased, due to the increased water vapor partial pressure conditions which were the underside of the film exposed to water. Similarly, in this study, PLA sheets were covered by soy protein and HPMC nanofibers and thickness of the sheets increased so WVP values increased, too. Moreover, (Busolo, Torres-giner, & Lagaron, 2009) produced multilayer film by incorporation of zein nanofibers to PLA sheets and it was observed that zein nanofibers did not enhance WVP of PLA. However, produced PLA/soy protein sheets had lower WVP values than soy protein films produced by casting method with having $268 \times 10^{-11} \text{ g m}^{-1} \text{ s}^{-1} \text{ Pa}^{-1}$ value (Rhim et al., 2007). Similarly, it

was reported that the WVP properties of HPMC films produced by casting method were between 6 and $9 \times 10^{-10} \text{ g m}^{-1} \text{ s}^{-1} \text{ Pa}^{-1}$ which was higher than WVP of PLA/HPMC nanofiber sheets (Akhtar et al., 2013b). Thus, instead of usage of soy protein and HPMC casting films as packaging materials, combination of them with PLA by electrospinning should be preferable.

3.5.2.4. FTIR Analysis

ATR-FTIR spectra of PLA, PLA-nanofibers and the polymer components are shown in Figure 3.25. The region between 750 cm^{-1} to 1500 cm^{-1} represents the fingerprint region that usually consists of bending vibrations within the molecule. A closer look to the fingerprint region of pure PLA, it exhibited absorption bands at 1082 and 1180 cm^{-1} due to the C-O stretching. In addition, the peak of 875 cm^{-1} corresponds to the stretching of the C-C single bond (Urbina et al., 2016). In PLA spectrum, it is worth mentioning the peak at 1751 cm^{-1} which was attributed to stretching of amorphous carbonyl group (C=O) assigned to lactides (Arrieta et al., 2014). A more detailed inspection of fingerprint region of soy protein, characteristic peaks at 1635, 1540 and 1244 cm^{-1} were observed. These peaks were assigned to amide I (C-O stretching), amide II (N-H bending), and amide III (C-N and N-H stretching). This was in agreement to the study of (X. Liu et al., 2017). All nanofibers showed the same peak that belongs to PLA and the components. That is the evidence that there is no chemical interaction between compounds.

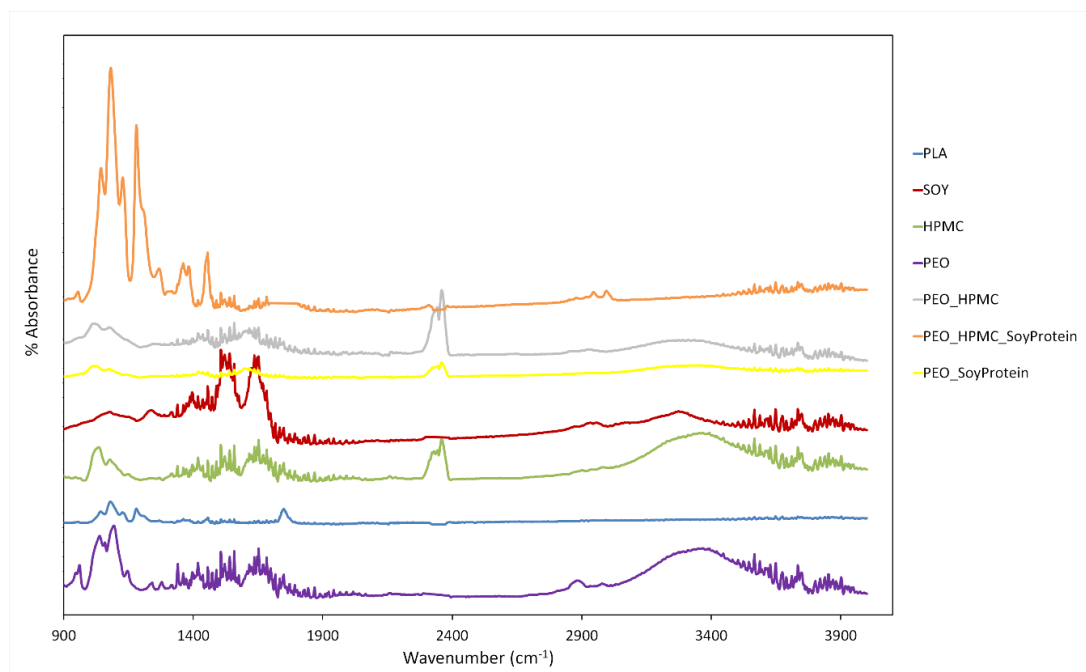


Figure 3.25 FTIR spectra of components and PLA-nanofiber sheets

3.5.2.5. TGA Analysis

For biocomposite development, thermal characterization of each component and composite materials is an important issue to take potential of thermal degradation into consideration. The TGA curves were shown in Figure 3.26. Pure PLA displays single stage degradation that began at onset temperature (T_{onset}) of 330 °C. In the study of Awal, Rana, & Sain (2015), PLA showed on step degradation with similar T_{onset} value. After decomposition almost 9% weight (metals, inorganic traces, mesolactide and lactide of sample remained (Marina Patricia Arrieta et al., 2013; Inkinen, Hakkarainen, Albertsson, & Södergard, 2011). As can be seen from Figure 3.26, soy protein lost weight before 100°C which was related to moisture evaporation. The main degradation occurred between 260-350 °C. Similar range was observed in the study of Yulong et al. (2010). This decomposition was mainly attributed to the breakage of the peptide bonds. Until ashes were just remained, S–S, O–N, and O–O linkages were ruptured (X. Xu et al., 2012). Although the degradation of soy protein began at about 300 °C which was lower than the temperatures at the degradation of other nanofibers

began, the degradation of soy protein was in the wide range of temperature (not step change). This was indication of the resistance of soy protein to thermal degradation. In contrast, the weight loss of HPMC containing samples was like step change (sharp decrease) that showed fast degradation. Therefore, the resistance of HPMC to degradation was lower. Moreover, above 450 °C, although still almost 30% weight of soy protein sample remained, the remaining weight of HPMC was significantly lower at same temperature. The lower weight loss is correlated with higher thermal stability (Guirguis & Moselhey, 2012). Moreover, in the studies of Issa, Al-maadeed, Luyt, Mrlik, & Hassan (2016) and Jakic, Vrandecic, & Erceg (2016), it was stated when the remaining weight loss after degradation was higher, it was indication of thermal stability. The pure HPMC powder showed one stage degradation with T_{onset} of 340 °C (Figure 3.6). Weight change of HPMC that was exposed to high temperature was about 11%. However, although T_{onset} of PEO was higher than the other polymer that used, weight loss of it was 96% which was the highest. In contrast, when the TGA curves of PLA- nanofiber sheets were investigated, it was seen that they represented two stage degradation. There was no chemical bonding between PLA and nanofibers, that's why bilayer sheets showed the properties of individual polymers. In PLA-nanofibers multilayer sheets, the first degradation process occurred at lower temperatures than the components (240-250°C). The second thermal degradation of PLA/nanofibers ranged between 350 and 380 °C. Similarly, the study of Arrieta et al. (2014) demonstrated that while PLA had one stage degradation, the PLA-PHB composite showed two step degradation with having lower first degradation temperature. Although the weight loss after first degradation of PEO_HPMC nanofiber sheets was lower than PEO_soy protein, the T_{onset} of soy protein nanofiber containing PLA sheets were higher than PEO_HPMC bilayer sheet. Moreover, T_{onset} values of second degradation of PEO/soy protein was highest one which was followed by PEO/soy protein/HPMC. Moreover, their weight losses were about 92% which was lower than PEO/HPMC sheet having 95%. It was concluded that nanofiber containing soy protein had higher thermal stability than HPMC containing nanofibers.

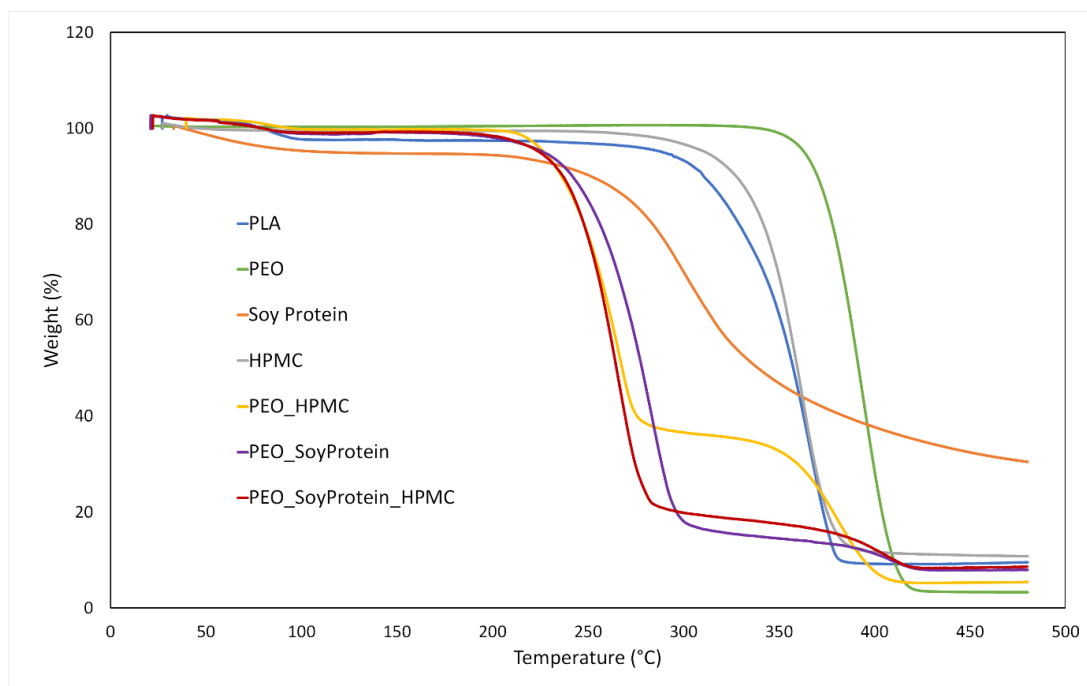


Figure 3.26 TGA curves of components and PLA-nanofiber sheets

3.5.2.6. DSC Analysis

The DSC thermograms of PLA and PLA-nanofiber combination were shown in Figure 3.27. PLA is a semi crystalline polymer containing both amorphous and crystalline domains, so it shows both melting temperature and glass transition temperature (T_g) (Cam & Marucci, 1997). T_g of PLA was determined as about 45 °C. However, it is hard to differentiate T_g from the enthalpic peak. This enthalpic relaxation is typical for a polymeric material in the glassy state that undergoes physical ageing (Pantani, Gorrasi, Vigliotta, Murariu, & Dubois, 2013). In addition, the melting temperature of PLA was determined as to be about 145 °C. In the study of Fabra et al. (2014), melting point of PLA was also reported as 150 °C. While melting is endothermic process, crystallization is exothermic, so the exothermic peak seen at DSC curve of PLA was related to crystallization of PLA. Cold crystallization temperature (T_{cc}) of PLA was found as about 115 °C which was confirmed by the study of Fabra et al. (2014). When the DSC curves of PLA-nanofibers were investigated, an endothermic peak at almost 62°C corresponding to the melting point of PEO was observed that differed from PLA

curve. The melting point of pure PEO powder was found as 68 °C but due to disruption of the crystalline structure of PEO with interaction between PEO and HPMC, the melting peak shifted to 56°C (Section 3.1.2.5). Similarly, in this study soy protein and HPMC disrupted crystalline structure of PEO and the melting point was depressed. All PLA-nanofibers bilayer sheets had similar DSC curve with pure PLA sheet. Therefore, PLA-nanofibers represented both T_g , crystallization and melting points which were close to neat PLA.

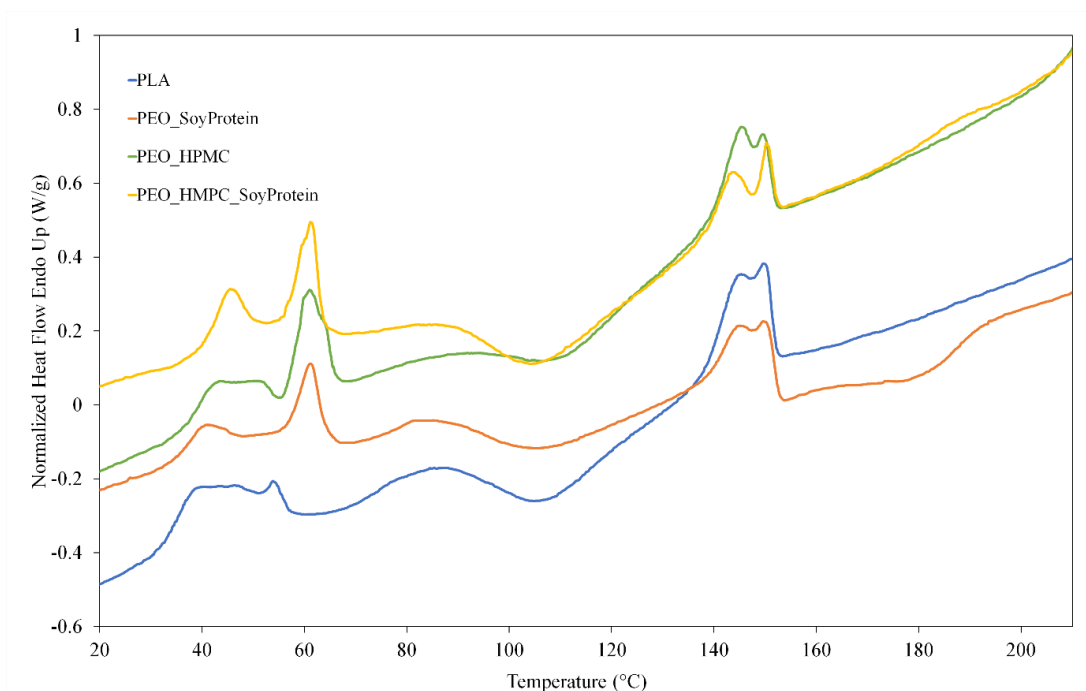


Figure 3.27 DSC curves of PLA and PLA-nanofiber sheets

CHAPTER 4

CONCLUSION

The aim of this study is to produce active packaging materials by encapsulating of gallic acid into HPMC and legume flours (lentil and pea flour) based electrospun nanofibers and examine the applicability of nanofibers as packaging material to prevent oxidation of walnuts during storage. In electrospinning method, optimization of electrospinning conditions and solution properties are crucial to obtain homogenous nanofibers. In this study, the effects of rheological properties and electrical conductivities of solution on fiber morphology were illustrated and it was observed that lower consistency index value and higher electrical conductivity values resulted in decrease in fiber diameters. Encapsulation of gallic acid as an antioxidant compound in HPMC, lentil flour and pea flour based nanofibers by means of electrospinning was successfully carried out. The obtained results indicated that gallic acid was encapsulated to nanofibers with a high loading efficiency and they had strong antioxidant activity. Incorporation of gallic acid into nanofibers was proven by TGA, DSC and FTIR analyses which indicated the interactions between gallic acid and polymers. Nanofibers showed different thermal and chemical properties than pure gallic acid which could be taken an evidence of gallic acid encapsulation. Gallic acid loaded HPMC and lentil flour-based nanofibers were used to pack walnuts. It was worth to state that fabricated active packages provided oxidation stability to walnuts. This study has given insight about the success of electrospinning to produce active packaging materials. In the light of being biodegradable with antioxidant activity, gallic acid loaded nanofibers have great potential to enhance the oxidative stability of foods. Moreover, soy protein and HPMC homogenous nanofibers were successfully collected onto PLA sheets. To determine the potential usage of PLA/nanofibers bilayer sheets as food packaging material, the opacity and permeability values were

investigated and compared to neat PLA sheet produced by casting method. Coating PLA sheets by nanofibers did not decrease the WVP of PLA sheets. However, it increased the opacity values significantly. Obtained PLA/nanofiber bilayer films by electrospinning method can potentially be employed for food packaging applications.

For future studies, electrospinning method could be applied to encapsulate different antimicrobial and antioxidant agents and the produced active packaging materials could be tested not only for antimicrobial but also for antioxidant activity. Packaging materials must show appropriate mechanical properties so the mechanical analyses to nanofibers should be determined. To improve mechanical properties of nanofibers, bilayer active packaging materials can be produced by covering the other type of biopolymer based packaging materials with nanofibers.

REFERENCES

- Abutaleb, A., Lolla, D., Aljuhani, A., & Shin, H. U. (2017). Effects of Surfactants on the Morphology and Properties of Electrospun Polyetherimide Fibers. *Fibers*, 5(33), 1–14. <https://doi.org/10.3390/fib5030033>
- Aceituno-Medina, M., Mendoza, S., Lagaron, J. M., & López-Rubio, A. (2015). Photoprotection of folic acid upon encapsulation in food-grade amaranth (*Amaranthus hypochondriacus* L.) protein isolate – Pullulan electrospun fibers. *LWT - Food Science and Technology*, 62(2), 970–975. <https://doi.org/10.1016/J.LWT.2015.02.025>
- Aceituno-Medina, M., Mendoza, S., María Lagaron, J., & opez-Rubio, A. L. (2015). Photoprotection of folic acid upon encapsulation in food-grade amaranth (*Amaranthus hypochondriacus* L.) protein isolate e Pullulan electrospun fibers. *LWT - Food Science and Technology*, 62, 970–975. <https://doi.org/10.1016/j.lwt.2015.02.025>
- Aceituno-Medina, M., Mendoza, S., Rodríguez, B. A., Lagaron, J. M., & López-Rubio, A. (2014). Improved antioxidant capacity of quercetin and ferulic acid during in-vitro digestion through encapsulation within food-grade electrospun fibers. *Journal of Functional Foods*, 12, 332–341. <https://doi.org/10.1016/j.jff.2014.11.028>
- Acta, A. C., Arecchi, A., Scampicchio, M., Drusch, S., & Mannino, S. (2010). Nanofibrous membrane based tyrosinase-biosensor for the detection of phenolic compounds. *Analytica Chimica Acta*, 659, 133–136. <https://doi.org/10.1016/j.aca.2009.11.039>
- Ahmed, S. H., Mohamed Ahmed, I. A., Eltayeb, M. M., Ahmed, S. O., & Babiker, E. E. (2011). Functional properties of grain legume flours. *Journal of Agricultural Technology*, 7(5), 1291–1302. Retrieved from <http://www.ijat-aatsea.com>
- Akhtar, M.-J., Jacquot, M., Jamshidian, M., Imran, M., Arab-Tehrany, E., & Desobry, S. (2013a). Fabrication and physicochemical characterization of HPMC films with commercial plant extract: Influence of light and film composition. *Food Hydrocolloids*, 31(2), 420–427. <https://doi.org/10.1016/j.foodhyd.2012.10.008>
- Akhtar, M.-J., Jacquot, M., Jamshidian, M., Imran, M., Arab-Tehrany, E., & Desobry, S. (2013b). Fabrication and physicochemical characterization of HPMC films with commercial plant extract: Influence of light and film composition. *Food Hydrocolloids*, 31, 420–427. <https://doi.org/10.1016/j.foodhyd.2012.10.008>
- Alborzi, S., Lim, L.-T., & Kakuda, Y. (2010). Electrospinning of sodium alginate-pectin ultrafine fibers. *Journal of Food Science*, 75(1), C100-7.

<https://doi.org/10.1111/j.1750-3841.2009.01437.x>

- Altan, A., Aytac, Z., & Uyar, T. (2018a). Carvacrol loaded electrospun fibrous films from zein and poly(lactic acid) for active food packaging. *Food Hydrocolloids*, *81*, 48–59. <https://doi.org/10.1016/j.foodhyd.2018.02.028>
- Altan, A., Aytac, Z., & Uyar, T. (2018b). Carvacrol loaded electrospun fibrous films from zein and poly(lactic acid) for active food packaging. *Food Hydrocolloids*, *81*, 48–59. <https://doi.org/10.1016/J.FOODHYD.2018.02.028>
- Anu Bhushani, J., & Anandharamakrishnan, C. (2014). Electrospinning and electrospaying techniques: Potential food based applications. *Trends in Food Science & Technology*, *38*(1), 21–33. <https://doi.org/10.1016/j.tifs.2014.03.004>
- Arrieta, M.P, Fortunati, E., Dominici, F., Rayón, E., López, J., & Kenny, J. M. (2014). Multifunctional PLA-PHB/cellulose nanocrystal films: Processing, structural and thermal properties. *Carbohydrate Polymers*, *107*, 16–24. <https://doi.org/10.1016/j.carbpol.2014.02.044>
- Arrieta, Marina P, Peltzer, M. A., Del, M., Garrigós, C., & Jiménez, A. (2013). Structure and mechanical properties of sodium and calcium caseinate edible active films with carvacrol. *Journal of Food Engineering*, *114*, 486–494. <https://doi.org/10.1016/j.jfoodeng.2012.09.002>
- Arrieta, Marina Patricia, Parres, F., López, J., & Jiménez, A. (2013). Development of a novel pyrolysis-gas chromatography/mass spectrometry method for the analysis of poly(lactic acid) thermal degradation products. *Journal of Analytical and Applied Pyrolysis*, *101*, 150–155. <https://doi.org/10.1016/J.JAAP.2013.01.017>
- Awal, A., Rana, M., & Sain, M. (2015). Thermorheological and mechanical properties of cellulose reinforced PLA bio-composites. *Mechanics of Materials*, *80*, 87–95. <https://doi.org/10.1016/j.mechmat.2014.09.009>
- Aydogdu, A., Kirtil, E., Sumnu, G., Oztop, M. H., & Aydogdu, Y. (2018). Utilization of lentil flour as a biopolymer source for the development of edible films. *Journal of Applied Polymer Science*, *135*(23), 46356. <https://doi.org/10.1002/app.46356>
- Ayrancı, E., Ukta, B. S. U., & Cetin, E. E. (1997). The Effect of Molecular Weight of Constituents on Properties of Cellulose-based Edible Films. *LWT - Food Science and Technology*, *30*, 101–104. Retrieved from http://ac.els-cdn.com/S0023643896901401/1-s2.0-S0023643896901401-main.pdf?_tid=bb7aeada-39a5-11e7-906e-00000aab0f27&acdnat=1494877143_965eba086baa66fd6e9467949ddb9f71
- Aytac, Z., Kusku, I., Durgun, E., & Uyar, T. (2016a). Encapsulation of gallic acid/cyclodextrin inclusion complex in electrospun polylactic acid nanofibers: Release behavior and antioxidant activity of gallic acid. *Materials Science &*

- Engineering C*, 63, 231–239. <https://doi.org/10.1016/j.msec.2016.02.063>
- Aytac, Z., Kusku, I., Durgun, E., & Uyar, T. (2016b). Quercetin/β-cyclodextrin inclusion complex embedded nanofibres: Slow release and high solubility. *Food Chemistry*, 197, 864–871. <https://doi.org/10.1016/j.foodchem.2015.11.051>
- Aytac, Z., & Uyar, T. (2016). Antioxidant activity and photostability of α-tocopherol/β-cyclodextrin inclusion complex encapsulated electrospun polycaprolactone nanofibers. *European Polymer Journal*, 79, 140–149. <https://doi.org/10.1016/J.EURPOLYMJ.2016.04.029>
- Bamdad, F., Goli, A. H., & Kadivar, M. (2006). Preparation and characterization of proteinous film from lentil (*Lens culinaris*): Edible film from lentil (*Lens culinaris*). *Food Research International*, 39(1), 106–111. <https://doi.org/10.1016/j.foodres.2005.06.006>
- Barbana, C., & Boye, J. I. (2013). In vitro protein digestibility and physico-chemical properties of flours and protein concentrates from two varieties of lentil (*Lens culinaris*). *Food and Function*, 4(2), 310–321. <https://doi.org/10.1039/c2fo30204g>
- Bhardwaj, N., & Kundu, S. C. (2010). Electrospinning: A fascinating fiber fabrication technique. *Biotechnology Advances*. <https://doi.org/10.1016/j.biotechadv.2010.01.004>
- Blanco-Padilla, A., López-Rubio, A., Loarca-Piña, G., Gómez-Mascaraque, L. G., & Mendoza, S. (2015). Characterization, release and antioxidant activity of curcumin-loaded amaranth-pullulan electrospun fibers. *LWT - Food Science and Technology*, 63, 1137–1144. <https://doi.org/10.1016/j.lwt.2015.03.081>
- Boy, R., Maness, C., & Kotek, R. (2016). Properties of chitosan/soy protein blended films with added plasticizing agent as a function of solvent type at acidic pH. *International Journal of Polymeric Materials and Polymeric Biomaterials*, 65(1), 11–17. <https://doi.org/10.1080/00914037.2015.1038821>
- Busolo, M. A., Torres-giner, S., & Lagaron, J. M. (2009). Enhancing the Gas Barrier Properties of Polylactic Acid by Means of Electrospun Ultrathin Zein Fibers, 2763–2767.
- Cael, J. J., Koenig, J. L., & Blackwell, J. (1975). Infrared and Raman spectroscopy of carbohydrates. Part VI: Normal coordinate analysis of V?? amylose. *Biopolymers*, 14(9), 1885–1903. <https://doi.org/10.1002/bip.1975.360140909>
- Cam, D., & Marucci, M. (1997). Influence of residual monomers and metals on poly (L-lactide) thermal stability. *Polymer*, 38(8), 1879–1997. Retrieved from https://ac.els-cdn.com/S0032386196007112/1-s2.0-S0032386196007112-main.pdf?_tid=df5244d2-a483-4a7a-9532-dd64006dd79b&acdnat=1545287142_b7efd136744b5cabbe67eb045bab5b6f

- Cano, A., Fortunati, E., Chafer, M., Kenny, J. M., Chiralt, A., & Gonzalez-Martinez, C. (2015). Properties and ageing behaviour of pea starch films as affected by blend with poly(vinyl alcohol). *Food Hydrocolloids*, *48*, 84–93. <https://doi.org/10.1016/j.foodhyd.2015.01.008>
- Celebioglu, A., & Uyar, T. (2013). Electrospinning of nanofibers from non-polymeric systems: Electrospun nanofibers from native cyclodextrins. <https://doi.org/10.1016/j.jcis.2013.04.034>
- Celebioglu, A., Yildiz, Z. I., & Uyar, T. (2018). Fabrication of Electrospun Eugenol/Cyclodextrin Inclusion Complex Nanofibrous Webs for Enhanced Antioxidant Property, Water Solubility, and High Temperature Stability. *Journal of Agricultural and Food Chemistry*, *66*, 457–466. <https://doi.org/10.1021/acs.jafc.7b04312>
- Chen, Z., Mo, X., & Qing, F. (2007). Electrospinning of collagen–chitosan complex. *Materials Letters*, *61*(16), 3490–3494. <https://doi.org/10.1016/J.MATLET.2006.11.104>
- Cho, D., Netravali, A. N., & Joo, Y. L. (2012). Mechanical properties and biodegradability of electrospun soy protein Isolate/ PVA hybrid nanofibers. *Polymer Degradation and Stability*, *97*, 747–754. <https://doi.org/10.1016/j.polymdegradstab.2012.02.007>
- Cho, D., Nnadi, O., Netravali, A., & Joo, Y. L. (2010). Electrospun hybrid soy protein/PVA fibers. *Macromolecular Materials and Engineering*, *295*(8), 763–773. <https://doi.org/10.1002/mame.201000161>
- Choi, J. S., Lee, S. W., Jeong, L., Bae, S.-H., Min, B. C., Youk, J. H., & Park, W. H. (2004). Effect of organosoluble salts on the nanofibrous structure of electrospun poly(3-hydroxybutyrate-co-3-hydroxyvalerate). *International Journal of Biological Macromolecules*, *34*(4), 249–256. <https://doi.org/10.1016/J.IJBIOMAC.2004.06.001>
- Chung, H.-J., Liu, Q., Hoover, R., Warkentin, T. D., & Vandenberg, B. (2008). In vitro starch digestibility, expected glycemic index, and thermal and pasting properties of flours from pea, lentil and chickpea cultivars. *Food Chemistry*, *111*, 316–321. <https://doi.org/10.1016/j.foodchem.2008.03.062>
- Chuysinuan, P., Chimnoi, N., Techasakul, S., & Supaphol, P. (2009). Gallic acid-loaded electrospun poly(L-lactic acid) fiber mats and their release characteristic. *Macromolecular Chemistry and Physics*, *210*(10), 814–822. <https://doi.org/10.1002/macp.200800614>
- Ćirin, D. M., Poša, M. M., Krstonošić, V. S., & Lj Milanović, M. (2012). Conductometric study of sodium dodecyl sulfate–nonionic surfactant (Triton X-100, Tween 20, Tween 60, Tween 80 or Tween 85) mixed micelles in aqueous solution. *Hemijaska Industrija*, *66*(1), 21–28.

<https://doi.org/10.2298/HEMIND110612059C>

- Coles, S. R., Jacobs, D. K., Meredith, J. O., Barker, G., Clark, A. J., Kirwan, K., ... Tucker, N. (2010). A Design of Experiments (DoE) Approach to Material Properties Optimization of Electrospun Nanofibers. *Journal of Applied Polymer Science*, *17*, 2251–2257. <https://doi.org/10.1002/app>
- Colín-Orozco, J., Zapata-Torres, M., Rodríguez-Gattorno, G., & Pedroza-Islas, R. (2015). Properties of Poly (ethylene oxide)/ whey Protein Isolate Nanofibers Prepared by Electrospinning. *Food Biophysics*, *10*, 134–144. <https://doi.org/10.1007/s11483-014-9372-1>
- Cozmuta, A. M., Apjok, R., Peter, A., Cozmuta, L. M., Nicula, C., Baia, M., & Vulpoi, A. (2018). Active papers coated with chitosan and containing TiO₂ and Ag/TiO₂ nanoparticles for increasing the shelf-life of walnut kernels. *Cellulose*, *25*, 5205–5225. <https://doi.org/10.1007/s10570-018-1925-x>
- Crews, C., Patrick, H., Godward, J., Brereton, P., Lees, M., Guiet, S., & Wilfried, W. (2005). Study of the Main Constituents of Some Authentic Walnut Oils. *Journal of Agricultural and Food Chemistry*, *53*(12), 4853–4860. <https://doi.org/10.1021/JF0478354>
- da Rosa, Cleonice Goncalves, Borges, C. D., Zambiazzi, R. C., Nunes, M. R., Benvenutti, E. V., Luz, S. R. da, ... Rutz, J. K. (2013). Microencapsulation of gallic acid in chitosan, β -cyclodextrin and xanthan. *Industrial Crops and Products*, *46*, 138–146. <https://doi.org/10.1016/j.indcrop.2012.12.053>
- Da Rosa, Cleonice Gonçalves, Borges, C. D., Zambiazzi, R. C., Rutz, J. K., da Luz, S. R., Krumreich, F. D., ... Nunes, M. R. (2014). Encapsulation of the phenolic compounds of the blackberry (*Rubus fruticosus*). *LWT - Food Science and Technology*, *58*(2), 527–533. <https://doi.org/10.1016/j.lwt.2014.03.042>
- de Moraes Crizel, T., de Oliveira Rios, A., D. Alves, V., Bandarra, N., Moldão-Martins, M., & Hickmann Flôres, S. (2018). Active food packaging prepared with chitosan and olive pomace. *Food Hydrocolloids*, *74*, 139–150. <https://doi.org/10.1016/J.FOODHYD.2017.08.007>
- de Vos, P., Faas, M. M., Spasojevic, M., & Sikkema, J. (2010). Encapsulation for preservation of functionality and targeted delivery of bioactive food components. *International Dairy Journal*, *20*, 292–302. <https://doi.org/10.1016/j.idairyj.2009.11.008>
- De Vrieze, S., Van Camp, T., Nelvig, A., Hagström, B., Westbroek, P., & De Clerck, K. (2009). The effect of temperature and humidity on electrospinning. *Journal of Materials Science*, *44*(5), 1357–1362. <https://doi.org/10.1007/s10853-008-3010-6>
- Deitzel, J. ., Kleinmeyer, J., Harris, D., & Beck Tan, N. . (2001). The effect of

- processing variables on the morphology of electrospun nanofibers and textiles. *Polymer*. [https://doi.org/10.1016/S0032-3861\(00\)00250-0](https://doi.org/10.1016/S0032-3861(00)00250-0)
- Demir, M. M., Yilgor, I., Yilgor, E., & Erman, B. (2002). Electrospinning of polyurethane fibers, *43*, 3303–3309.
- Deng, L., Kang, X., Liu, Y., Feng, F., & Zhang, H. (2017). Effects of surfactants on the formation of gelatin nanofibres for controlled release of curcumin. *Food Chemistry*, *231*, 70–77. <https://doi.org/10.1016/J.FOODCHEM.2017.03.027>
- Dick, M., Costa, T. M. H., Gomaa, A., Subirade, M., Rios, A. D. O., & Flôres, S. H. (2015). Edible film production from chia seed mucilage: Effect of glycerol concentration on its physicochemical and mechanical properties. *Carbohydrate Polymers*, *130*, 198–205. <https://doi.org/10.1016/j.carbpol.2015.05.040>
- Ding, C., Zhang, M., & Li, G. (2015). Preparation and characterization of collagen/hydroxypropyl methylcellulose (HPMC) blend film. *Carbohydrate Polymers*, *119*, 194–201. <https://doi.org/10.1016/j.carbpol.2014.11.057>
- Doshi, J., & Reneker, D. H. (1995). Electrospinning Process and Applications of Electrospun Fibers. *Journal of Electrostatics*, *35*, 151–160. <https://doi.org/10.1002/jcb.23036>
- Drosou, C. G., Krokida, M. K., & Biliaderis, C. G. (2017). Encapsulation of bioactive compounds through electrospinning/electrospraying and spray drying: A comparative assessment of food-related applications. *Drying Technology*, *35*(2), 139–162. <https://doi.org/10.1080/07373937.2016.1162797>
- El-Aassar, M. R. (2013). Journal of Molecular Catalysis B : Enzymatic Functionalized electrospun nanofibers from poly (AN-co-MMA) for enzyme immobilization. *Journal of Molecular Catalysis B: Enzymatic*, *85–86*, 140–148. <https://doi.org/10.1016/j.molcatb.2012.09.002>
- El-Moghazy, A. Y., Soliman, E. A., Ibrahim, H. Z., Marty, J. L., Istamboulie, G., & Noguier, T. (2016). Biosensor based on electrospun blended chitosan-poly (vinyl alcohol) nanofibrous enzymatically sensitized membranes for pirimiphos-methyl detection in olive oil. *Talanta*, *155*, 258–264. <https://doi.org/10.1016/j.talanta.2016.04.018>
- Elizalde, B. E., Bartholomai, G. B., & Pilosof, A. M. R. (1996). The Effect of pH on the Relationship Between Hydrophilic/Lipophilic Characteristics and Emulsification Properties of Soy Proteins. *LWT - Food Science and Technology*, *29*, 334–339. Retrieved from https://ac.els-cdn.com/S002364389690050X/1-s2.0-S002364389690050X-main.pdf?_tid=69813749-7a2d-4ad4-907f-3b443ab1d422&acdnat=1544659101_f94ebb503ceae1fa5ab3868156a5d1b5
- Fabra, Maria Jose, Lopez-Rubio, A., & Lagaron, J. M. (2015). Effect of the film-processing conditions, relative humidity and ageing on wheat gluten films coated

- with electrospun polyhydroxyalkanoate. *Food Hydrocolloids*, 44, 292–299. <https://doi.org/10.1016/j.foodhyd.2014.09.032>
- Fabra, Maria Jose, Lopez-Rubio, A., & Lagaron, J. M. (2016). Use of the electrohydrodynamic process to develop active/bioactive bilayer films for food packaging applications. *Food Hydrocolloids*, 55, 11–18. <https://doi.org/10.1016/j.foodhyd.2015.10.026>
- Fabra, María José, Lopez-rubio, A., & Lagaron, J. M. (2014). Nanostructured interlayers of zein to improve the barrier properties of high barrier polyhydroxyalkanoates and other polyesters. *Journal of Food Engineering*, 127, 1–9. <https://doi.org/10.1016/j.jfoodeng.2013.11.022>
- Fabra, María José, Lopez-Rubio, A., & Lagaron, J. M. (2013). High barrier polyhydroxyalkanoate food packaging film by means of nanostructured electrospun interlayers of zein. *Food Hydrocolloids*, 32(1), 106–114. <https://doi.org/10.1016/J.FOODHYD.2012.12.007>
- Fabra, María José, López-Rubio, A., & Lagaron, J. M. (2014). On the use of different hydrocolloids as electrospun adhesive interlayers to enhance the barrier properties of polyhydroxyalkanoates of interest in fully renewable food packaging concepts. *Food Hydrocolloids*, 39, 77–84. <https://doi.org/10.1016/J.FOODHYD.2013.12.023>
- Fabra, María José, López-Rubio, A., & Lagaron, J. M. (2015). Three-Layer Films Based on Wheat Gluten and Electrospun PHA. *Food and Bioprocess Technology*, 2330–2340. <https://doi.org/10.1007/s11947-015-1590-0>
- Fazel, R., Torabi, S., Naseri-nosar, P., Ghasempur, S., Ranaei-siadat, S., & Khajeh, K. (2016). Enzyme and Microbial Technology Electrospun polyvinyl alcohol / bovine serum albumin biocomposite membranes for horseradish peroxidase immobilization. *Enzyme and Microbial Technology*, 93–94, 1–10. <https://doi.org/10.1016/j.enzmictec.2016.07.002>
- Fernandez, A., Torres-Giner, S., & Lagaron, J. M. (2009). Novel route to stabilization of bioactive antioxidants by encapsulation in electrospun fibers of zein prolamine. *Food Hydrocolloids*, 23(5), 1427–1432. <https://doi.org/10.1016/J.FOODHYD.2008.10.011>
- Fong, H., Chun, I., & Reneker, D. H. (1999). Beaded nanofibers formed during electrospinning. *Polymer*, 40, 4585–4592. Retrieved from https://ac.els-cdn.com/S0032386199000683/1-s2.0-S0032386199000683-main.pdf?_tid=f7d46558-ba65-43f9-b0ef-baa397d17f1a&acdnat=1551591296_92e4c57f3bd52ace628d476a70f98f9d
- Ford, J. L. (1999). Thermal analysis of hydroxypropylmethylcellulose and methylcellulose: powders, gels and matrix tablets. *International Journal of Pharmaceutics*, 179, 209–228.

- Formhals, A. (1934). Process and Apparatus for Preparing Artificial Threads. <https://doi.org/D01D5/00>
- Fortunati, E., Puglia, D., Luzi, F., Santulli, C., Kenny, J. M., & Torre, L. (2013). Binary PVA bio-nanocomposites containing cellulose nanocrystals extracted from different natural sources: Part I. *Carbohydrate Polymers*, *97*(2), 825–836. <https://doi.org/10.1016/J.CARBPOL.2013.03.075>
- Friedman, M., & Jü, H. S. (2000). Effect of pH on the Stability of Plant Phenolic Compounds. *Journal of Agricultural and Food Chemistry*, *48*, 2101–2110. <https://doi.org/10.1021/jf990489j>
- Fuller, C. ., MacRae, R. ., Walther, M., & Cameron, R. . (2001). Interactions in poly(ethylene oxide)–hydroxypropyl methylcellulose blends. *Polymer*, *42*(23), 9583–9592. [https://doi.org/10.1016/S0032-3861\(01\)00477-3](https://doi.org/10.1016/S0032-3861(01)00477-3)
- Furlan, R., Rosado, J. a. M., Rodriguez, G. G., Fachini, E. R., da Silva, a. N. R., & da Silva, M. L. P. (2012). Formation and Characterization of Oriented Micro- and Nanofibers Containing Poly (ethylene oxide) and Pectin. *Journal of the Electrochemical Society*, *159*(3), K66–K71. <https://doi.org/10.1149/2.057203jes>
- Geng, X., Kwon, O.-H., & Jang, J. (2005). Electrospinning of chitosan dissolved in concentrated acetic acid solution. *Biomaterials*, *26*(27), 5427–5432. <https://doi.org/10.1016/j.biomaterials.2005.01.066>
- Geoffrey R Mitchell (Ed.). (2015). *Electrospinning Principles, Practice and Possibilities*. Royal Society of Chemistry.
- Ghiteșcu, R.-E., Popa, A.-M., Popa, V. I., Rossi, R. M., & Fortunato, G. (2015). Encapsulation of polyphenols into pHEMA e-spun fibers and determination of their antioxidant activities. *International Journal of Pharmaceutics*, *494*(1), 278–287. <https://doi.org/10.1016/J.IJPHARM.2015.08.020>
- Ghorani, B., & Tucker, N. (2015). Fundamentals of electrospinning as a novel delivery vehicle for bioactive compounds in food nanotechnology. *Food Hydrocolloids*, *51*, 227–240. <https://doi.org/10.1016/j.foodhyd.2015.05.024>
- Guirguis, O. W., & Moselhey, M. T. H. (2012). Thermal and structural studies of poly (vinyl alcohol) and hydroxypropyl cellulose blends. *Natural Science*, *04*(01), 57–67. <https://doi.org/10.4236/ns.2012.41009>
- Guo, C., Zhou, L., & Lv, J. (2013). Effects of expandable graphite and modified ammonium polyphosphate on the flame-retardant and mechanical properties of wood flour-polypropylene composites. *Polymers and Polymer Composites*, *21*(7), 449–456. <https://doi.org/10.1002/app>
- Gupta, D., Jassal, M., & Agrawal, A. K. (2015). Electrospinning of Poly(vinyl alcohol)-Based Boger Fluids To Understand the Role of Elasticity on Morphology of Nanofibers. *Industrial & Engineering Chemistry Research*, *54*,

1547–1554. <https://doi.org/10.1021/ie504141c>

- Gupta, P., Elkins, C., Long, T. E., & Wilkes, G. L. (2005). Electrospinning of linear homopolymers of poly(methyl methacrylate): exploring relationships between fiber formation, viscosity, molecular weight and concentration in a good solvent. *Polymer*, *46*, 4799–4810. <https://doi.org/10.1016/j.polymer.2005.04.021>
- Haghi, A. K., & Akbari, M. (2007). Trends in electrospinning of natural nanofibers. In *Physica Status Solidi (A) Applications and Materials Science* (Vol. 204, pp. 1830–1834). <https://doi.org/10.1002/pssa.200675301>
- Haider, A., Haider, S., & Kang, I.-K. (2018). A comprehensive review summarizing the effect of electrospinning parameters and potential applications of nanofibers in biomedical and biotechnology. *Arabian Journal of Chemistry*, *11*, 1165–1188. Retrieved from https://ac.els-cdn.com/S1878535215003275/1-s2.0-S1878535215003275-main.pdf?_tid=a222a972-c478-4362-b280-612e23578151&acdnat=1551389861_786a412d7d4a498fc60a9894bb788fe5
- Hardiansyah, A., Tanadi, H., Yang, M., & Liu, T. (2015). Electrospinning and antibacterial activity of chitosan-blended poly (lactic acid) nanofibers. *Journal of Polymer Research*, *22*(59), 1–10. <https://doi.org/10.1007/s10965-015-0704-8>
- Hosseini, S. F., Nahvi, Z., & Zandi, M. (2019). Antioxidant peptide-loaded electrospun chitosan/poly(vinyl alcohol) nanofibrous mat intended for food biopackaging purposes. *Food Hydrocolloids*, *89*, 637–648. <https://doi.org/10.1016/j.foodhyd.2018.11.033>
- Hottle, T. A., Bilec, M. M., & Landis, A. E. (2013). Sustainability assessments of bio-based polymers. *Polymer Degradation and Stability*, *98*, 1898–1907. <https://doi.org/10.1016/j.polymdegradstab.2013.06.016>
- Huang, L., Nagapudi, K., P.Apkarian, R., & Chaikof, E. L. (2001). Engineered collagen–PEO nanofibers and fabrics. *Journal of Biomaterials Science, Polymer Edition*, *12*(9), 979–993. <https://doi.org/10.1163/156856201753252516>
- Huang, Z.-M., Zhang, Y.-Z., Kotaki, M., & Ramakrishna, S. (2003). A review on polymer nanofibers by electrospinning and their applications in nanocomposites. *Composites Science and Technology*, *63*(15), 2223–2253. [https://doi.org/10.1016/S0266-3538\(03\)00178-7](https://doi.org/10.1016/S0266-3538(03)00178-7)
- Inkinen, S., Hakkarainen, M., Albertsson, A.-C., & Södergard, A. (2011). From Lactic Acid to Poly(lactic acid) (PLA): Characterization and Analysis of PLA and Its Precursors. *Biomacromolecules*, *12*, 523–532. <https://doi.org/10.1021/bm101302t>
- Islam, M. S., & Karim, M. R. (2010). Fabrication and characterization of poly(vinyl alcohol)/alginate blend nanofibers by electrospinning method. *Colloids and Surfaces A: Physicochemical and Engineering Aspects*, *366*(1–3), 135–140.

<https://doi.org/10.1016/j.colsurfa.2010.05.038>

- Issa, A. A., Al-maadeed, M., Luyt, A. S., Mrlik, M., & Hassan, M. K. (2016). Investigation of the physico-mechanical properties of electrospun PVDF / cellulose (nano) fibers. *Journal of Applied Polymer Science*, 43594, 2–13. <https://doi.org/10.1002/app.43594>
- Jacic, M., Vrandecic, N. S., & Erceg, M. (2016). Kinetic analysis of the non-isothermal degradation of poly(vinyl chloride)/poly(ethylene oxide) blends. *Journal of Thermal Analysis and Calorimetry*, 123(2), 1513–1522. <https://doi.org/10.1007/s10973-015-5096-9>
- Jia, Y. T., Gong, J., Gu, X. H., Kim, H. Y., Dong, J., & Shen, X. Y. (2007). Fabrication and characterization of poly (vinyl alcohol)/chitosan blend nanofibers produced by electrospinning method. *Carbohydrate Polymers*, 67(3), 403–409. <https://doi.org/10.1016/j.carbpol.2006.06.010>
- Jiang, H., Fang, D., Hsiao, B., Chu, B., & Chen, W. (2004). Preparation and characterization of ibuprofen-loaded poly(lactide-co-glycolide)/poly(ethylene glycol)-g-chitosan electrospun membranes. *Journal of Biomaterials Science. Polymer Edition*, 15(3), 279–296. Retrieved from <http://www.ncbi.nlm.nih.gov/pubmed/15147162>
- Jimenez, A., Fabra, M. J., Talens, P., & Chiralt, A. (2012). Effect of re-crystallization on tensile, optical and water vapour barrier properties of corn starch films containing fatty acids. *Food Hydrocolloids*, 26(1), 302–310. <https://doi.org/10.1016/j.foodhyd.2011.06.009>
- Kararli, T. T., Hurlbut, J. B., & Needham, T. E. (1990). Glass–Rubber Transitions of Cellulosic Polymers by Dynamic Mechanical Analysis. *Journal of Pharmaceutical Sciences*, 79(9), 845–848. <https://doi.org/10.1002/jps.2600790922>
- Kattamuri, N., Shin, J. H., Kang, B., Lee, C. G., Lee, J. K., & Sung, C. (2005). Development and surface characterization of positively charged filters. *Journal of Materials Science*, 40(17), 4531–4539. <https://doi.org/10.1007/s10853-005-2803-0>
- Katti, D. S., Robinson, K. W., Ko, F. K., & Laurencin, C. T. (2004). Bioresorbable nanofiber-based systems for wound healing and drug delivery: Optimization of fabrication parameters. *Journal of Biomedical Materials Research*, 70B(2), 286–296. <https://doi.org/10.1002/jbm.b.30041>
- Kayaci, F., & Uyar, T. (2012). Encapsulation of vanillin/cyclodextrin inclusion complex in electrospun polyvinyl alcohol (PVA) nanoweb: Prolonged shelf-life and high temperature stability of vanillin. *Food Chemistry*, 133(3), 641–649. <https://doi.org/10.1016/J.FOODCHEM.2012.01.040>

- Kessick, R., & Tepper, G. (2004). Microscale polymeric helical structures produced by electrospinning. *Applied Physics Letter*, 84(23), 4807–4809. <https://doi.org/10.1063/1.1762704>
- Ki, C. S., Baek, D. H., Gang, K. D., Lee, K. H., Um, I. C., & Park, Y. H. (2005). Characterization of gelatin nanofiber prepared from gelatin–formic acid solution. *Polymer*, 46(14), 5094–5102. <https://doi.org/10.1016/j.polymer.2005.04.040>
- Kim, Y.-J. (2007). Antimelanogenic and Antioxidant Properties of Gallic Acid. *Biological & Pharmaceutical Bulletin*. <https://doi.org/10.1248/bpb.30.1052>
- Kizil, R., Irudayaraj, J., And, †, & Seetharaman, K. (2002). Characterization of Irradiated Starches by Using FT-Raman and FTIR Spectroscopy. *Journal of Agr*, 50, 3912–3918. <https://doi.org/10.1021/jf011652p>
- Klossner, R. R., Queen, H. A., Coughlin, A. J., & Krause, W. E. (2008). Correlation of Chitosan's Rheological Properties and Its Ability to Electrospin. *Biomacromolecules*, 9, 2947–2953. <https://doi.org/10.1021/bm800738u>
- Kong, L., & Ziegler, G. R. (2014). Rheological aspects in fabricating pullulan fibers by electro-wet- spinning. *Food Hydrocolloids*, 38, 220–226. <https://doi.org/10.1016/j.foodhyd.2013.12.016>
- Kriegel, C., Arecchi, A., Arrecchi, A., Kit, K., McClements, D. J., & Weiss, J. (2008). Fabrication, functionalization, and application of electrospun biopolymer nanofibers. *Critical Reviews in Food Science and Nutrition*, 48(8), 775–797. <https://doi.org/10.1080/10408390802241325>
- Kriegel, C., Kit, K. M., McClements, D. J., & Weiss, J. (2009a). Electrospinning of chitosan–poly(ethylene oxide) blend nanofibers in the presence of micellar surfactant solutions. *Polymer*, 50(1), 189–200. <https://doi.org/10.1016/J.POLYMER.2008.09.041>
- Kriegel, C., Kit, K. M., McClements, D. J., & Weiss, J. (2009b). Influence of Surfactant Type and Concentration on Electrospinning of Chitosan–Poly(Ethylene Oxide) Blend Nanofibers. *Food Biophysics*, 4(3), 213–228. <https://doi.org/10.1007/s11483-009-9119-6>
- Kumar, N., Kaur, P., & Bhatia, S. (2017). Advances in bio-nanocomposite materials for food packaging: a review. *Bio-Nanocomposite Materials*, 47(4), 591–606. <https://doi.org/10.1108/00346651111151384>
- Lala, N. L., Ramaseshan, R., Bojun, L., Sundarajan, S., Barhate, R. S., Ying-jun, L., & Ramakrishna, S. (2007). Fabrication of nanofibers with antimicrobial functionality used as filters: protection against bacterial contaminants. *Biotechnology and Bioengineering*, 97(6), 1357–1365. <https://doi.org/10.1002/bit.21351>
- Lee, S. (2009). Developing UV-protective textiles based on electrospun zinc oxide

- nanocomposite fibers. *Fibers and Polymers*. <https://doi.org/10.1007/s12221-009-0295-2>
- Lee, Y. J., Shin, D. S., Kwon, O. W., Park, W. H., Choi, H. G., Lee, Y. R., ... Lyoo, W. S. (2007). Preparation of atactic poly(vinyl alcohol)/sodium alginate blend nanowebs by electrospinning. *Journal of Applied Polymer Science*, *106*(2), 1337–1342. <https://doi.org/10.1002/app.26568>
- Li, J., Kim, S. Y., Chen, X., & Park, H. J. (2016). Calcium-alginate beads loaded with gallic acid: Preparation and characterization. *LWT - Food Science and Technology*, *68*, 667–673. <https://doi.org/10.1016/J.LWT.2016.01.012>
- Li, W.-J., Laurencin, C. T., Caterson, E. J., Tuan, R. S., & Ko, F. K. (2002). Electrospun nanofibrous structure: A novel scaffold for tissue engineering. *Journal of Biomedical Materials Research*, *60*(4), 613–621. <https://doi.org/10.1002/jbm.10167>
- Li, Z., & Wang, C. (2013). *One dimensional Nanostructures Electrospinning Technique and Unique Nanofibers*. London: Springer. <https://doi.org/10.1007/978-3-642-36427-3>
- Lim, Y.-M., Gwon, H.-J., Pyo Jeun, J., & Nho, Y.-C. (2010). Preparation of Cellulose-based Nanofibers Using Electrospinning. In A. Kumar (Ed.), *Nanofibers*. Retrieved from <http://cdn.intechweb.org/pdfs/8643.pdf>
- Lin, S., Breene, W. M., & Sargent, J. S. (1990). Effects of pH, Sodium Chloride, Polysaccharides, and Surfactants on the Pasting Characteristics of Pea Flours (*Pisum sativum*). *Cereal Chemistry*. Retrieved from https://www.aaccnet.org/publications/cc/backissues/1990/Documents/67_14.pdf
- Lin, Y., Yao, Y., Yang, X., Wei, N., Li, X., Gong, P., ... Wu, D. (2008). Preparation of Poly(ether sulfone) Nanofibers by Gas-Jet/Electrospinning. *Journal of Applied Polymer Science*, *107*, 909–917. <https://doi.org/10.1002/app>
- Liu, F., Guo, R., Shen, M., Wang, S., & Shi, X. (2009). Effect of processing variables on the morphology of electrospun poly[(lactic acid)-co-(glycolic acid)] nanofibers. *Macromolecular Materials and Engineering*, *294*(10), 666–672. <https://doi.org/10.1002/mame.200900110>
- Liu, J., Niu, J., Yin, L., & Jiang, F. (2011). In situ encapsulation of laccase in nanofibers by electrospinning for development of enzyme biosensors for chlorophenol monitoring. *Analyst*, *136*(4802). <https://doi.org/10.1039/c1an15649g>
- Liu, W., Sun, D., Li, C., Liu, Q., & Xu, J. (2006). Formation and stability of paraffin oil-in-water nano-emulsions prepared by the emulsion inversion point method. *Journal of Colloid and Interface Science*, *303*(2), 557–563.

<https://doi.org/10.1016/j.jcis.2006.07.055>

- Liu, X., Song, R., Zhang, W., Qi, C., Zhang, S., & Li, J. (2017). *Development of Eco-friendly Soy Protein Isolate Films with High Mechanical Properties through HNTs, PVA, and PTGE Synergism Effect OPEN*. <https://doi.org/10.1038/srep44289>
- Liu, Y., Gu, J., Zhang, J., Yu, F., Wang, J., Nie, N., & Li, W. (2015). LiFePO₄ nanoparticles growth with preferential (010) face modulated by Tween-80. *Rsc Advances*, 5(13), 9745–9751. <https://doi.org/10.1039/c4ra14791j>
- Lopez-Amoros, M. L., Hernandez, T., & Estrella, I. (2006). Effect of germination on legume phenolic compounds and their antioxidant activity. *Journal of Food Composition and Analysis*, 19, 277–283. Retrieved from https://ac.els-cdn.com/S0889157504001218/1-s2.0-S0889157504001218-main.pdf?_tid=ba386dd1-c298-4b8a-a67b-b8b0621e704e&acdnat=1545950001_fa2dd781beefc118e06cfdcdc39fc2f7
- Lu, J.-W., Zhu, Y.-L., Guo, Z.-X., Hu, P., & Yu, J. (2006). Electrospinning of sodium alginate with poly(ethylene oxide). *Polymer*, 47(23), 8026–8031. <https://doi.org/10.1016/j.polymer.2006.09.027>
- Luca, A., Cilek, B., Hasirci, V., Sahin, S., & Sumnu, G. (2013). Effect of Degritting of Phenolic Extract from Sour Cherry Pomace on Encapsulation Efficiency-Production of Nano-suspension. *Food and Bioprocess Technology*, 6(9), 2494–2502. <https://doi.org/10.1007/s11947-012-0880-z>
- Mascheroni, E., Fuenmayor, C. A., Cosio, M. S., Di Silvestro, G., Piergiovanni, L., Mannino, S., & Schiraldi, A. (2013). Encapsulation of volatiles in nanofibrous polysaccharide membranes for humidity-triggered release. *Carbohydrate Polymers*, 98(1), 17–25. <https://doi.org/10.1016/J.CARBPOL.2013.04.068>
- McHugh, T. H., Avenabustillos, R., & Krochta, J. M. (1993). Hydrophilic Edible Films - Modified Procedure for Water-Vapor Permeability and Explanation of Thickness Effects. *J Food Sci*, 58(4), 899–903. <https://doi.org/10.1111/j.1365-2621.1993.tb09387.x>
- McKee, M. G., Wilkes, G. L., Colby, R. H., & Long, T. E. (2004). Correlations of Solution Rheology with Electrospun Fiber Formation of Linear and Branched Polyesters. *Macromolecules*, 37(5), 1760–1767. <https://doi.org/10.1021/ma035689h>
- Meechaisue, C., Dubin, R., Supaphol, P., Hoven, V. P., & Kohn, J. (2006). Electrospun mat of tyrosine-derived polycarbonate fibers for potential use as tissue scaffolding material. *Journal of Biomaterials Science. Polymer Edition*, 17(9), 1039–1056. Retrieved from <https://www.ncbi.nlm.nih.gov/pubmed/17094641>

- Megelski, S., Stephens, J. S., Chase, D. B., & Rabolt, J. F. (2002). Micro-and Nanostructured Surface Morphology on Electrospun Polymer Fibers. *Macromolecules*, *35*, 8456–8466. <https://doi.org/10.1021/ma020444a>
- Mit-Uppatham, C., Nithitanakul, M., & Supaphol, P. (2004). Ultrafine electrospun polyamide-6 fibers: Effect of solution conditions on morphology and average fiber diameter. *Macromolecular Chemistry and Physics*, *205*(17), 2327–2338. <https://doi.org/10.1002/macp.200400225>
- Moomand, K., & Lim, L.-T. (2014). Oxidative stability of encapsulated fish oil in electrospun zein fibres. *Food Research International*, *62*, 523–532. <https://doi.org/10.1016/J.FOODRES.2014.03.054>
- Nawab, A., Alam, F., Haq, M. A., Lutfi, Z., & Hasnain, A. (2018). Effect of mango kernel starch coatings on the shelf life of almond (*Prunus dulcis*) kernels. *Journal of Food Processing and Preservation*, *42*(2), 1–7. <https://doi.org/10.1111/jfpp.13449>
- Neo, Y. P., Ray, S., Easteal, A. J., Nikolaidis, M. G., & Quek, S. Y. (2012). Influence of solution and processing parameters towards the fabrication of electrospun zein fibers with sub-micron diameter. *Journal of Food Engineering*, *109*(4), 645–651. <https://doi.org/10.1016/j.jfoodeng.2011.11.032>
- Neo, Y. P., Ray, S., Jin, J., Gizdavic-Nikolaidis, M., Nieuwoudt, M. K., Liu, D., & Quek, S. Y. (2013). Encapsulation of food grade antioxidant in natural biopolymer by electrospinning technique: a physicochemical study based on zein-gallic acid system. *Food Chemistry*, *136*(2), 1013–1021. <https://doi.org/10.1016/j.foodchem.2012.09.010>
- Nidhi, K., Indrajeet, S., Khushboo, M., Gauri, K., & Sen, D. J. (2011). Hydrotropy: A promising tool for solubility enhancement: A review. *International Journal of Drug Development and Research*, *3*(2), 26–33. <https://doi.org/10.1002/jps>
- Nieuwland, M., Geerdink, P., Brier, P., van den Eijnden, P., Henket, J. T. M. M., Langelaan, M. L. P., ... Martin, A. H. (2013). Food-grade electrospinning of proteins. *Innovative Food Science & Emerging Technologies*, *20*, 269–275. <https://doi.org/10.1016/j.ifset.2013.09.004>
- Oguz, S., Tam, N., Aydogdu, A., Sumnu, G., & Sahin, S. (2018). Development of novel pea flour-based nanofibres by electrospinning method. *International Journal of Food Science and Technology*, *53*(5), 1269–1277. <https://doi.org/10.1111/ijfs.13707>
- Okutan, N., Terzi, P., & Altay, F. (2014). Affecting parameters on electrospinning process and characterization of electrospun gelatin nanofibers. *Food Hydrocolloids*, *39*, 19–26. <https://doi.org/10.1016/j.foodhyd.2013.12.022>
- Olga, G., Styliani, C., & Ioannis, R. G. (2015). Coencapsulation of Ferulic and Gallic

- acid in hp-b-cyclodextrin. *Food Chemistry*, *185*, 33–40. <https://doi.org/10.1016/j.foodchem.2015.03.058>
- Oriero, D. A., Gyan, I. O., Bolshaw, B. W., Cheng, I. F., & Aston, D. E. (2015). Electrospun biocatalytic hybrid silica-PVA-tyrosinase fiber mats for electrochemical detection of phenols. *Microchemical Journal*, *118*, 166–175. <https://doi.org/10.1016/j.microc.2014.09.005>
- Oriero, D. A., Jabal, J. M. F., Deobald, L., Weakley, A. T., & Aston, D. E. (2011). A potential enzyme-encapsulating, ultrafine fiber for phenol detection. *Reactive and Functional Polymers*, *71*, 870–880. <https://doi.org/10.1016/j.reactfunctpolym.2011.05.004>
- Ozdemir, M., & Floros, J. D. (2008). Optimization of edible whey protein films containing preservatives for water vapor permeability, water solubility and sensory characteristics. *Journal of Food Engineering*, *86*(2), 215–224. <https://doi.org/10.1016/j.jfoodeng.2007.09.028>
- Pakravan, M., Heuzey, M.-C., & Ajji, A. (2011). A fundamental study of chitosan/PEO electrospinning. *Polymer*, *52*(21), 4813–4824. <https://doi.org/10.1016/j.polymer.2011.08.034>
- Pantani, R., Gorrasi, G., Vigliotta, G., Murariu, M., & Dubois, P. (2013). PLA-ZnO nanocomposite films: Water vapor barrier properties and specific end-use characteristics. *European Polymer Journal*, *49*, 3471–3482. <https://doi.org/10.1016/j.eurpolymj.2013.08.005>
- Park, J.-Y., & Lee, I.-H. (2010). Relative Humidity Effect on the Preparation of Porous Electrospun Polystyrene Fibers. *Journal of Nanoscience and Nanotechnology*, *10*(5), 3473–3477. <https://doi.org/10.1166/jnn.2010.2349>
- Patel, A. C., Li, S., Yuan, J. M., & Wei, Y. (2006). In situ encapsulation of horseradish peroxidase in electrospun porous silica fibers for potential biosensor applications. *Nano Letters*, *6*(5), 1042–1046. <https://doi.org/10.1021/nl0604560>
- Pelegri, D. H. G., & Gasparetto, C. A. (2005). Whey proteins solubility as function of temperature and pH. *LWT - Food Science and Technology*, *38*(1), 77–80. <https://doi.org/10.1016/J.LWT.2004.03.013>
- Pelipenko, J., Kristl, J., Jankov, B., Baumgartner, S., & Kocbek, P. (2013). The impact of relative humidity during electrospinning on the morphology and mechanical properties of nanofibers. *International Journal of Pharmaceutics*, *456*, 125–134. <https://doi.org/10.1016/j.ijpharm.2013.07.078>
- Pelissari, F. M., Andrade-Mahecha, M. M., Sobral, P. J. D. A., & Menegalli, F. C. (2013). Comparative study on the properties of flour and starch films of plantain bananas (*Musa paradisiaca*). *Food Hydrocolloids*, *30*(2), 681–690. <https://doi.org/10.1016/j.foodhyd.2012.08.007>

- Pereira de Abreu, D. a., Paseiro Losada, P., Maroto, J., & Cruz, J. M. (2011). Natural antioxidant active packaging film and its effect on lipid damage in frozen blue shark (*Prionace glauca*). *Innovative Food Science & Emerging Technologies*, *12*(1), 50–55. <https://doi.org/10.1016/j.ifset.2010.12.006>
- Phiriyawirut, M., & Phaechamud, T. (2012). Gallic Acid-loaded Cellulose Acetate Electrospun Nanofibers : Thermal Properties , Mechanical Properties , and Drug Release Behavior. *Open Journal of Polymer Chemistry*, *2*(1), 21–29. <https://doi.org/http://dx.doi.org/10.4236/ojpcem.2012.21004>
- Pielichowski, K., & Flejtuch, K. (2005). Non-oxidative thermal degradation of poly(ethylene oxide): kinetic and thermoanalytical study. *Journal of Analytical and Applied Pyrolysis*, *73*, 131–138. <https://doi.org/10.1016/j.jaap.2005.01.003>
- Pralhad, T., & Rajendrakumar, K. (2004). Study of freeze-dried quercetin–cyclodextrin binary systems by DSC, FT-IR, X-ray diffraction and SEM analysis. *Journal of Pharmaceutical and Biomedical Analysis*, *34*(2), 333–339. [https://doi.org/10.1016/S0731-7085\(03\)00529-6](https://doi.org/10.1016/S0731-7085(03)00529-6)
- Ramakrishna, S., Fujihara, K., Teo, W. E., Lim, T.-C., & Ma, Z. (2005a). *An Introduction to Electrospinning and Nanofibers*. Singapore: World Scientific Publishing.
- Ramakrishna, S., Fujihara, K., Teo, W. E., Lim, T.-C., & Ma, Z. (2005b). *An Introduction to Electrospinning and Nanofibers*. Singapore: world scientific publishing.
- Ramji, K., & Shah, R. N. (2014). Electrospun soy protein nanofiber scaffolds for tissue regeneration. *Journal of Biomaterials Applications*, *29*(3), 411–422. <https://doi.org/10.1177/0885328214530765>
- Ren, G., Xu, X., Liu, Q., Cheng, J., Yuan, X., Wu, L., & Wan, Y. (2006). Electrospun poly(vinyl alcohol)/glucose oxidase biocomposite membranes for biosensor applications. *Reactive and Functional Polymers*, *66*(12), 1559–1564. <https://doi.org/10.1016/J.REACTFUNCTPOLYM.2006.05.005>
- Rhim, J.-W., Lee, J. H., & Ng, P. K. W. (2007). Mechanical and barrier properties of biodegradable soy protein isolate-based films coated with polylactic acid. *LWT - Food Science and Technology*, *40*, 232–238. <https://doi.org/10.1016/j.lwt.2005.10.002>
- Rho, K. S., Jeong, L., Lee, G., Seo, B.-M., Park, Y. J., Hong, S.-D., ... Min, B.-M. (2006). Electrospinning of collagen nanofibers: Effects on the behavior of normal human keratinocytes and early-stage wound healing. *Biomaterials*, *27*(8), 1452–1461. <https://doi.org/10.1016/j.biomaterials.2005.08.004>
- Rieger, K. A., Birch, N. P., & Schiffman, J. D. (2016). Electrospinning chitosan/poly(ethylene oxide) solutions with essential oils: Correlating solution

- rheology to nanofiber formation. *Carbohydrate Polymers*, 139, 131–138. <https://doi.org/10.1016/j.carbpol.2015.11.073>
- Robert, P., García, P., Reyes, N., Chávez, J., & Santos, J. (2012). Acetylated starch and inulin as encapsulating agents of gallic acid and their release behaviour in a hydrophilic system. *Food Chemistry*, 134(1), 1–8. <https://doi.org/10.1016/j.foodchem.2012.02.019>
- Rocco, A. M., Moreira, D. P., & Pereira, R. P. (2003). Specific interactions in blends of poly(ethylene oxide) and poly(bisphenol A-co-epichlorohydrin): FTIR and thermal study. *European Polymer Journal*, 39(9), 1925–1934. [https://doi.org/10.1016/S0014-3057\(03\)00098-3](https://doi.org/10.1016/S0014-3057(03)00098-3)
- Rodríguez-deLuna, S. E., Moreno-Cortez, I. E., Garza-Navarro, M. A., Lucio-Porto, R., López Pavón, L., & González-González, V. A. (2017). Thermal stability of the immobilization process of horseradish peroxidase in electrospun polymeric nanofibers. *Journal of Applied Polymer Science*, 134(19). <https://doi.org/10.1002/app.44811>
- Safi, S., Morshed, M., Hosseini Ravandi, S. A., & Ghiaci, M. (2007). Study of electrospinning of sodium alginate, blended solutions of sodium alginate/poly(vinyl alcohol) and sodium alginate/poly(ethylene oxide). *Journal of Applied Polymer Science*, 104(5), 3245–3255. <https://doi.org/10.1002/app.25696>
- Salas, C., Ago, M., Lucia, L. a., & Rojas, O. J. (2014). Synthesis of soy protein–lignin nanofibers by solution electrospinning. *Reactive and Functional Polymers*, 85, 221–227. <https://doi.org/10.1016/j.reactfunctpolym.2014.09.022>
- Sapountzi, E., Braiek, M., Vocanson, F., Chateaux, J. F., Jaffrezic-Renault, N., & Lagarde, F. (2017). Gold nanoparticles assembly on electrospun poly(vinyl alcohol)/poly(ethyleneimine)/glucose oxidase nanofibers for ultrasensitive electrochemical glucose biosensing. *Sensors and Actuators, B: Chemical*, 238, 392–401. <https://doi.org/10.1016/j.snb.2016.07.062>
- Sardar, N., & Kamil, M. (2012). Interaction between Nonionic Polymer Hydroxypropyl Methyl Cellulose (HPMC) and Cationic Gemini/Conventional Surfactants. *Industrial & Engineering Chemistry Research*, 51, 1227–1235. <https://doi.org/10.1021/ie2010725>
- Shevkani, K., Singh, N., Kaur, A., & Rana, J. C. (2015). Structural and functional characterization of kidney bean and field pea protein isolates: A comparative study. *Food Hydrocolloids*, 43, 679–689. <https://doi.org/10.1016/j.foodhyd.2014.07.024>
- Sill, T. J., & Von Recum, H. A. (2008). Electrospinning: Applications in drug delivery and tissue engineering. *Biomaterials*, 29, 1989–2006. <https://doi.org/10.1016/j.biomaterials.2008.01.011>

- Sim, L. H., Gan, S. N., Chan, C. H., & Yahya, R. (2010). Spectrochimica Acta Part A: Molecular and Biomolecular Spectroscopy ATR-FTIR studies on ion interaction of lithium perchlorate in polyacrylate/poly(ethylene oxide) blends. *Spectrochimica Acta Part A*, 76, 287–292. <https://doi.org/10.1016/j.saa.2009.09.031>
- Singh, D., Singh Maniyari Rawat, M., Semalty, A., & Semalty, M. (2011). Gallic Acid-Phospholipid Complex: Drug Incorporation and Physicochemical Characterization. *Letters in Drug Design & Discovery*, 8(3), 284–291. <https://doi.org/10.2174/157018011794578240>
- Soares, R. M. D., Siqueira, N. M., Prabhakaram, M. P., & Ramakrishna, S. (2018). Electrospinning and electrospray of bio-based and natural polymers for biomaterials development. *Materials Science and Engineering: C*, 92, 969–982. <https://doi.org/10.1016/J.MSEC.2018.08.004>
- Son, W. K., Youk, J. H., Lee, T. S., & Park, W. H. (2004). The effects of solution properties and polyelectrolyte on electrospinning of ultrafine poly(ethylene oxide) fibers. *Polymer*, 45, 2959–2966. <https://doi.org/10.1016/j.polymer.2004.03.006>
- Stanger, J., Tucker, N., & Staiger, M. (2005). *Electrospinning* (Vol. 16).
- Sullivan, S. T., Tang, C., Kennedy, A., Talwar, S., & Khan, S. a. (2014). Electrospinning and heat treatment of whey protein nanofibers. *Food Hydrocolloids*, 35, 36–50. <https://doi.org/10.1016/j.foodhyd.2013.07.023>
- Sun, B., Long, Y. Z., Zhang, H. D., Li, M. M., Duvail, J. L., Jiang, X. Y., & Yin, H. L. (2014). Advances in three-dimensional nanofibrous macrostructures via electrospinning. *Progress in Polymer Science*, 39, 862–890. <https://doi.org/10.1016/j.progpolymsci.2013.06.002>
- Tam, N., Oguz, S., Aydogdu, A., Sumnu, G., & Sahin, S. (2017). Influence of solution properties and pH on the fabrication of electrospun lentil flour/HPMC blend nanofibers. *Food Research International*, 102, 616–624. <https://doi.org/10.1016/j.foodres.2017.09.049>
- Tampau, A., González-Martinez, C., & Chiralt, A. (2017). Carvacrol encapsulation in starch or PCL based matrices by electrospinning. *Journal of Food Engineering*, 214, 245–256. <https://doi.org/10.1016/J.JFOODENG.2017.07.005>
- Tan, S. H., Inai, R., Kotaki, M., & Ramakrishna, S. (2005). Systematic parameter study for ultra-fine fiber fabrication via electrospinning process. *Polymer*, 46(16), 6128–6134. <https://doi.org/10.1016/j.polymer.2005.05.068>
- Tavassoli-Kafrani, E., Goli, S. A. H., & Fathi, M. (2017). Fabrication and characterization of electrospun gelatin nanofibers crosslinked with oxidized phenolic compounds. *International Journal of Biological Macromolecules*, 103,

1062–1068. <https://doi.org/10.1016/J.IJBIOMAC.2017.05.152>

- Tavassoli-Kafrani, E., Goli, S. A. H., & Fathi, M. (2018). Encapsulation of Orange Essential Oil Using Cross-linked Electrospun Gelatin Nanofibers. *Food and Bioprocess Technology*, *11*(2), 427–434. <https://doi.org/10.1007/s11947-017-2026-9>
- Teepoo, S., Dawan, P., & Barnthip, N. (2017). Electrospun Chitosan-Gelatin Biopolymer Composite Nanofibers for Horseradish Peroxidase Immobilization in a Hydrogen Peroxide Biosensor. *Biosensors*, *7*. <https://doi.org/10.3390/bios7040047>
- Torres-Giner, S., Ocio, M. J., & Lagaron, J. M. (2009a). Novel antimicrobial ultrathin structures of zein/chitosan blends obtained by electrospinning. *Carbohydrate Polymers*, *77*(2), 261–266. <https://doi.org/10.1016/j.carbpol.2008.12.035>
- Torres-Giner, S., Ocio, M. J., & Lagaron, M. (2009b). Novel antimicrobial ultrathin structures of zein/chitosan blends obtained by electrospinning. *Carbohydrate Polymers*, *77*, 261–266. <https://doi.org/10.1016/j.carbpol.2008.12.035>
- Tort, S., & Acartürk, F. (2016). Preparation and characterization of electrospun nanofibers containing glutamine. *Carbohydrate Polymers*, *152*, 802–814. <https://doi.org/10.1016/j.carbpol.2016.07.028>
- Urbina, L., Algar, I., García-Astrain, C., Gabilondo, N., González, A., Corcuera, M., ... Retegi, A. (2016). Biodegradable composites with improved barrier properties and transparency from the impregnation of PLA to bacterial cellulose membranes. *Journal of Applied Polymer Science*, *133*(28), 1–10. <https://doi.org/10.1002/app.43669>
- Valenzuela, C., Abugoch, L., Tapia, C., & Gamboa, A. (2013). Effect of alkaline extraction on the structure of the protein of quinoa (*Chenopodium quinoa* Willd.) and its influence on film formation. *International Journal of Food Science & Technology*, *48*(4), 843–849. <https://doi.org/10.1111/ijfs.12035>
- Vanhanen, L. P., & Savage, G. P. (2006). The use of peroxide value as a measure of quality for walnut flour stored at five different temperatures using three different types of packaging. *Food Chemistry*, *99*(1), 64–69. <https://doi.org/10.1016/J.FOODCHEM.2005.07.020>
- Vega-Lugo, A.-C., & Lim, L.-T. (2009). Controlled release of allyl isothiocyanate using soy protein and poly(lactic acid) electrospun fibers. *Food Research International*, *42*(8), 933–940. <https://doi.org/10.1016/j.foodres.2009.05.005>
- Vega-Lugo, A.-C., & Lim, L.-T. (2012). Effects of poly(ethylene oxide) and pH on the electrospinning of whey protein isolate. *Journal of Polymer Science Part B: Polymer Physics*, *50*(16), 1188–1197. <https://doi.org/10.1002/polb.23106>
- Wang, Hong, Shao, H., & Hu, X. (2006). Structure of silk fibroin fibers made by an

- electrospinning process from a silk fibroin aqueous solution. *Journal of Applied Polymer Science*, 101(2), 961–968. <https://doi.org/10.1002/app.24024>
- Wang, Hualin, Hao, L., Niu, B., Jiang, S., Cheng, J., & Jiang, S. (2016). Kinetics and Antioxidant Capacity of Proanthocyanidins Encapsulated in Zein Electrospun Fibers by Cyclic Voltammetry. *Journal of Agricultural and Food Chemistry*, 64(15), 3083–3090. <https://doi.org/10.1021/acs.jafc.6b00540>
- Wang, S.-C., Wei, T.-C., Chen, W.-B., & Tsao, H.-K. (2004). Effects of surfactant micelles on viscosity and conductivity of poly(ethylene glycol) solutions Effects of surfactant micelles on viscosity and conductivity of poly " ethylene glycol... solutions. *The Journal of Chemical Physics*, 120(4980). <https://doi.org/10.1063/1.1644798>
- Wang, S., Marcone, M. F., Barbut, S., & Lim, L.-T. (2013). Electrospun soy protein isolate-based fiber fortified with anthocyanin-rich red raspberry (*Rubus strigosus*) extracts. *Food Research International*, 52(2), 467–472. <https://doi.org/10.1016/j.foodres.2012.12.036>
- Wang, X., Um, I. C., Fang, D., Okamoto, A., Hsiao, B. S., & Chu, B. (2005). Formation of water-resistant hyaluronic acid nanofibers by blowing-assisted electro-spinning and non-toxic post treatments. *Polymer*, 46, 4853–4867. Retrieved from https://ac.els-cdn.com/S003238610500323X/1-s2.0-S003238610500323X-main.pdf?_tid=ad022603-14e0-4e42-826a-8a8302a6a2e7&acdnat=1552775820_45d7577917a1fba64eea289667ab2671
- Wang, Y., Zhang, Q., Zhang, C.-L., & Li, P. (2012). Characterisation and cooperative antimicrobial properties of chitosan/nano-ZnO composite nanofibrous membranes. *Food Chemistry*, 132, 419–427. <https://doi.org/10.1016/j.foodchem.2011.11.015>
- Wen, P., Zhu, D.-H., Feng, K., Liu, F.-J., Lou, W.-Y., Li, N., ... Wu, H. (2016). Fabrication of electrospun polylactic acid nanofilm incorporating cinnamon essential oil/ β -cyclodextrin inclusion complex for antimicrobial packaging. *Food Chemistry*, 196, 996–1004. <https://doi.org/10.1016/J.FOODCHEM.2015.10.043>
- Wen, P., Zong, M.-H., Linhardt, R. J., Feng, K., & Wu, H. (2017). Electrospinning: A novel nano-encapsulation approach for bioactive compounds. *Trends in Food Science & Technology*, 70, 56–68. <https://doi.org/10.1016/J.TIFS.2017.10.009>
- Wu, C., Tian, J., Li, S., Wu, T., Hu, Y., Chen, S., ... Ye, X. (2016). Structural properties of films and rheology of film-forming solutions of chitosan gallate for food packaging. *Carbohydrate Polymers*, 146, 10–19. <https://doi.org/10.1016/J.CARBPOL.2016.03.027>
- Wu, J., & Yin, F. (2013). Sensitive enzymatic glucose biosensor fabricated by electrospinning composite nanofibers and electrodepositing Prussian blue film. *Journal of Electroanalytical Chemistry*, 694, 1–5.

<https://doi.org/10.1016/j.jelechem.2013.02.003>

- Wu, L., Yuan, X., & Sheng, J. (2005). Immobilization of cellulase in nanofibrous PVA membranes by electrospinning. *Journal of Membrane Science*, 250(1–2), 167–173. <https://doi.org/10.1016/J.MEMSCI.2004.10.024>
- Xie, J., & Hsieh, Y.-L. (2003). Ultra-high surface fibrous membranes from electrospinning of natural proteins: casein and lipase enzyme. *Journal of Materials Science*, 38, 2125–2133. Retrieved from <https://link.springer.com/content/pdf/10.1023%2FA%3A1023763727747.pdf>
- Xu, F., Sheardown, H., & Hoare, T. (2016). Reactive electrospinning of degradable poly(oligoethylene glycol methacrylate)-based nanofibrous hydrogel networks. *Chemical Communications*, 52(7), 1451–1454. <https://doi.org/10.1039/C5CC08053C>
- Xu, J., Carson, B., & Kim, S. (2015). The pH Dependence on the Rheology of Wheat Protein Isolate Suspensions. *Polymer Sciences*, 1(1), 1. <https://doi.org/10.21767/2471-9935.100005>
- Xu, X., Jiang, L., Zhou, Z., Wu, X., & Wang, Y. (2012). Preparation and Properties of Electrospun Soy Protein Isolate / Polyethylene Oxide Nano fiber Membranes. *ACS Applied Materials & Interfaces*, 4, 4331–4337.
- Yang, F., Murugan, R., Ramakrishna, S., Wang, X., Ma, Y.-X., & Wang, S. (2004). Fabrication of nano-structured porous PLLA scaffold intended for nerve tissue engineering. *Biomaterials*, 25(10), 1891–1900. <https://doi.org/10.1016/j.biomaterials.2003.08.062>
- Yang, Q., Zhenyu, L. I., Hong, Y., Zhao, Y., Qiu, S., Wang, C. E., & Wei, Y. (2004). Influence of solvents on the formation of ultrathin uniform poly(vinyl pyrrolidone) nanofibers with electrospinning. *Journal of Polymer Science, Part B: Polymer Physics*, 42(20), 3721–3726. <https://doi.org/10.1002/polb.20222>
- Yang, W., Sousa, A. M. M., Fan, X., Jin, T., Li, X., Tomasula, P. M., & Liu, L. (2017). Electrospun ultra-fine cellulose acetate fibrous mats containing tannic acid-Fe³⁺ complexes. *Carbohydrate Polymers*, 157, 1173–1179. <https://doi.org/10.1016/J.CARBPOL.2016.10.078>
- Yao, C., Li, X., & Song, T. (2006). Electrospinning and Crosslinking of Zein Nanofiber Mats. *Journal of Applied Polymer Science*, 103, 380–385. <https://doi.org/10.1002/app>
- Yin, J., Luo, K., Chen, X., & Khutoryanskiy, V. V. (2006). Miscibility studies of the blends of chitosan with some cellulose ethers. *Carbohydrate Polymers*, 63(2), 238–244. <https://doi.org/10.1016/j.carbpol.2005.08.041>
- Ying Yang, Zhidong Jia, Qiang Li, & Zhicheng Guan. (2006). Experimental

- investigation of the governing parameters in the electrospinning of polyethylene oxide solution. *IEEE Transactions on Dielectrics and Electrical Insulation*, 13(3), 580–585. <https://doi.org/10.1109/tdei.2006.1657971>
- Yuan, X. Y., Zhang, Y. Y., Dong, C., & Sheng, J. (2004). Morphology of ultrafine polysulfone fibers prepared by electrospinning. *Polymer International*, 53, 1704–1710. <https://doi.org/10.1002/pi.1538>
- Yulong, Z., Huang, Z., Zhang, J., Wenyu, W. U., Wang, M., & Lili, F. (2010). Thermal Degradation of Sodium Alginate-Incorporated Soy Protein Isolate/Glycerol Composite Membranes. In *17th IAPRI World Conference on Packaging* (pp. 402–405). Retrieved from <http://file.scirp.org/pdf/21-1.98.pdf>
- Zeleny, J. (1914). The electrical discharge from liquid points, and a hydrostatic method of measuring the electric intensity at their surfaces. *Physical Review*, 3(2), 69–91. <https://doi.org/10.1103/PhysRev.3.69>
- Zeng, J., Xu, X., Chen, X., Liang, Q., Bian, X., Yang, L., & Jing, X. (2003). *Biodegradable electrospun fibers for drug delivery*. *Journal of Controlled Release* (Vol. 92). [https://doi.org/10.1016/S0168-3659\(03\)00372-9](https://doi.org/10.1016/S0168-3659(03)00372-9)
- Zhang, C., Yuan, X., Wu, L., Han, Y., & Sheng, J. (2004). Study on morphology of electrospun poly(vinyl alcohol) mats. *European Polymer Journal*, 41, 423–432. <https://doi.org/10.1016/j.eurpolymj.2004.10.027>
- Zhang, Y., Yang, L., Zu, Y., Chen, X., Wang, F., & Liu, F. (2010). Oxidative stability of sunflower oil supplemented with carnosic acid compared with synthetic antioxidants during accelerated storage. *Food Chemistry*, 118(3), 656–662. <https://doi.org/10.1016/j.foodchem.2009.05.038>
- Zhao, S., Wu, X., Wang, L., & Huang, Y. (2004). Electrospinning of Ethyl – Cyanoethyl Cellulose / Tetrahydrofuran Solutions. *Journal of Applied Microbiology*, 91, 242–246.
- Zheng, J., Zhuang, M., Yu, Z., Zheng, G., Zhao, Y., Wang, H., & Sun, D. (2014). The Effect of Surfactants on the Diameter and Morphology of Electrospun Ultrafine Nanofiber. *Journal of Nanomaterials*, 2014.
- Zong, X., Kim, K., Fang, D., Ran, S., Hsiao, B. S., & Chu, B. (2002). Structure and process relationship of electrospun bioabsorbable nanofiber membranes. *Polymer*, 43(16), 4403–4412. [https://doi.org/10.1016/S0032-3861\(02\)00275-6](https://doi.org/10.1016/S0032-3861(02)00275-6)

APPENDICES

A. ANOVA TABLES

Table A. 1 *One way Analysis of Variance (ANOVA) and Tukey's comparison test for consistency index (k) values of solutions containing different amount of HPMC/PEO.*

Factor	Type	Levels	Values
solution	fixed	12	1.5/1.5, 1/1, 1/2, 2/1, 2/1.5, 2/2, 3/1.5, 3/2, 4.5/1.5, 4/1, 4/2, 5/1

Analysis of Variance for k, using Adjusted SS for Tests

Source	DF	Seq SS	Adj SS	Adj MS	F	P
solution	11	2108.67	2108.67	191.70	167.18	0.000
Error	24	27.52	27.52	1.15		
Total	35	2136.19				

S = 1.07080 R-Sq = 98.71% R-Sq(adj) = 98.12%

Grouping Information Using Tukey Method and 95.0% Confidence

solution	N	Mean	Grouping
4.5/1.5	3	20.3	A
5/1	3	19.3	A
4/2	3	17.5	A B
4/1	3	15.5	B
3/2	3	6.8	C
3/1.5	3	5.9	C
2/2	3	2.6	D
2/1.5	3	2.0	D
2/1	3	1.4	D
1.5/1.5	3	1.1	D
1/2	3	0.6	D
1/1	3	0.3	D

Means that do not share a letter are significantly different.

Table A. 2 One way Analysis of Variance (ANOVA) and Tukey's comparison test for flow behavior index (n) values of solutions containing different amount of HPMC/PEO.

Factor	Type	Levels	Values
solution	fixed	12	1.5/1.5, 1/1, 1/2, 2/1, 2/1.5, 2/2, 3/1.5, 3/2, 4.5/1.5, 4/1, 4/2, 5/1

Analysis of Variance for n, using Adjusted SS for Tests

Source	DF	Seq SS	Adj SS	Adj MS	F	P
solution	11	0.633539	0.633539	0.057594	108.70	0.000
Error	24	0.012717	0.012717	0.000530		
Total	35	0.646256				

S = 0.0230189 R-Sq = 98.03% R-Sq(adj) = 97.13%

Grouping Information Using Tukey Method and 95.0% Confidence

solution	N	Mean	Grouping
1/1	3	0.9	A
1/2	3	0.9	A
1.5/1.5	3	0.9	A B
2/1	3	0.9	B
2/1.5	3	0.9	B
2/2	3	0.9	B
3/2	3	0.8	C
3/1.5	3	0.7	C
4/2	3	0.6	D
4.5/1.5	3	0.6	D
5/1	3	0.6	D
4/1	3	0.5	E

Means that do not share a letter are significantly different.

Table A. 3 *One way Analysis of Variance (ANOVA) and Tukey's comparison test for electrical conductivity values of solutions containing different amount of HPMC/PEO.*

Factor	Type	Levels	Values
solution	fixed	12	1.5/1.5, 1/1, 1/2, 2/1, 2/1.5, 2/2, 3/1.5, 3/2, 4.5/1.5, 4/1, 4/2, 5/1

Analysis of Variance for conductivity, using Adjusted SS for Tests

Source	DF	Seq SS	Adj SS	Adj MS	F	P
solution	11	15793.2	15793.2	1435.7	112.37	0.000
Error	12	153.3	153.3	12.8		
Total	23	15946.5				

S = 3.57445 R-Sq = 99.04% R-Sq(adj) = 98.16%

Grouping Information Using Tukey Method and 95.0% Confidence

solution	N	Mean	Grouping
4.5/1.5	2	215.0	A
4/2	2	209.0	A B
3/1.5	2	200.0	B C
5/1	2	200.0	B C
4/1	2	191.4	C D
3/2	2	189.1	C D
2/1.5	2	182.5	D
2/2	2	180.7	D
1.5/1.5	2	158.7	E
1/2	2	154.2	E
2/1	2	147.6	E
1/1	2	128.6	F

Means that do not share a letter are significantly different.

Table A. 4 One way Analysis of Variance (ANOVA) and Tukey's comparison test for diameter values of nanofibers containing different amount of HPMC/PEO.

Factor	Type	Levels	Values
nanofiber	fixed	8	2/1, 2/1.5, 2/2, 3/1.5, 3/2, 4.5/1.5, 4/1, 4/2

Analysis of Variance for diameter, using Adjusted SS for Tests

Source	DF	Seq SS	Adj SS	Adj MS	F	P
nanofiber	7	1572894	1572894	224699	66.83	0.000
Error	858	2885005	2885005	3362		
Total	865	4457898				

S = 57.9869 R-Sq = 35.28% R-Sq(adj) = 34.76%

Grouping Information Using Tukey Method and 95.0% Confidence

nanofiber	N	Mean	Grouping
4.5/1.5	110	316.7	A
4/2	116	311.7	A
4/1	102	301.1	A B
3/2	123	279.9	B
2/2	103	235.2	C
3/1.5	112	235.2	C
2/1.5	104	211.3	C D
2/1	96	202.3	D

Means that do not share a letter are significantly different.

Table A. 5 One way Analysis of Variance (ANOVA) and Tukey's comparison test for WVP values of nanofibers containing different amount of HPMC/PEO.

Factor	Type	Levels	Values
Nanofiber	fixed	6	2/1, 2/1.5, 2/2, 4.5/1.5, 4/2, 5/1

Analysis of Variance for WVP, using Adjusted SS for Tests

Source	DF	Seq SS	Adj SS	Adj MS	F	P
Nanofiber	5	46.1752	46.1752	9.2350	18.42	0.000
Error	9	4.5117	4.5117	0.5013		
Total	14	50.6869				

S = 0.708026 R-Sq = 91.10% R-Sq(adj) = 86.15%

Grouping Information Using Tukey Method and 95.0% Confidence

Nanofiber	N	Mean	Grouping
2/1	3	12.0	A
2/1.5	2	10.2	A B
2/2	2	8.4	B C
5/1	3	7.8	C
4.5/1.5	3	7.5	C
4/2	2	7.4	C

Means that do not share a letter are significantly different.

Table A. 6 One way Analysis of Variance (ANOVA) and Tukey's comparison test for glass transition temperature (Tg) values of nanofibers containing different amount of HPMC/PEO.

Factor	Type	Levels	Values
Nanofiber	fixed	6	2/1, 2/1.5, 2/2, 4.5/1.5, 4/2, 5/1

Analysis of Variance for Tg, using Adjusted SS for Tests

Source	DF	Seq SS	Adj SS	Adj MS	F	P
Nanofiber	5	6674.0	6674.0	1334.8	672.24	0.000
Error	16	31.8	31.8	2.0		
Total	21	6705.8				

S = 1.40912 R-Sq = 99.53% R-Sq(adj) = 99.38%

Grouping Information Using Tukey Method and 95.0% Confidence

Nanofiber	N	Mean	Grouping
4/2	4	181.3	A
4.5/1.5	4	179.1	A
5/1	3	168.8	B
2/1	3	160.3	C
2/1.5	4	144.1	D
2/2	4	136.5	E

Means that do not share a letter are significantly different.

Table A. 7 *One way Analysis of Variance (ANOVA) and Tukey's comparison test for melting temperature (T_m) values of nanofibers containing different amount of HPMC/PEO.*

Factor	Type	Levels	Values
Nanofiber	fixed	6	2/1, 2/1.5, 2/2, 4.5/1.5, 4/2, 5/1

Analysis of Variance for T_m, using Adjusted SS for Tests

Source	DF	Seq SS	Adj SS	Adj MS	F	P
Nanofiber	5	12.8998	12.8998	2.5800	24.42	0.000
Error	8	0.8453	0.8453	0.1057		
Total	13	13.7451				

S = 0.325054 R-Sq = 93.85% R-Sq(adj) = 90.01%

Grouping Information Using Tukey Method and 95.0% Confidence

Nanofiber	N	Mean	Grouping
2/2	2	56.1	A
4/2	2	55.7	A B
5/1	3	55.0	B C
4.5/1.5	2	54.5	B C
2/1.5	3	54.1	C D
2/1	2	53.1	D

Means that do not share a letter are significantly different.

Table A. 8 *One way Analysis of Variance (ANOVA) and Tukey's comparison test for melting enthalpy (ΔH_m) values of nanofibers containing different amount of HPMC/PEO.*

Factor	Type	Levels	Values
Nanofiber	fixed	6	2/1, 2/1.5, 2/2, 4.5/1.5, 4/2, 5/1

Analysis of Variance for Enthalpy, using Adjusted SS for Tests

Source	DF	Seq SS	Adj SS	Adj MS	F	P
Nanofiber	5	616.21	616.21	123.24	47.44	0.000
Error	18	46.76	46.76	2.60		
Total	23	662.97				

S = 1.61174 R-Sq = 92.95% R-Sq(adj) = 90.99%

Grouping Information Using Tukey Method and 95.0% Confidence

Nanofiber	N	Mean	Grouping
2/2	4	23.3	A
2/1.5	5	23.1	A
2/1	3	18.4	B
4/2	3	14.5	B C
5/1	4	14.0	C
4.5/1.5	5	10.5	D

Means that do not share a letter are significantly different.

Table A. 9 *One way Analysis of Variance (ANOVA) and Tukey's comparison test for consistency index (k) values of HPMC/PEO solutions containing different amount of gallic acid.*

Factor	Type	Levels	Values
Solution	fixed	4	0, 10, 2, 5

Analysis of Variance for k, using Adjusted SS for Tests

Source	DF	Seq SS	Adj SS	Adj MS	F	P
Solution	3	127.594	127.594	42.531	86.34	0.000
Error	7	3.448	3.448	0.493		
Total	10	131.042				

S = 0.701867 R-Sq = 97.37% R-Sq(adj) = 96.24%

Grouping Information Using Tukey Method and 95.0% Confidence

Solution	N	Mean	Grouping
0	3	15.5	A
2	3	11.6	B
5	2	8.0	C
10	3	7.0	C

Means that do not share a letter are significantly different.

Table A. 10 *One way Analysis of Variance (ANOVA) and Tukey's comparison test for flow behavior index (n) values of HPMC/PEO solutions containing different amount of gallic acid*

Factor	Type	Levels	Values
Solution	fixed	4	0, 10, 2, 5

Analysis of Variance for n, using Adjusted SS for Tests

Source	DF	Seq SS	Adj SS	Adj MS	F	P
Solution	3	0.030644	0.030644	0.010215	23.40	0.001
Error	7	0.003056	0.003056	0.000437		
Total	10	0.033700				

S = 0.0208935 R-Sq = 90.93% R-Sq(adj) = 87.05%

Grouping Information Using Tukey Method and 95.0% Confidence

Solution	N	Mean	Grouping
10	3	0.7	A
5	2	0.7	A B
2	3	0.6	B
0	3	0.5	C

Means that do not share a letter are significantly different.

Table A. 11 One way Analysis of Variance (ANOVA) and Tukey's comparison test for electrical conductivity values of HPMC/PEO solutions containing different amount of gallic acid.

Factor	Type	Levels	Values
solution	fixed	4	0, 2, 5, 10

Analysis of Variance for electrical conductivity, using Adjusted SS for Tests

Source	DF	Seq SS	Adj SS	Adj MS	F	P
solution	3	118684	118684	39561	4128.15	0.000
Error	8	77	77	10		
Total	11	118761				

S = 3.09570 R-Sq = 99.94% R-Sq(adj) = 99.91%

Grouping Information Using Tukey Method and 95.0% Confidence

solution	N	Mean	Grouping
2	3	438.0	A
10	3	410.0	A
5	3	409.3	A
0	3	191.0	B

Means that do not share a letter are significantly different.

Table A. 12 *One way Analysis of Variance (ANOVA) and Tukey's comparison test for diameter values of HPMC/PEO nanofibers containing different amount of gallic acid.*

Factor	Type	Levels	Values
Nanofiber	fixed	4	0; 10; 2; 5

Analysis of Variance for Diameter, using Adjusted SS for Tests

Source	DF	Seq SS	Adj SS	Adj MS	F	P
Nanofiber	3	0.062745	0.062745	0.020915	12.59	0.000
Error	409	0.679267	0.679267	0.001661		
Total	412	0.742012				

S = 0.0407529 R-Sq = 8.46% R-Sq(adj) = 7.78%

Grouping Information Using Tukey Method and 95.0% Confidence

Fiber	N	Mean	Grouping
0	102	0.3	A
2	103	0.3	B
5	99	0.3	B C
10	109	0.3	C

Means that do not share a letter are significantly different.

Table A. 13 *One way Analysis of Variance (ANOVA) and Tukey's comparison test for gallic acid loading efficiency values of HPMC/PEO nanofibers containing different amount of gallic acid.*

Factor	Type	Levels	Values
nanofiber	fixed	3	10, 2, 5

Analysis of Variance for loading eff, using Adjusted SS for Tests

Source	DF	Seq SS	Adj SS	Adj MS	F	P
nanofiber	2	261.65	261.65	130.82	98.09	0.000
Error	18	24.01	24.01	1.33		
Total	20	285.66				

S = 1.15488 R-Sq = 91.60% R-Sq(adj) = 90.66%

Grouping Information Using Tukey Method and 95.0% Confidence

nanofiber	N	Mean	Grouping
10	11	69.0	A
5	5	62.2	B
2	5	61.6	B

Means that do not share a letter are significantly different.

Table A. 14 *One way Analysis of Variance (ANOVA) and Tukey's comparison test for antioxidant activity values of HPMC/PEO nanofibers containing different amount of gallic acid.*

Factor	Type	Levels	Values
nanofiber	fixed	3	2, 5, 10

Analysis of Variance for AA, using Adjusted SS for Tests

Source	DF	Seq SS	Adj SS	Adj MS	F	P
nanofiber	2	399.34	399.34	199.67	1241.86	0.000
Error	3	0.48	0.48	0.16		
Total	5	399.83				

S = 0.400980 R-Sq = 99.88% R-Sq(adj) = 99.80%

Grouping Information Using Tukey Method and 95.0% Confidence

nanofiber	N	Mean	Grouping
10	2	24.7	A
5	2	12.4	B
2	2	5.0	C

Means that do not share a letter are significantly different.

Table A. 15 One way Analysis of Variance (ANOVA) and Tukey's comparison test for p_anisidin values of walnuts packed in HPMC/PEO packages

Factor	Type	Levels	Values
nanofiber	fixed	2	0, 10

Analysis of Variance for p_anisidin, using Adjusted SS for Tests

Source	DF	Seq SS	Adj SS	Adj MS	F	P
nanofiber	1	5.3799	5.3799	5.3799	131.50	0.000
Error	5	0.2046	0.2046	0.0409		
Total	6	5.5844				

S = 0.202268 R-Sq = 96.34% R-Sq(adj) = 95.60%

Grouping Information Using Tukey Method and 95.0% Confidence

nanofiber	N	Mean	Grouping
0	4	2.4	A
10	3	0.6	B

Means that do not share a letter are significantly different.

Table A. 16 *One way Analysis of Variance (ANOVA) and Tukey's comparison test for peroxide value values of walnuts packed in HPMC/PEO packages*

Factor	Type	Levels	Values
nanofiber	fixed	2	0, 10

Analysis of Variance for PV, using Adjusted SS for Tests

Source	DF	Seq SS	Adj SS	Adj MS	F	P
nanofiber	1	0.60840	0.60840	0.60840	82.22	0.012
Error	2	0.01480	0.01480	0.00740		
Total	3	0.62320				

S = 0.0860233 R-Sq = 97.63% R-Sq(adj) = 96.44%

Grouping Information Using Tukey Method and 95.0% Confidence

nanofiber	N	Mean	Grouping
0	2	1.4	A
10	2	0.6	B

Means that do not share a letter are significantly different.

Table A. 17 *One way Analysis of Variance (ANOVA) and Tukey's comparison test for TBARS values of walnuts packed in HPMC/PEO packages*

Factor	Type	Levels	Values
nanofiber	fixed	2	0, 10

Analysis of Variance for TBARS, using Adjusted SS for Tests

Source	DF	Seq SS	Adj SS	Adj MS	F	P
nanofiber	1	0.0000699	0.0000699	0.0000699	2.89	0.140
Error	6	0.0001453	0.0001453	0.0000242		
Total	7	0.0002152				

S = 0.00492076 R-Sq = 32.48% R-Sq(adj) = 21.23%

Grouping Information Using Tukey Method and 95.0% Confidence

nanofiber	N	Mean	Grouping
0	4	0.1	A
10	4	0.1	A

Means that do not share a letter are significantly different.

Table A. 18 *Two way Analysis of Variance (ANOVA) and Tukey's comparison test for the effect of pH and gallic acid on consistency index (k) values of solutions containing lentil flour/PEO.*

Factor	Type	Levels	Values
pH	fixed	2	1, 10
gallic acid	fixed	2	0, 10

Analysis of Variance for k, using Adjusted SS for Tests

Source	DF	Seq SS	Adj SS	Adj MS	F	P
pH	1	2.4428	2.4428	2.4428	650.98	0.000
gallic acid	1	1.0476	1.0476	1.0476	279.16	0.000
pH*gallic acid	1	0.7323	0.7323	0.7323	195.15	0.000
Error	8	0.0300	0.0300	0.0038		
Total	11	4.2527				

S = 0.0612581 R-Sq = 99.29% R-Sq(adj) = 99.03%

Grouping Information Using Tukey Method and 95.0% Confidence

pH	N	Mean	Grouping
10	6	1.6	A
1	6	0.7	B

Means that do not share a letter are significantly different.

Grouping Information Using Tukey Method and 95.0% Confidence

gallic acid	N	Mean	Grouping
0	6	1.4	A
10	6	0.8	B

Means that do not share a letter are significantly different.

Grouping Information Using Tukey Method and 95.0% Confidence

pH	gallic acid	N	Mean	Grouping
10	0	3	2.1	A
10	10	3	1.0	B
1	0	3	0.7	C
1	10	3	0.6	C

Means that do not share a letter are significantly different.

Table A. 19 *Two way Analysis of Variance (ANOVA) and Tukey's comparison test for the effect of pH and gallic acid on flow behavior index values (n) of solutions containing lentil flour/PEO.*

Factor	Type	Levels	Values
pH	fixed	2	1, 10
gallic acid	fixed	2	0, 10

Analysis of Variance for n, using Adjusted SS for Tests

Source	DF	Seq SS	Adj SS	Adj MS	F	P
pH	1	0.0065147	0.0065147	0.0065147	145.08	0.000
gallic acid	1	0.0005201	0.0005201	0.0005201	11.58	0.009
pH*gallic acid	1	0.0003786	0.0003786	0.0003786	8.43	0.020
Error	8	0.0003592	0.0003592	0.0000449		
Total	11	0.0077726				

S = 0.00670106 R-Sq = 95.38% R-Sq(adj) = 93.65%

Grouping Information Using Tukey Method and 95.0% Confidence

pH	N	Mean	Grouping
1	6	1.0	A
10	6	0.9	B

Means that do not share a letter are significantly different.

Grouping Information Using Tukey Method and 95.0% Confidence

gallic acid	N	Mean	Grouping
10	6	0.9	A
0	6	0.9	B

Means that do not share a letter are significantly different.

Grouping Information Using Tukey Method and 95.0% Confidence

gallic acid		N	Mean	Grouping
pH	10	3	1.0	A
	1	3	1.0	A
10	10	3	0.9	B
10	0	3	0.9	C

Means that do not share a letter are significantly different.

Table A. 20 Two way Analysis of Variance (ANOVA) and Tukey's comparison test for the effect of pH and gallic acid on electrical conductivity values of solutions containing lentil flour/PEO.

Factor	Type	Levels	Values
pH	fixed	2	1, 10
gallic acid	fixed	2	0, 10

Analysis of Variance for conductivity, using Adjusted SS for Tests

Source	DF	Seq SS	Adj SS	Adj MS	F	P
pH	1	1051799113	1051799113	1051799113	62256.89	0.000
gallic acid	1	374113	374113	374113	22.14	0.009
pH*gallic acid	1	29146612	29146612	29146612	1725.21	0.000
Error	4	67578	67578	16894		
Total	7	1081387416				

S = 129.979 R-Sq = 99.99% R-Sq(adj) = 99.99%

Grouping Information Using Tukey Method and 95.0% Confidence

pH	N	Mean	Grouping
1	4	26425.0	A
10	4	3492.5	B

Means that do not share a letter are significantly different.

Grouping Information Using Tukey Method and 95.0% Confidence

gallic acid	N	Mean	Grouping
0	4	15175.0	A
10	4	14742.5	B

Means that do not share a letter are significantly different.

Grouping Information Using Tukey Method and 95.0% Confidence

gallic acid		N	Mean	Grouping
pH	0	2	28550.0	A
1	10	2	24300.0	B
10	10	2	5185.0	C
10	0	2	1800.0	D

Means that do not share a letter are significantly different.

Table A. 21 *Two way Analysis of Variance (ANOVA) and Tukey's comparison test for the effect of pH and gallic acid on total phenolic content (TPC) values of solutions containing lentil flour/PEO.*

Factor	Type	Levels	Values
pH	fixed	2	1, 10
gallic acid	fixed	2	0, 10

Analysis of Variance for TPC, using Adjusted SS for Tests

Source	DF	Seq SS	Adj SS	Adj MS	F	P
pH	1	11874	9970	9970	419.29	0.000
gallic acid	1	33902	23551	23551	990.42	0.000
pH*gallic acid	1	9853	9853	9853	414.36	0.000
Error	11	262	262	24		
Total	14	55891				

S = 4.87632 R-Sq = 99.53% R-Sq(adj) = 99.40%

Grouping Information Using Tukey Method and 95.0% Confidence

pH	N	Mean	Grouping
1	9	74.5	A
10	6	19.8	B

Means that do not share a letter are significantly different.

Grouping Information Using Tukey Method and 95.0% Confidence

gallic acid	N	Mean	Grouping
10	9	89.2	A
0	6	5.2	B

Means that do not share a letter are significantly different.

Grouping Information Using Tukey Method and 95.0% Confidence

pH	gallic acid	N	Mean	Grouping
1	10	5	143.7	A
10	10	4	34.7	B
1	0	4	5.3	C
10	0	2	5.0	C

Means that do not share a letter are significantly different.

Table A. 22 *One way Analysis of Variance (ANOVA) and Tukey's comparison test for total phenolic content values of lentil flour/PEO nanofibers prepared at different pH values*

Factor	Type	Levels	Values
nanofiber	fixed	2	1, 10

Analysis of Variance for TPC, using Adjusted SS for Tests

Source	DF	Seq SS	Adj SS	Adj MS	F	P
nanofiber	1	13606	13606	13606	116.76	0.000
Error	6	699	699	117		
Total	7	14305				

S = 10.7947 R-Sq = 95.11% R-Sq(adj) = 94.30%

Grouping Information Using Tukey Method and 95.0% Confidence

nanofiber	N	Mean	Grouping
1	4	89.5	A
10	4	7.0	B

Means that do not share a letter are significantly different.

Table A. 23 One way Analysis of Variance (ANOVA) and Tukey's comparison test for antioxidant activity values of lentil flour/PEO nanofibers prepared at different pH values

Factor	Type	Levels	Values
nanofiber	fixed	2	1, 10

Analysis of Variance for AA, using Adjusted SS for Tests

Source	DF	Seq SS	Adj SS	Adj MS	F	P
nanofiber	1	1016.4	1016.4	1016.4	696.08	0.000
Error	9	13.1	13.1	1.5		
Total	10	1029.6				

S = 1.20839 R-Sq = 98.72% R-Sq(adj) = 98.58%

Grouping Information Using Tukey Method and 95.0% Confidence

nanofiber	N	Mean	Grouping
1	5	20.9	A
10	6	1.6	B

Means that do not share a letter are significantly different.

Table A. 24 *One way Analysis of Variance (ANOVA) and Tukey's comparison test for per oxide values of walnuts packed in lentil flour/PEO packages*

Factor	Type	Levels	Values
nanofiber	fixed	2	0, 10

Analysis of Variance for per oxide, using Adjusted SS for Tests

Source	DF	Seq SS	Adj SS	Adj MS	F	P
nanofiber	1	1.0000	1.0000	1.0000	50.00	0.019
Error	2	0.0400	0.0400	0.0200		
Total	3	1.0400				

S = 0.141421 R-Sq = 96.15% R-Sq(adj) = 94.23%

Grouping Information Using Tukey Method and 95.0% Confidence

nanofiber	N	Mean	Grouping
0	2	2.3	A
10	2	1.3	B

Means that do not share a letter are significantly different.

Table A. 25 *One way Analysis of Variance (ANOVA) and Tukey's comparison test for p-anisidin values of walnuts packed in lentil flour/PEO packages*

Factor	Type	Levels	Values
nanofiber	fixed	2	0, 10

Analysis of Variance for p anisidin, using Adjusted SS for Tests

Source	DF	Seq SS	Adj SS	Adj MS	F	P
nanofiber	1	0.9998	0.9998	0.9998	7.12	0.018
Error	2	0.2809	0.2809	0.1405		
Total	3	1.2807				

S = 0.374785 R-Sq = 98.07% R-Sq(adj) = 97.10%

Grouping Information Using Tukey Method and 95.0% Confidence

nanofiber	N	Mean	Grouping
0	2	2.1	A
10	2	1.1	B

Means that do not share a letter are significantly different.

Table A. 26 *One way Analysis of Variance (ANOVA) and Tukey's comparison test for TBARS values of walnuts packed in lentil flour/PEO packages*

Factor	Type	Levels	Values
nanofiber	fixed	2	0, 10

Analysis of Variance for TBARS, using Adjusted SS for Tests

Source	DF	Seq SS	Adj SS	Adj MS	F	P
nanofiber	1	0.004684	0.004684	0.004684	4.21	0.067
Error	10	0.011123	0.011123	0.001112		
Total	11	0.015807				

S = 0.0333515 R-Sq = 29.63% R-Sq(adj) = 22.59%

Grouping Information Using Tukey Method and 95.0% Confidence

nanofiber	N	Mean	Grouping
10	4	0.1	A
0	8	0.1	A

Means that do not share a letter are significantly different.

Table A. 27 One way Analysis of Variance (ANOVA) and Tukey's comparison test for consistency index (k) values of Pea flour/PEO solutions containing different amount of gallic acid.

Factor	Type	Levels	Values
solution	fixed	3	0, 5, 10

Analysis of Variance for k, using Adjusted SS for Tests

Source	DF	Seq SS	Adj SS	Adj MS	F	P
solution	2	2.0091	2.0091	1.0046	308.73	0.000
Error	5	0.0163	0.0163	0.0033		
Total	7	2.0254				

S = 0.0570423 R-Sq = 99.20% R-Sq(adj) = 98.88%

Grouping Information Using Tukey Method and 95.0% Confidence

solution	N	Mean	Grouping
0	3	2.7	A
5	2	2.3	B
10	3	1.5	C

Means that do not share a letter are significantly different.

Table A. 28 *One way Analysis of Variance (ANOVA) and Tukey's comparison test for flow behavior index (n) values of pea flour/PEO solutions containing different amount of gallic acid.*

Factor	Type	Levels	Values
solution	fixed	3	0, 5, 10

Analysis of Variance for n, using Adjusted SS for Tests

Source	DF	Seq SS	Adj SS	Adj MS	F	P
solution	2	0.0021398	0.0021398	0.0010699	16.72	0.006
Error	5	0.0003199	0.0003199	0.0000640		
Total	7	0.0024598				

S = 0.00799923 R-Sq = 86.99% R-Sq(adj) = 81.79%

Grouping Information Using Tukey Method and 95.0% Confidence

solution	N	Mean	Grouping
10	3	0.9	A
0	3	0.9	A
5	2	0.8	B

Means that do not share a letter are significantly different.

Table A. 29 *One way Analysis of Variance (ANOVA) and Tukey's comparison test for electrical conductivity values of pea flour/PEO solutions containing different amount of gallic acid.*

Factor	Type	Levels	Values
solution	fixed	3	0, 5, 10

Analysis of Variance for electrical conductivity, using Adjusted SS for Tests

Source	DF	Seq SS	Adj SS	Adj MS	F	P
solution	2	2124509192	2124509192	1062254596	2937.64	0.000
Error	6	2169606	2169606	361601		
Total	8	2126678798				

S = 601.333 R-Sq = 99.90% R-Sq(adj) = 99.86%

Grouping Information Using Tukey Method and 95.0% Confidence

solution	N	Mean	Grouping
10	3	38433.3	A
5	3	14033.3	B
0	3	1419.3	C

Means that do not share a letter are significantly different.

Table A. 30 One way Analysis of Variance (ANOVA) and Tukey's comparison test for total phenolic content (TPC) values of pea flour/PEO solutions containing different amount of gallic acid.

Factor	Type	Levels	Values
solution	fixed	3	0, 5, 10

Analysis of Variance for TPC, using Adjusted SS for Tests

Source	DF	Seq SS	Adj SS	Adj MS	F	P
solution	2	1391.46	1391.46	695.73	1356.39	0.000
Error	10	5.13	5.13	0.51		
Total	12	1396.59				

S = 0.716189 R-Sq = 99.63% R-Sq(adj) = 99.56%

Grouping Information Using Tukey Method and 95.0% Confidence

solution	N	Mean	Grouping
10	3	36.5	A
5	6	14.5	B
0	4	9.4	C

Means that do not share a letter are significantly different.

Table A. 31 *One way Analysis of Variance (ANOVA) and Tukey's comparison test for diameter values of pea flour/PEO nanofibers containing different amount of gallic acid.*

Factor	Type	Levels	Values
nanofiber	fixed	3	0, 5, 10

Analysis of Variance for diameter, using Adjusted SS for Tests

Source	DF	Seq SS	Adj SS	Adj MS	F	P
nanofiber	2	590504	590504	295252	103.67	0.000
Error	293	834427	834427	2848		
Total	295	1424931				

S = 53.3655 R-Sq = 41.44% R-Sq(adj) = 41.04%

Grouping Information Using Tukey Method and 95.0% Confidence

nanofiber	N	Mean	Grouping
0	97	297.4	A
5	99	219.3	B
10	100	191.7	C

Means that do not share a letter are significantly different.

Table A. 32 One way Analysis of Variance (ANOVA) and Tukey's comparison test for total phenolic content (TPC) values of pea flour/PEO nanofibers containing different amount of gallic acid.

Factor	Type	Levels	Values
nanofiber	fixed	2	5, 10

Analysis of Variance for TPC, using Adjusted SS for Tests

Source	DF	Seq SS	Adj SS	Adj MS	F	P
nanofiber	1	282.94	282.94	282.94	243.65	0.000
Error	4	4.65	4.65	1.16		
Total	5	287.59				

S = 1.07763 R-Sq = 98.38% R-Sq(adj) = 97.98%

Grouping Information Using Tukey Method and 95.0% Confidence

nanofiber	N	Mean	Grouping
10	3	27.2	A
5	3	13.4	B

Means that do not share a letter are significantly different.

Table A. 33 *One way Analysis of Variance (ANOVA) and Tukey's comparison test for antioxidant activity values of pea flour/PEO nanofibers containing different amount of gallic acid.*

Factor	Type	Levels	Values
nanofiber	fixed	2	5, 10

Analysis of Variance for AA, using Adjusted SS for Tests

Source	DF	Seq SS	Adj SS	Adj MS	F	P
nanofiber	1	0.4036	0.4036	0.4036	0.95	0.361
Error	7	2.9635	2.9635	0.4234		
Total	8	3.3671				

S = 0.650659 R-Sq = 11.99% R-Sq(adj) = 0.00%

Grouping Information Using Tukey Method and 95.0% Confidence

nanofiber	N	Mean	Grouping
10	5	5.7	A
5	4	5.3	A

Means that do not share a letter are significantly different.

Table A. 34 *One way Analysis of Variance (ANOVA) and Tukey's comparison test for consistency index (k) values of solutions containing PEO/soy protein/HPMC.*

Factor	Type	Levels	Values
solution	fixed	3	HPMC/PEO, HPMC/Soy/PEO, Soy/PEO

Analysis of Variance for k, using Adjusted SS for Tests

Source	DF	Seq SS	Adj SS	Adj MS	F	P
solution	2	610.70	610.70	305.35	7799.97	0.000
Error	3	0.12	0.12	0.04		
Total	5	610.82				

S = 0.197857 R-Sq = 99.98% R-Sq(adj) = 99.97%

Grouping Information Using Tukey Method and 95.0% Confidence

solution	N	Mean	Grouping
HPMC/PEO	2	24.1	A
HPMC/Soy/PEO	2	6.4	B
Soy/PEO	2	0.3	C

Means that do not share a letter are significantly different.

Table A. 35 *One way Analysis of Variance (ANOVA) and Tukey's comparison test for flow behavior index (n) values of solutions containing PEO/soy protein/HPMC.*

Factor	Type	Levels	Values
solution	fixed	3	HPMC/PEO, HPMC/Soy/PEO, Soy/PEO

Analysis of Variance for n, using Adjusted SS for Tests

Source	DF	Seq SS	Adj SS	Adj MS	F	P
solution	2	0.073408	0.073408	0.036704	2918.41	0.000
Error	3	0.000038	0.000038	0.000013		
Total	5	0.073445				

S = 0.00354636 R-Sq = 99.95% R-Sq(adj) = 99.91%

Grouping Information Using Tukey Method and 95.0% Confidence

solution	N	Mean	Grouping
Soy/PEO	2	1.0	A
HPMC/Soy/PEO	2	0.9	B
HPMC/PEO	2	0.7	C

Means that do not share a letter are significantly different.

Table A. 36 One way Analysis of Variance (ANOVA) and Tukey's comparison test for diameter values of nanofibers containing PEO/soy protein/HPMC.

Factor	Type	Levels	Values
nanofiber	fixed	3	hpmc, soy, soy/hpmc

Analysis of Variance for diameter, using Adjusted SS for Tests

Source	DF	Seq SS	Adj SS	Adj MS	F	P
nanofiber	2	532423	532423	266212	59.39	0.000
Error	294	1317824	1317824	4482		
Total	296	1850247				

S = 66.9507 R-Sq = 28.78% R-Sq(adj) = 28.29%

Grouping Information Using Tukey Method and 95.0% Confidence

nanofiber	N	Mean	Grouping
hpmc	99	342.4	A
soy/hpmc	100	288.5	B
soy	98	238.5	C

Means that do not share a letter are significantly different.

Table A. 37 One way Analysis of Variance (ANOVA) and Tukey's comparison test for opacity values of sheets containing PEO/soy protein/HPMC and PLA

Factor	Type	Levels	Values
nanofiber	fixed	4	HPMC/PEO, HPMC/Soy/PEO, PLA, soy/PEO

Analysis of Variance for opacity, using Adjusted SS for Tests

Source	DF	Seq SS	Adj SS	Adj MS	F	P
nanofiber	3	3062.1	3062.1	1020.7	546.06	0.000
Error	8	15.0	15.0	1.9		
Total	11	3077.0				

S = 1.36718 R-Sq = 99.51% R-Sq(adj) = 99.33%

Grouping Information Using Tukey Method and 95.0% Confidence

nanofiber	N	Mean	Grouping
soy/PEO	2	43.7	A
HPMC/Soy/PEO	2	42.4	A B
HPMC/PEO	4	39.7	B
PLA	4	7.6	C

Means that do not share a letter are significantly different.

Table A. 38 *One way Analysis of Variance (ANOVA) and Tukey's comparison test for WVP values of sheets containing PEO/soy protein/HPMC and PLA.*

Factor	Type	Levels	Values
nanofiber	fixed	4	HPMC/PEO, HPMC/soy/PEO, PLA, soy/PEO

Analysis of Variance for WVP, using Adjusted SS for Tests

Source	DF	Seq SS	Adj SS	Adj MS	F	P
nanofiber	3	16.0736	16.0736	5.3579	31.04	0.003
Error	4	0.6905	0.6905	0.1726		
Total	7	16.7642				

S = 0.415497 R-Sq = 95.88% R-Sq(adj) = 92.79%

Grouping Information Using Tukey Method and 95.0% Confidence

nanofiber	N	Mean	Grouping
soy/PEO	2	6.2	A
HPMC/PEO	2	5.9	A
HPMC/soy/PEO	2	4.9	A
PLA	2	2.6	B

Means that do not share a letter are significantly different.

CURRICULUM VITAE

PERSONAL INFORMATION

Surname, Name : Aydođdu, Ayça
Nationality : Turkish (TC)
Date and Place of Birth : 13 July 1988, Elazığ
Phone : +90 537 610 2617
E-mail : e156152@metu.edu.tr

EDUCATION

Degree	Institution	Year of Graduation
MS	METU Food Engineering	2014
BS	METU Food Engineering	2011
High School	Elazığ Anadolu High School, Elazığ	2006

WORK EXPERIENCE

Year	Place	Enrollment
2012-2018	Middle East Technical University	Research Assistant
2011-2012	Konya Necmettin Erbakan University	Research Assistant

FOREIGN LANGUAGES

Advanced English, Basic German

PUBLICATIONS

1. Barskiy, D., Tayler, M., Marco, I., Kentner, A., Vigneron, D., Cikrikci, S., Aydogdu, A., Reh, M., Pravdivtsev, A., Hovener, J., Blanchard, J., Wu, T., Budker, D., & Pines, A.. Zero-Field Nuclear Magnetic Resonance of pH-dependent Chemical Exchange. Nature Communications.
2. Aydogdu, A., Yildiz, E., Aydogdu, Y., Sumnu, G., Sahin, S. and Ayhan, Z. “Enhancing oxidative stability of walnuts by using gallic acid loaded lentil flour based electrospun nanofibers as active packaging material”, Food Hydrocolloids, 95, 245-255 (2019)
3. Aydogdu, A., Yildiz, E., Ayhan, Z., Aydogdu, Y., Sumnu, G. and Sahin, S. “Nanostructured Poly (lactic acid)/Soy Protein/HPMC films by

- electrospinning for potential applications in food industry”, *European Polymer Journal*, 112, 477-486 (2019)
4. Aydogdu, A., Sumnu, G. and Sahin, S. “Fabrication of gallic acid loaded Hydroxypropyl methylcellulose nanofibers by electrospinning technique as active packaging material”, *Carbohydrate Polymers*, 208, 241–250 (2019)
 5. Aydogdu, A., Sumnu, G. and Sahin, S. “A novel electrospun hydroxypropyl methylcellulose/polyethylene oxide blend nanofibers: Morphology and physicochemical properties”, *Carbohydrate Polymers*, 181, 234–246 (2018)
 6. Aydogdu, A., Kirtil, E., Sumnu, G., Oztop, M. H. and Aydogdu, Y. “Utilization of lentil flour as a biopolymer source for the development of edible films”, *Journal of Applied Polymer Science*, 135(23), 46356 (2018)
 7. Oguz, S., Tam, N., Aydogdu, A., Sumnu, G. and Sahin, S. “Development of novel pea flour-based nanofibres by electrospinning method”, *International Journal of Food Science and Technology*, 53(5), 1269–1277 (2018)
 8. Tam, N., Oguz, S., Aydogdu, A., Sumnu, G. and Sahin, S. “Influence of solution properties and pH on the fabrication of electrospun lentil flour/HPMC blend nanofibers”, *Food Research International*, 102, 616–624 (2017)
 9. Aydogdu, A., Sumnu, G. and Sahin, S. “Effects of addition of different fibers on rheological characteristics of cake batter and quality of cakes”, *Journal of Food Science and Technology*, 55(2), 667–677 (2017)
 10. Kirtil, E., Tonyali, B., Aydogdu, A., Bulut, Y. and Cilek Tatar, B. “Visualisation of cakes differing in oil content with magnetic resonance imaging”, *International Journal of Food Properties*, 20, 1025–1036 (2017)
 11. Kirtil, E., Aydogdu, A. and Oztop, M. H. “Investigation of physical properties and moisture sorption behaviour of different marshmallow formulations”, *Acta Horticulture*, (2017)
 12. Aydogdu, A., Ozkahraman, B.C., Sumnu, G. and Sahin, S. “Effects of legume flours on batter rheology and cake physical quality”, *Acta Horticulture*, (2017)
 13. Aydogdu, A., Sumnu, G. and Sahin, S. “Effects of Microwave-Infrared Combination Drying on Quality of Eggplants”, *Food and Bioprocess Technology*, 8, 1198–1210 (2015)

SELECTED ORAL and POSTER PRESENTATIONS

1. Barskiy D., Reh M., Cikrikci S., Aydogdu A., Blanchard J., Budker D., & Pines A. (2018). Zero-Field NMR of Quadrupolar Nuclei and Exchanging Systems. HYP18-An International Conference on Nuclear Hyperpolarization. Southampton, UK (Abstract-Poster Presentation)
2. Tam, N., Oguz, S., Aydogdu, A., Sumnu, G., & Sahin, S. (2017). Mercimek Unu ve HPMC Konsantrasyonunun Elektroeğirme Çözültisi ve Nanolif Özelliklerine Olan Etkileri. 10. Gıda Mühendisliği Kongresi. Antalya, Turkey (Abstract-Poster Presentation)
3. Aydogdu, A., Ozkahraman, B.C., Sumnu, G., Sahin, S. (2016). Effects of legume flours on batter rheology and cake quality. International Conference on Agricultural

and Food Engineering (Cafei2016), Kuala Lumpur, Malaysia (Full text-Oral presentation)

4. Aydogdu, A., Sumnu, G., Sahin, S. (2016). Limon Lifinin Kek Hamuru ve Kekin Kalite Parametrelerine Olan Etkisinin İncelenmesi. Türkiye 12. Gıda Kongresi, Edirne (Abstract-Poster Presentation)

Kirtil,E., Aydogdu,A., Elik, S., Oztop,M.H. (2015). Effect of sugar type and water content on the physical properties of marshmallows. 4th International Conference and Exhibition on Food Processing & Technology, London, UK (Abstract-Poster Presentation)

6. Aydogdu, A., Sumnu, G., Sahin, S. (2015). The Effect of Microwave-Infrared Combination Drying on Quality of Osmotically Dehydrated Eggplants. 4th International Conference and Exhibition on Food Processing & Technology, London,UK (Abstract-Poster Presentation)

7. Aydogdu, A., Sumnu, G., Sahin, S. (2015). Mikrodalga-kızıl ötesi kombinasyonu ile kurutmanın ön işlem görmüş patlıcanların kuruma davranışı üzerindeki etkileri. Pamukkale University, Gıda Sempozyumu III, Denizli,Turkey (Abstract-Poster Presentation)

8. Aydogdu, A., Sumnu, G., Sahin, S. (2014). Pore size distribution of eggplants dried by different drying methods. Food Balt 2014 9th Baltic Conference on Food Science and Technology “Food for consumer well-being, Jelgava, Latvia (Full Text- Poster Presentation)

9. Kirtil,E., Yildiz, E., Cilek,B., Tonyali, B., Aydogdu, A., Yucekutlu, M., Oztop, M.H. (2014). Investigating Effect of Fat Content and Peanut/Raisin Addition to Cake Batters on Texture Moisture Content and Weight Loss with Magnetic Resonance Imaging (MRI). Institute of Food Technologists –IFT 14 Annual Meeting + Food Expo, New Orleans, USA (Abstract-Poster Presentation)

10. Aydogdu, A., Sumnu, G., Sahin, S. (2013). Infrared assisted microwave drying of eggplants. 4th International Conference on Food Engineering and Biotechnology – ICFEB, Copenhagen, Denmark (Full Text-Oral Presentation)

11. Aydogdu, A., Sumnu, G., Sahin, S. (2013). Comparison of microwave-infrared combination drying and hot air drying of eggplants. Institute of Food Technologists – IFT 13 Annual Meeting + Food Expo, Chicago, USA (Abstract-Poster Presentation)

12. Aydogdu, A., Sumnu, G., Sahin, S. (2013). The effects of microwave-infrared combination drying on drying characteristics of eggplants. II. Traditional Foods from Adriatic to Caucas, Ohrid, Macedonia (Abstract-Poster Presentation)

HOBBIES

Traveling, photography